AD 714825

Aperture Synthesis for HF Radio Signals Propagated via the F Layer of the Ionosphere

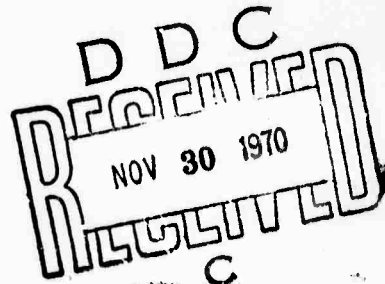by

J. T. Lynch

September 1970

Technical Report N° 161

DDC
RECEIVED
NOV 30 1970
C

RADIOSCIENCE LABORATORY

STANFORD ELECTRONICS LABORATORIES

STANFORD UNIVERSITY · STANFORD, CALIFORNIA

DISCLAIMER NOTICE

THIS DOCUMENT IS THE BEST
QUALITY AVAILABLE.

COPY FURNISHED CONTAINED
A SIGNIFICANT NUMBER OF
PAGES WHICH DO NOT
REPRODUCE LEGIBLY.

APERTURE SYNTHESIS FOR HF RADIO SIGNALS
PROPAGATED VIA THE F LAYER OF THE IONOSPHERE

by

J. T. Lynch

September 1970

Technical Report No. 161

Radioscience Laboratory
Stanford Electronics Laboratories
Stanford University   Stanford, California

BLANK PAGE

ABSTRACT

A portable high-frequency (HF) radio aperture up to 70 km in length was synthesized by receiving ionospherically propagated signals in a DC-3 airplane. By thus moving a small antenna rapidly over a long distance, a narrow receiving beam width (high azimuthal resolution) was achieved. It is believed that the synthetic aperture described here is the first in the world developed for HF, although the concept has been used successfully at microwave frequencies.

When HF radio signals are propagated by refraction from the ionosphere, inhomogeneities in the electron density of the medium distort the refracted signals and limit the azimuthal resolution which can be achieved. Using a statistical model of the ionospheric distortion a theoretical analysis was made to predict the performance of the HF synthetic aperture, determine its limitations and compare its performance with that of a ground-based fixed array.

Using continuous wave (CW) signals transmitted from a point 2600 km to the east, it was shown that with compensation for the deviations of the airplane from a straight line course, a 10 km aperture yielded a 1/12 deg beam width (at 23 MHz) for about 20 per cent of the data tested, while a 5 km aperture yielded a 1/6 deg beam for about 50 per cent of the data tested. Based on results obtained by receiving the same signal at a fixed antenna on the ground, it is believed that both spatial and temporal variations of the ionosphere were limiting the achievable beam width. In another method of operation a sequence of swept frequency CW (SFCW) signals was transmitted from California, backscattered from ground areas 2600 km to the east, and received in the airplane, thus yielding an HF reflectivity image of the area. An HF repeater was located near the terrain to be imaged and was used as a reference to compensate for flight-path deviations and ionospheric distortion. A second repeater located 1000 m away from the reference repeater was used to simulate a strong backscatter return. An HF back-scatter map was made using a 70 km synthetic aperture which had a 500 m range and a 500 m cross-range (lateral) resolution. The two repeaters

SEL-70-066

were distinguishable in cross range. On the basis of the theoretical analysis, and the characteristics of the two repeaters as revealed in the backscatter map, it is believed that objects should be within 3 to 5 km of the reference repeater in order to be imaged without significant distortion.

The above results were obtained on a midlatitude east-west path which is known to have favorable characteristics. The data were taken during a period of low magnetic activity and in general the ionosphere was undisturbed.

It is concluded that aperture-synthesis techniques at HF are particularly attractive for apertures of between 1 and 10 km in length. For the shorter apertures, 1 to 3 km, it should be possible to obtain full benefit of the aperture by using a medium-sized airplane and simple processing techniques which would not compensate for course deviations of the plane from a straight line. Longer apertures, 6 to 10 km, could be used effectively at least part of the time, if compensation for course variations could be provided.

CONTENTS

CONTENTS (Cont)

ILLUSTRATIONS

ILLUSTRATIONS (Cont)

ILLUSTRATIONS (Cont)

TABLES

ACKNOWLEDGMENT

I. INTRODUCTION

A. PURPOSE AND MOTIVATION

The purpose of this research was to explore the possibilities of synthesizing an extremely long, high-frequency (HF) radio receiving array. This synthetic aperture is used to obtain the narrow beam width (high azimuthal resolution) possible with a large aperture by moving a small antenna rapidly over a large distance. This was accomplished by flying HF receiving equipment in an airplane over a path which formed the center line of the synthetic array. A sequence of pulsed signals propagated a long distance by means of an ionospheric reflection was received by the plane in flight. The information received at each position along the flight path was essentially equivalent to a signal received by a hypothetical dipole of a fixed array at that position. By receiving data in this manner in a plane traveling about 180 mph for up to 20 minutes it should be possible to synthesize arrays up to 100 km in length.

The investigation was undertaken because previous work in the ionospheric propagation of HF signals had shown that at least under favorable ionospheric conditions, the spread in azimuthal angle of arrival caused by irregularities in the ionosphere was often smaller than could be detected by arrays of the sizes used in the measurements. Some of these measurements have been made on what is believed to be the longest ground HF array now available, a 2.5 km phased array operated by the Stanford Radioscience Laboratory[1] at Los Banos, California. It was hoped that the synthetic aperture technique would demonstrate that apertures much longer than 2.5 km could be used at HF to form very narrow beam widths. The synthetic-aperture concept is very attractive at HF because of the large size of the physical structures otherwise required to obtain very narrow beam widths. The cost and time of laying cables for even a 10 km array are prohibitively large. The synthetic-aperture technique has proven successful at microwave frequencies;[2] however, the use of this technique at HF poses many new problems because

1

of the much longer wave lengths and therefore the much longer arrays which are required to obtain narrow azimuthal beams, and also because of the inhomogeneous nature of the ionosphere, which has a pronounced effect at HF.

There appear to be many potential applications for HF synthetic apertures, such as obtaining more detailed backscatter images of the HF reflectivity of the ground. It has been known for decades that HF radio signals can be propagated via the ionosphere to distant regions of the earth, scattered, and reflected back to a receiver near the source. For even the best existing HF backscatter sounding systems, the cross-range (measured perpendicular to signal path and is proportional to the angle of arrival times the range) resolution (10,000 m at a range of 2600 km), or detail obtained in this "backscatter" process is about two orders of magnitude less than the range resolution (measured parallel to signal path and is proportional to signal delay) (300 m). The backscatter records therefore contain only spatially averaged information about the ground scattering characteristics.

Using a 100 km aperture, a cross-range resolution of about 500 m at a range of 2600 km could theoretically be possible. With a cross-range resolution and a range resolution of about 500 m each, it might be possible to identify individual scatterers on the ground.

This research should also have implications regarding the ability of fixed arrays on the ground to obtain much narrower beam widths than previously demonstrated. There may be applications for which the cost and complexity of a large fixed array would be warranted if some assurance could be given that it would produce very narrow beam widths.

B. PREVIOUS WORK IN THE FIELD

Synthetic-aperture radars have been successfully used at microwave frequencies for many years.[2,3] These radars often operate at wave lengths of a few centimeters and at a line-of-sight distance from the terrain they image. They produce optical-quality radar reflectivity maps at least as useful as optical photographs.

A synthetic aperture for HF has been proposed by Shearman,[4] who

2

described an incoherent processing technique similar to the radio-astronomy approach. The incoherent HF technique takes advantage of the temporal variations of the ionosphere, requires a long averaging time, and depends on the randomness of the phase fluctuations. It is not obvious, however, that the statistics of the phase fluctuations of ionospherically propagated signals have the necessary properties in order for the incoherent approach to work. Therefore, the technique and implementation described here are based on coherent processing just as is the microwave technique. The coherent processing approach is used in this study because, as is later described, the ionosphere appears to preserve signal coherence over distances on the order of 2-10 km. It was also desired that the results apply directly to conventional large arrays which use coherent processing.

Many solutions to problems of the microwave synthetic aperture are directly translatable to the HF implementation. A problem not encountered at microwave frequencies, however, is the distortion caused by inhomogeneities in the propagating media. The ionospheric distortion may not limit the performance of arrays of about 2 to 10 km in length; however, the induced signal incoherence may be severe for arrays longer than 10 or 20 km. To determine the effect of the inhomogeneities on the performance of an HF array it is necessary to know the spatial and temporal statistics of the amplitude and phase distortion of obliquely propagated HF signals. While much is known about such ionospheric inhomogeneities, as is described below, there are many unanswered questions which the synthetic aperture experiment might help answer.

The ionosphere is composed of free ions, electrons and neutral particles as a result of solar radiation interaction with the earth's atmosphere. The electrons exert the major influence on HF radio signals by decreasing the refractive index thus causing radio rays from the earth to bend and return to earth. Although the process is often a gradual bending of the ray the term reflection is used to emphasize the major effect. The maximum electron density is near 300 km (which varies diurnally and seasonally) and drops off nearly monotonically to approximately zero both near the earth and in interplanetary space. The

3

signals used in this study were reflected by the F layer, which is the region of the ionosphere near the electron density maximum. At a lower height there is sometimes a local maximum of electron density or sometimes just a variation in the rate of change with height of the electron density which is called the E-layer. Propagation using the E-layer can have more stable characteristics than F-layer propagation. It can be used, however, only for distances shorter than those used in this study. All signals used in this study were propagated via a single ionospheric reflection, i.e., one hop. Two and three hop signals are common; however the intervening ground reflection can greatly distort the signal.

The electron density in the ionosphere is spatially inhomogeneous as a result of many different mechanisms such as temperature fluctuations, solar radiation changes, interaction of the plasma with neutral winds and wave motions and the passage of meteors. Traveling ionospheric disturbances with spatial periods of 50 to 500 km are often observed (see Georges[5] for a review). Satellite-to-ground radio measurements[6] indicate regions of the irregularities near or above the F-region peak. Size estimates for these irregularities are on the order of 1 km. However, the nature of the irregularities below the F-region peak is of most interest here, since obliquely propagated HF signals are always below this level.

Vertical incidence measurements[7] and incoherent scatter observations of traveling disturbances have also been made (see Thome[8, 9]) with a sensitivity of about 1 per cent of the ambient electron density.

The techniques mentioned above do not appear to be sensitive to the presence of weak irregularities which appear to exist even under quiet conditions. To avoid confusion in interpreting results, it would be best to make observations of the irregularities with obliquely propagated HF signals if the effect of the irregularities on this type of signal is to be determined.

The oblique measurements should be made using a signal propagated by only a one hop path. The intervening ground reflection of the multi-hop case and the interference between the several modes apparently explains why most of the research so far conducted shows a low degree of

4

spatial and temporal coherence. There have been a few experiments reported which use a single mode and significantly conclude that the wave coherence is very good.

In a 1951 paper entitled "Measurements of the Direction of Arrival of Short Radio Waves Reflected at the Ionosphere," Bramley and Ross[10] report that direction-of-arrival measurements, made at two sites laterally separated by 27 km, were highly correlated. This suggests that large inhomogeneities in the ionosphere are responsible for the angle-of-arrival fluctuations. Bramley and Ross indicate that there may also exist smaller, weaker, irregularities which could affect the phase of HF signals. A 1953 paper by Bramley[11] is similar to the earlier one but investigates more fully the nature of large-scale irregularities and their effect on angle-of-arrival measurements. The characteristics of the large disturbances are of considerable interest in HF direction finding. A paper reviewing this subject has been written by Getting.[12]

Recent measurements made at Stanford University provided basic information and were a motivating factor for the research described here. These measurements indicated that one-hop signals can be more phase coherent than previously thought. Delay-resolution measurements of one-hop F-layer signals by Lynch et al[13] show that 1 to 5 μsec pulses can be propagated without significant spreading, at least during favorable conditions. These conditions include a midlatitude path, propagating in winter at midday, using a one-hop F lower ray mode and an operating frequency about 70 per cent of the maximum usable frequency (MUF). Coherent band widths of 500 kHz are possible at least part of the time under these conditions.

Angular resolution measurements have been made by Sweeney[1] using HF antenna elements which span 2.5 km. Mode-resolved amplitude and phase measurements made at eight elements of this a y indicate that the wave fronts are nearly linear for the ideal propagation conditions described above. This implies that beam widths at least as good as 1/4 deg at 30 MHz are possible at least part of the time over a favorable path. In a recent paper, Fialer[14] indicates that there are weak

5

(1 per cent or less) slow-moving irregularities with a typical size of about 35 km.

Mode-resolved measurements made by other researchers also indicate a high degree of coherence for one-hop F-layer signals. A paper written by Balser and Smith in 1962[15] reports on amplitude measurements made on a 1500 km path with a lateral separation between receiving antennas of up to 700 m. Balser and Smith assume that the amplitude variations were caused by scattering from many inhomogeneities in the ionosphere, and they are able to relate the amplitude correlations to the angular spread of the scattered signals. They estimate that the spreading was about 0.2 deg in azimuth, much less than predicted in earlier research. Regardless of the validity of their assumptions and conclusions of the analysis, their experimental results, indicating a high degree of spatial amplitude correlation in ionospherically propagated signals, are significant. Measurements of temporal variations have been made; however, only a few of these measure the frequency spread introduced by the ionosphere. Sheperd and Lomax[16] report frequency spreads of less than 1/10 Hz for one-hop F or E modes.

Mode-resolved measurements of phase difference of obliquely propagated signals at points separated by more than 3 km have apparently not been made. Thus the upper limit on how far HF arrays can be extended and still achieve the beam widths predicted from theory has not been determined. The synthetic-aperture technique offers the possibility of determining a lower bound on the performance of large arrays. Such a bound is determined because the temporal variations of the ionosphere degrade the performance of the synthetic aperture but do not affect the fixed aperture.

C. APPROACH USED IN PRESENT STUDY

The approach used in this investigation is to show the feasibil'ty and determine the fundamental limitations of HF synthetic apertures by using a simple but realistic analysis and experimental measurements designed to use existing equipment and techniques whenever possible. Three possible methods of operation have been developed for the

6

synthetic aperture. These methods are:

1. Operation <u>without</u> compensation for airplane flight
    path deviations from a straight line or for
    ionospheric distortion.

2. Operation <u>with</u> compensation for flight path deviations
    by means of an airplane tracking system, but without
    compensation for ionospheric distortion.

3. Operation with an HF repeater used to provide a
    reference signal to compensate for both flight-path
    deviations and ionospheric distortion.

The first method, in which no compensation is used, is by far the
simplest in terms of signal processing and is attractive for this reason.

The second method, in which compensation for airplane course
deviations is made, requires some technique to accurately determine the
coordinates of the plane as a function of time. Thus the measurements
will indicate the limitations imposed by the ionosphere on a synthetic
aperture.

The third method, in which compensation for airplane course
deviations and ionospheric distortion is made, offers the possibility
of obtaining extremely long synthetic apertures. The use of an HF
repeater to measure the distortion is similar to the use of a reference
beam in optical holography to reduce image distortion. It has been
shown by Goodman[17] that holograms are superior to conventional incoher-
ent images if the medium through which the light passes is turbulent.
If the object and the reference beam are close enough to each other,
the random phase variations in the optical signal are cancelled because
the reference beam for the hologram and the light from the object pass
through nearly the same random variations in refractive index.

The principal features of the experimental program are:

1. Verification of airplane tracking subsystem performance.

2. Measurement of beam width achievable with synthetic
    aperture when receiving a CW signal transmitted from
    Bearden, Arkansas (CW forward-propagation experiment).
    In this test, compensation was made for deviations of the

7

airplane from a linear flight path by the use of the airplane tracking data.

3. Demonstration of feasibility of obtaining two-dimensional backscatter data (range vs cross range) without compensating for ionospheric distortion or deviations of the airplane from a linear flight path.

4. Investigation of the use of an HF repeater at Bearden to provide a reference signal in compensating for airplane flight path deviations and ionospheric distortion, for the purpose of obtaining extremely high azimuthal resolution in backscatter mapping.

The CW forward propagation experiment has the advantage of much simpler signal processing requirements, thus making it easier and less expensive to process more data. The backscatter experiments are important, however, to illustrate application of synthetic apertures to HF backscatter imaging. The use of both approaches also makes it easier to compare the results obtained with both forward propagation and backscatter studies being performed by the Stanford Radioscience Laboratory with the 2.5 km array at Los Banos.

As indicated earlier, the experimental design was to use existing facilities and equipment whenever possible. Thus the Stanford Radio-science Laboratory's existing wide-band, high-power, narrow-beam transmitter at Lost Hills, California, the transmitter and repeater at Bearden, Arkansas, and the swept frequency CW (SFCW) sounding equipment were all part of the design. The digital computer processing is available at Stanford and allows considerable flexibility in specifying and changing the signal processing. It is expensive to use a large computer such as the IBM 360; but as only a few backscatter images were to be made, this was cheaper than other approaches. The use of a digital computer also makes it possible to implement more complex signal processing techniques.

D. CONTRIBUTIONS OF THIS RESEARCH

During the course of this research the following original contributions were made in the field of ionospheric propagation of HF radio signals:

8

1. A portable HF radio antenna aperture of up to 70 km
    in length was synthesized by installing receiving
    equipment aboard an airplane which flew a substantially
    straight course while receiving ionospherically
    propagated signals. It is believed that this long
    synthetic aperture is the first in the world to be
    developed for operation at HF.

2. A theoretical analysis was made to predict the
    performance of such a synthetic aperture, determine
    its limitations and compare its performance with
    that of a ground-based fixed antenna array.

3. The problem of restoring signals to their undistorted
    form was studied for application to HF synthetic
    apertures. The improvement afforded by a reference
    signal was calculated in order to predict how far a
    point to be imaged could be from the reference and
    still have a small degree of distortion.

4. Using such compensation techniques it was shown
    experimentally that a very high degree of azimuthal
    resolution can be obtained within 3 to 5 km of an
    HF repeater used as a reference signal. An HF
    backscatter map using a 70 km aperture was made
    showing a second repeater used to simulate ground
    backscatter.

5. It was also shown experimentally that synthetic
    apertures 6 to 10 km in length can be used effectively
    at least part of the time (i.e., under favorable
    ionospheric conditions) if compensation for only
    flight path deviations are made.

II. ANALYSIS OF AN HF SYNTHETIC APERTURE

A. BASIC RELATIONSHIPS

The use of a synthetic aperture for HF radio reception is a technique for obtaining the narrow beam width (high azimuthal resolution) possible with a large aperture by moving a small aperture rapidly over a large distance. Consider a sequence of HF pulses from a distant fixed source with a period of T_f sec. The pulses are identical, and each pulse has a plane wave front. A small receiving antenna moves at a uniform velocity of v_a m/sec, as shown in Fig. 1. The antenna, in effect, samples each arriving pulse at uniformly spaced points along the wave front. If N pulses are coherently processed, the result should be equivalent to that obtained if signals were processed from N fixed elements spaced $T_f v_a$ meters apart along the flight path of the airplane. The beam width of the synthetic aperture is equal to the wave length λ divided by the total equivalent aperture length $N T_f v_a$, or $\lambda/N T_f v_a$ radians beam width.

An equivalent point of view considers the frequency shift ("doppler") introduced by the motion of the receiving antenna. If N pulses are coherently processed, the integration time is $N T_f$ sec, and the frequency (doppler) resolution is $1/N T_f$ Hz. This resolution is a measure of how closely spaced in frequency two signals can be, and yet be distinguished from each other. A distant source whose signal arrives perpendicularly to the path of motion of the antenna has zero doppler shift. A source θ radians from the first has a doppler shift f_d given by

$$f_d = \frac{v_a}{\lambda} \sin \theta \quad .$$

For small θ, where $\sin \theta \cong \theta$, the angular resolution is the "doppler resolution" $(1/N T_f)$ times λ/v_a, giving a resolution of $\lambda/(N T_f v_a)$

Preceding page blank
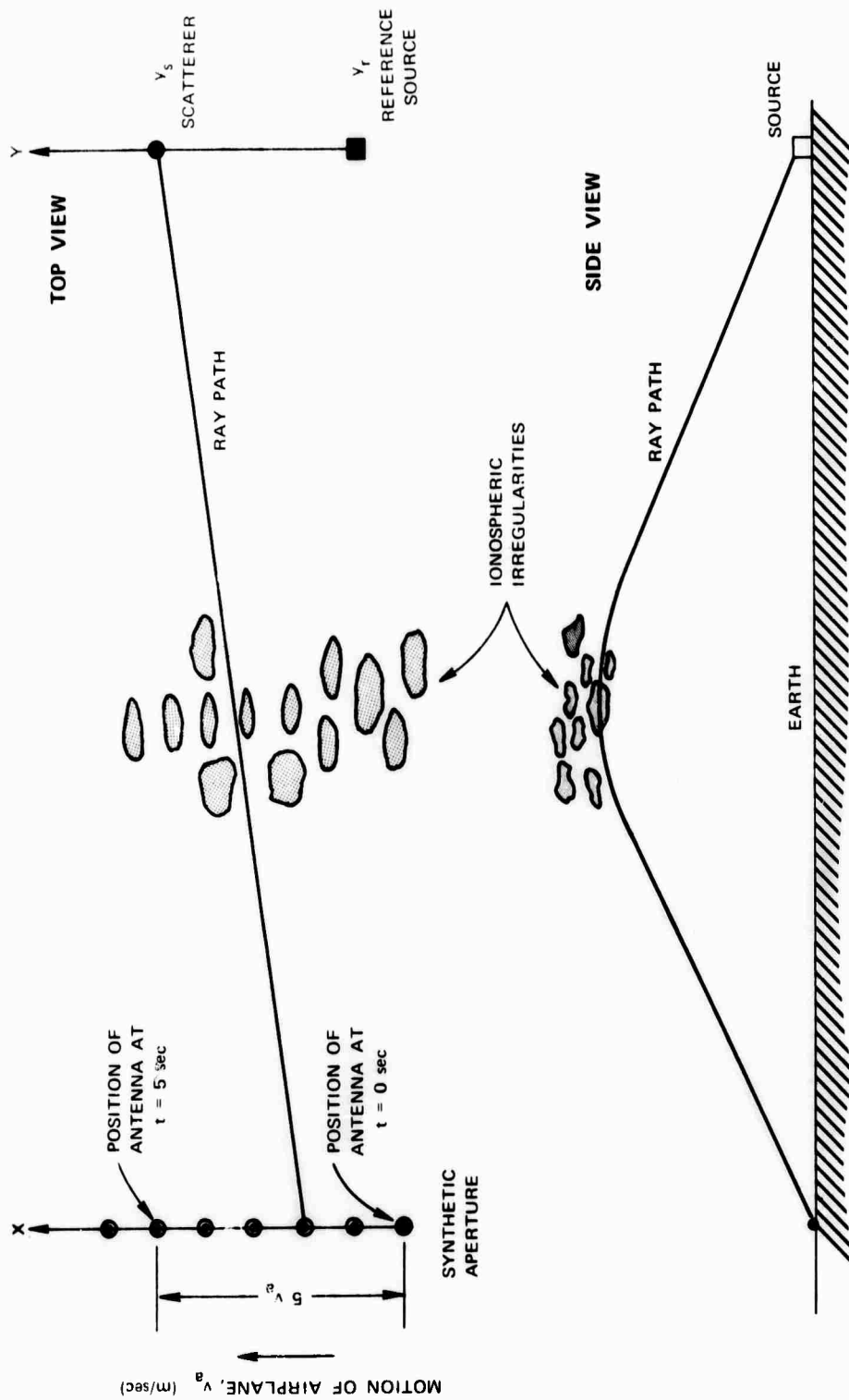
Figure 1   Geometry of HF synthetic aperture.

12

radians. Thus the analysis gives the same conclusion regardless of the point of view.

The first point of view--i.e., that of an equivalent array fixed in space--will be taken to describe the performance of the synthetic array. Although the synthetic array is actually composed of discrete equivalent elements, it is convenient to describe its performance in terms of continuous rather than discrete variables. It is assumed that in practice the elements of the array are close enough together to avoid a problem of multiple side lobes caused by spatial aliasing ("grating lobes").

Let the received signal voltage at a point x along the array of length L be represented by the real part of

$$s(x) = A(x) e^{j\varphi(x)} ,$$

where $A(x)$ =   the amplitude of the received signal

$\varphi(x)$ =   the "phase"--i.e., the phase difference between the incident wave and the local oscillator of the receiver.

Let $S(\theta)$ be the complex angular distribution of signal amplitude and phase; then (see Bracewell[18])

$$S(\theta) = \frac{1}{L} \int_{-L/2}^{L/2} s(x) \exp\left(-j \frac{2\pi x \sin\theta}{\lambda}\right) dx . \tag{1}$$

For small angles $(\sin\theta \cong \theta)$, Eq. (1) becomes a Fourier transform with the quantity θ/λ interpreted as a spatial frequency.

If the signal amplitude across an aperture of length L is unity, and the phase φ is linear according to the relation

13

$$\varphi(x) = 2\pi \frac{\theta_o}{\lambda} x ,$$

where θ_o is a constant expressed in radians, then the distribution of received power vs angle (often called the "array power pattern") is given by:

$$|S(\theta)|^2 = \left| \frac{\sin \frac{\pi(\theta - \theta_o) L}{\lambda}}{\frac{\pi(\theta - \theta_o) L}{\lambda}} \right|^2 . \tag{2}$$

The resolution of the antenna is determined by its beam width and side-lobe level. The beam width is often defined as the width of the main lobe of the antenna at the half-power point (3 dB below the peak), although a point 10 or 20 dB down is also often used. The 3 dB width of the antenna pattern described by Eq. (2) is about λ/L radians. The largest side lobe is 13 dB below the peak. Techniques to reduce the side-lobe level are well known,[19] and one of the simplest will be used here. The reduction is achieved by multiplying the data along the aperture by a weighting function $W(x)$ given by:

$$W(x) = \begin{cases} 1 + \cos \frac{2\pi x}{L} , & -\frac{L}{2} < x < \frac{L}{2} ; \\ 0 & \text{otherwise} . \end{cases} \tag{3}$$

The effect of the weighting is to broaden the main lobe slightly and to reduce the largest side lobe amplitude to approximately 30 dB below the peak amplitude.

14

B. EFFECT OF IONOSPHERIC IRREGULARITIES ON A FIXED HF ARRAY

The angular resolution of an antenna may be lost if the wave fronts are no longer planar as was assumed in the initial model. Wave-front distortion can be caused by irregularities in the medium through which the signal passes. A statistical model of these wave-front distortions is used to analyze their effect on the array. The array performance is characterized by the statistical expectation (mean) of its power pattern.

The random wave-front distortion can be considered to be made up of two components, a random tilt or change in the apparent direction of arrival of a signal, and the variations about the tilt (see Fig. 2). A changing random wave-front tilt displaces in azimuthal angle the signals received by the array, but does not degrade the resolution by widening the main lobe or increasing the side lobes if the data are collected, or time averaged, in a time interval short relative to the time required for changes in the wave-front tilt. This case is referred to here as the short-term average.case. In the long-term average case the changing wave front tilt will smear the received signal in azimuthal angle. The situation is analogous to photography with a moving camera. The blurring caused by the camera motion can be reduced by making the film exposure-time interval shorter. The analysis for the long-term average therefore includes the effect of changing random wave-front tilts, while the short-term average excludes them. Each equivalent element of a synthetic aperture receives data essentially instantaneously; therefore the short-term average case also applies to synthetic apertures regardless of the temporal variation of the propagation medium.

The distinction between long- and short-term has been made in the context of optical imaging by Fried[20] and Heidbreder.[21] Their analyses are more complicated and more difficult to interpret than that to be presented here, because they used an accurate but awkward definition of wave front tilt, and also because they characterized the wave front variations with a statistical model which, though not necessarily more accurate than the one used here, was far more difficult to treat analytically.

15

DIRECTION
OF SIGNAL

WAVEFRONT φ (x)

TANGENT TO
WAVEFRONT AT
POINT x

CENTER LINE
OF ARRAY

x

$$\text{TILT } T(x) = \frac{d\,\varphi\,(x)}{dx}$$
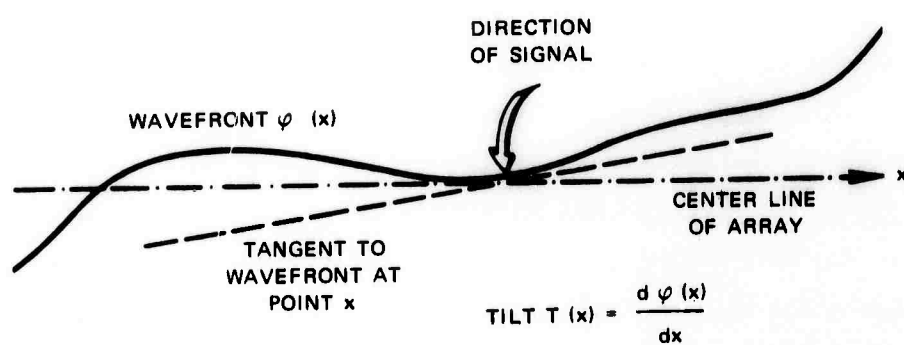
Figure 2   Wavefront after undergoing distortion.

1. <u>Wave-Front Distortion Model and Mean Power Pattern of Array</u>

The electron density in the ionosphere is temporally changing
and spatially inhomogeneous as a result of many different mechanisms
such as temperature fluctuations, solar radiation changes, interaction
of the plasma with winds of neutral particles and wave motions, and the
passage of meteors. These changing ionospheric inhomogeneities cause
the wave-front distortion just discussed. These distortions are char-
acterized here by a phase distortion in the received signal. The phase
distortion is the phase difference between the phase which would have
been measured in the absence of ionospheric inhomogeneities and the
phase which is actually measured in the presence of the inhomogeneities.
For the purpose of the analysis it is assumed here that the phase distor-
tion φ , is a stationary gaussian, zero-mean random process with a
correlation function given by

$$K_{\varphi}(\Delta x) = E[\varphi(x) \varphi(x - \Delta x)]$$
$$= \sigma_{\varphi}^2 \exp\left[-\left(\frac{\Delta x}{\Lambda}\right)^2\right] \ , \tag{4}$$

where Δx is the distance between two points at which the phase is
measured; σ_{φ}^2 is the "phase variance"--i.e., the mean square of the
phase φ ; Λ is the phase correlation distance; and $E[\cdot]$ denotes a
statistical expectation (here called the mean). This is clearly a very
simple model of a complicated phenomenon; however, it has several char-
acteristics required by the physical mechanisms involved. For example,
the phase variance is bounded, the correlation function is monotonically
decreasing, and the correlation function is differentiable (thus, the
phase process is uniformly continuous). A more complicated model could
be developed by using a correlation function which is the sum of several
functions similar to the above with different correlation distances Λ .
The simple function (4) should be useful, however, in relating the

17

correlation distance Λ to the performance of the antenna system. It is to be noted that nonstationary variations, such as would be caused by diurnal effects, are disregarded. The only cases considered here are those in which amplitude distortion caused by focusing of the beam by the ionospheric irregularities is small.

The phase-structure function is defined by

$$D_{\varphi}(\Delta x) \triangleq E[|\varphi(x) - \varphi(x - \Delta x)|^2] \quad . \tag{5a}$$

It is related to the correlation function by

$$D_{\varphi}(\Delta x) = 2[K_{\varphi}(0) - K_{\varphi}(\Delta x)] \quad ,$$

and for the assumed correlation function Eq. (4), the phase-structure function is given by

$$D_{\varphi}(\Delta x) = 2 \sigma_{\varphi}^2 \left\{ 1 - \exp\left[-\left(\frac{\Delta x}{\Lambda}\right)^2 \right] \right\} \quad . \tag{5b}$$

A simple, already-known result will now be described which relates the phase-structure function to the distorted power pattern of an array. Since it includes the effect of random wave-front tilts the following result is for the long-term average case.

Let $h_{LT}(\Delta x)$ be a distortion function defined by

$$h_{LT}(x) \triangleq \exp\left[-\tfrac{1}{2}D_{\varphi}(\Delta x) \right] \quad , \tag{6}$$

18

and let $H_{LT}(\theta)$ be given by

$$H_{LT}(\theta) \triangleq \int_{-\infty}^{\infty} h_{LT}(\Delta x) \exp\left[- j \frac{2\pi\theta}{\lambda} \Delta x\right] d\Delta x \quad .$$

where $d\Delta x$ is the differential of Δx . Then the mean array power pattern, $E[|S(\theta)|^2]$, is (see Gaskill[22])

$$E[|S(\theta)|^2] = \frac{1}{L} \int_{-\infty}^{\infty} \left\{ \int_{-\infty}^{\infty} \frac{1}{L} p(x) p(x - \Delta x) dx \right\}$$

$$h_{LT}(\Delta x) e^{- j \frac{2\pi\theta}{\lambda} \Delta x} d\Delta x \tag{7}$$

Equation 7 is a special case of a more general result which is derived in the following section. This is a special case because $D_{\varphi}(\Delta x)$ does not depend on x (only on Δx).

2. Calculation of the Mean Array Power Pattern for Case of Short-Term Averaging

The distortion function defined in (6) is appropriate to the case of long-term averages because it includes the effect of random wave-front tilts. The wave-front tilt, $T(x)$, is defined as the slope of the phase of the signal at any point x (see Fig. 2). The angle of arrival θ_o , of a signal received at a point $x = 0$, is related to the tilt by $\theta_o = T(0) \frac{\lambda}{2\pi}$. The tilt at a point x is given by

$$T(x) \triangleq \frac{d\varphi(x)}{dx} = \lim_{\delta x \to 0} \left\{ \frac{\varphi(x) - \varphi(x - \delta x)}{\delta x} \right\} , \tag{8}$$

where δx represents an incremental value of x (not to be confused

19

with Δx , the distance between two discrete points at which the phase is measured). The variance of the tilt, σ_T^2 , is given by

$$E\left| T(x) \right|^2 = \frac{2\sigma_\varphi^2}{\Lambda^2} \tag{9a}$$

and the variance of the angle of arrival $\sigma_{\theta_o}^2$ is therefore

$$\sigma_{\theta_o}^2 = \frac{2\sigma_\varphi^2}{(2\pi)^2} \left(\frac{\lambda}{\Lambda} \right)^2 \tag{9b}$$

The short-term average distortion function is designated by $h_{ST}(x)$, and is calculated with the linear phase-vs-distance part of the phase distortion removed. Define $D_{NL}(\Delta x)$ as the "nonlinear" phase-structure function--i.e., the function with an approximation to the linear phase term removed. An approximation to the short-term average distortion function is then given by

$$h_{ST}(\Delta x) = \exp\left[-\tfrac{1}{2} D_{NL}(\Delta x) \right] .$$

The approach taken here is to approximate the exact result by subtracting from the phase difference $\{\varphi(x) - \varphi(x - \Delta x)\}$ a phase which depends on the wave front tilt at the center of the array $(x = 0)$. This approach will yield a lower bound on the antenna performance, since the actual amount of displacement of the array beam is given by the average tilt across the entire aperture. Thus there may be some

20

residual tilt left in the calculations presented here which will cause the distortion predicted to be greater than the actual distortion.

In the derivation[22] of the expression for $E[|S(\theta)|^2]$, Eq. 7, it was assumed by Gaskill that the phase structure function $D_\varphi(\Delta x)$, Eq. 5a, depends only on Δx but not on x . In the development to follow it is found that $D_{NL}(\Delta x)$ depends on x as well as Δx and therefore it is necessary to derive a new expression which is an upper bound on the quantity $E[|S(\theta)|^2]$. This bound is consistent with the use of the wave front tilt measured at the midpoint of the array since it too places an upper bound on the array performance, i.e., the actual performance is better than the predicted performance.

Define an "aperture function" $p(x)$ by

$$p(x) \;=\; \begin{cases} 1 & -\dfrac{L}{2} \le x \le \dfrac{L}{2} \\[2ex] 0 & \text{otherwise} \end{cases}$$

and let the received signal $s(x)$ be given by

$$s(x) \;=\; e^{j\left(\varphi(x) \,-\, (x)\,\cdot\, T(0)\right)}$$

where a linear phase due to the wave front tilt has been subtracted and where the amplitude is assumed to be unity. Using Eq. 1 the mean square power pattern of the array is given by

21

$$E|S(\theta)|^2 = E\left[\frac{1}{L} \int_{-\infty}^{+\infty} p(x_1) \; s(x_1) \; \exp\left(- j \frac{2\pi x_1 \theta}{\lambda}\right) dx_1 \right.$$

$$\left. \times \; \frac{1}{L} \int_{-\infty}^{+\infty} p(x_2) \; s*(x_2) \; \exp\left(+ j \frac{2\pi x_2 \theta}{\lambda}\right) dx_2 \right]$$

where $s*(x_2)$ denotes the complex conjugate of $s(x_2)$.

The previous equation can be rewritten by forming a double integral, taking the expectation inside the integral and using the fact that (see Gaskill[22]) for a zero mean gaussian random variable "a",

$$E[\exp(\pm \; ja)] = \exp[-\tfrac{1}{2}E(a^2)]$$

Thus the expression for $E[|S(\theta)|^2]$ becomes

$$E[|S(\theta)|^2] = \frac{1}{L^2} \iint_{-\infty}^{+\infty} p(x_1) \; p(x_2) \; \exp\left\{ - \tfrac{1}{2}E[\left|\varphi(x_1) - \varphi(x_2)\right.\right.$$

$$\left.\left. - (x_1 - x_2)T(0)\right|^2] \right\} \exp\left\{ - j \frac{2\pi(x_1 - x_2)\theta}{\lambda} \right\} dx_1 dx_2$$

Let $x_1 - x_2 = \Delta x$ and define a nonlinear phase structure function $D_{NL}(\Delta x, x_1)$ by

$$D_{NL}(\Delta x, x_1) \triangleq E[\left|\varphi(x_1) - \varphi(x_1 - \Delta x) - (\Delta x)T(0)\right|^2]$$

22

The expression for $E[|S(\theta)|^2]$ can be written as

$$E[|S(\theta)|^2] = \frac{1}{L^2} \int_{-\infty}^{+\infty}\int p(x_1)\, p(x_1 - \Delta x) \exp\left[-\tfrac{1}{2}D_{NL}(\Delta x, x_1)\right]$$

$$\exp\left(-j\frac{2\pi\Delta x\theta}{\lambda}\right) dx_1\, d\Delta x$$

Rearranging, it appears as:

$$E[|S(\theta)|^2] = \frac{1}{L}\int_{-\infty}^{+\infty}\left\{\frac{1}{L}\int_{-\infty}^{+\infty} p(x_1)\, p(x_1 - \Delta x)\exp\left[-\tfrac{1}{2}D_{NL}(\Delta x, x_1)\right]dx_1\right\}$$

$$\exp\left(-j\frac{2\pi\Delta x\theta}{\lambda}\right)dx_1$$

$$= \frac{1}{L}\int_{-\infty}^{+\infty} h_{ST}(\Delta x)\exp\left(-j\frac{2\pi\Delta x\theta}{\lambda}\right)d\Delta x \qquad (10)$$

where $h_{ST}(\Delta x)$ will be called the short term distortion function. The distortion function $h_{ST}(\Delta x)$ is essentially an aperture weighting function. If $h_{ST}(\Delta x)$ becomes small for large Δx then there is a restriction on the maximum size of the aperture which can be effectively used and therefore there is an expected beam width defined. By approximating $h_{ST}(\Delta x)$ with functions which are always smaller than $h_{ST}(\Delta x)$ an upper bound for $E[|S(\theta)|^2]$ can be found. That is the actual performance will be better than that predicted by the calculation. The first step is to upper bound the integral in the above equation which depends on x_1. This is done by noting that for positive Δx the

23

limits of the integral can be modified (see Fig. 3 for illustration on integration limits) to account for the function $p(x_1)$ as follows

$$E\left[|S(\theta)|^2\right] = \frac{1}{L} \int_{-\infty}^{+\infty} p(x_1)\, p(x_1 - \Delta x)\, \exp\left[-\tfrac{1}{2} D_{NL}(\Delta x, x_1)\right] dx_1$$

$$= \begin{cases} \dfrac{1}{L} \displaystyle\int_{-(L/2-\Delta x)}^{L/2} \exp\left[-\tfrac{1}{2} D_{NL}(\Delta x, x_1)\right] dx_1 , & 0 \le \Delta x < L \\[4mm] 0 & \Delta x > L \end{cases} \tag{11}$$

The symmetry in the definitions of $D_{NL}(\Delta x, x_1)$ implies that the result of the integration is even in Δx, thus it suffices to evaluate the above for positive Δx.

The next step is to place an upper bound on the second integral. This is done by noting that e^{-z_1} is a convex function, namely

$$\tfrac{1}{2}\left[e^{-z_1} + e^{-z_2}\right] \ge e^{-\tfrac{1}{2}(z_1 + z_2)} .$$

It follows that, for $0 \le \Delta x < L$,

$$\frac{1}{L-\Delta x} \int_{-(L/2-\Delta x)}^{L/2} \exp\left[-b(z)\right] dz \ge \exp\left[-\frac{1}{L-\Delta x} \int_{-(L/2-\Delta x)}^{L/2} b(z)\, dz\right]$$

where $b(z)$ is any integrable function. Using this inequality and Eq. 11, we can now write

24
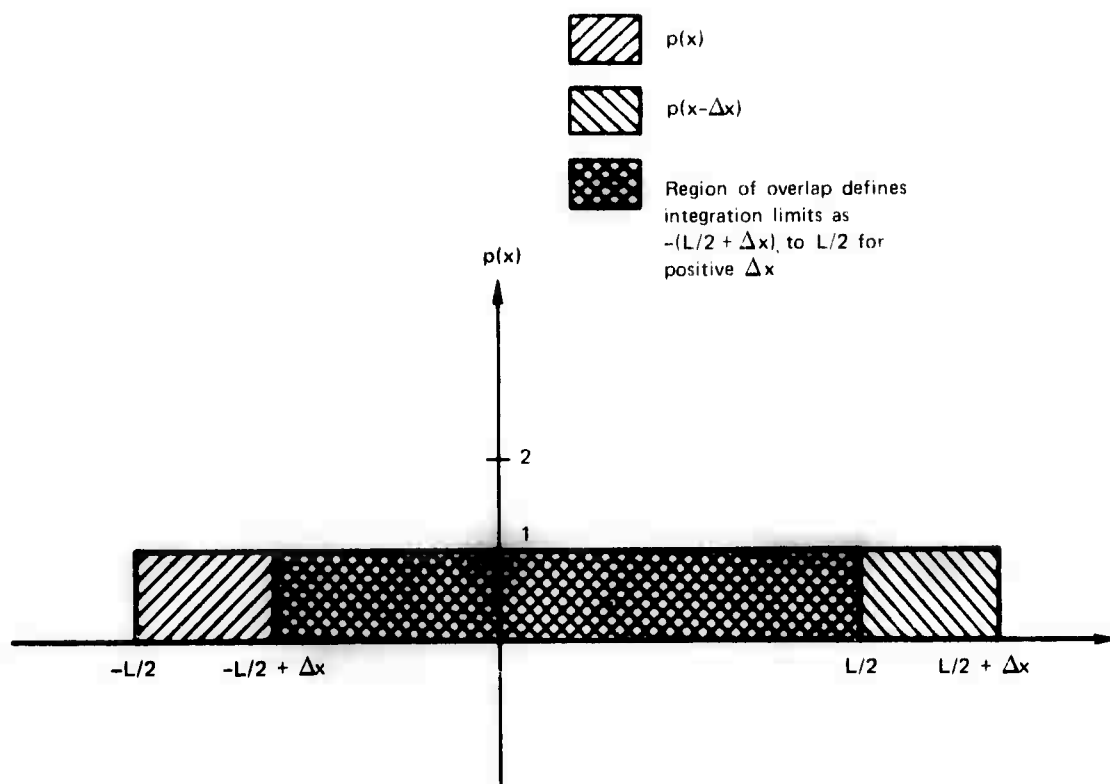
Figure 3   Sketch showing limits of integration in evaluating $h_{ST}(\Delta x)$.

$$\frac{L - \Delta x}{L} \quad \cdot \quad \frac{1}{L - \Delta x} \int_{-(L/2 - \Delta x)}^{L/2} e^{-\frac{1}{2} D_{NL}(\Delta x, x_1)} \, dx_1$$

$$\geq \frac{L - \Delta x}{L} \exp \left\{ - \left[\frac{1}{2(L - \Delta x)} \int_{-(L/2 - \Delta x)}^{L/2} D_{NL}(\Delta x, x_1) \, dx_1 \right] \right\}$$

and the term in the exponential is written as

$$<D_{NL}(\Delta x)> = \frac{1}{L - \Delta x} \int_{-(L/2 - \Delta x)}^{L/2} D_{NL}(\Delta x, x_1) \, dx_1$$

to indicate a spatial average over x_1 . Here $\tilde{h}_{ST}(\Delta x)$ is a lower bound on the actual distortion function $h_{ST}(\Delta x)$ defined in Eq. 10.

The function $D_{NL}(\Delta x, x)$ is now evaluated and the integral performed. Using the definition of tilt in Eq. 8 the correlation function defined in Eq. 4, and the phase structure function in Eq. 5a $D_{NL}(\Delta x, x)$ can be evaluated to be

$$D_{NL}(\Delta x, x) = D_\varphi(\Delta x) + (\Delta x)^2 \sigma_T^2 - 2\Delta x \, K_\varphi'(-x) + 2\Delta x \, K_\varphi'(\Delta x - x)$$

where $K_\varphi'(\Delta x) \overset{\Delta}{=} \frac{d}{dx} K_\varphi(\Delta x)$ and σ_T^2 is the variance of the tilt $T(0)$.

26

The integral of the preceeding equation is easy to evaluate since the first two terms do not depend on x and the second two terms are differentials. We therefore find that

$$\langle D_{NL}(\Delta x)\rangle = D_\varphi(\Delta x) + (\Delta x)^2 \sigma_T^2 + \frac{2\Delta x}{L - \Delta x}\left\{2K_\varphi\left(\frac{L}{2}\right)\right.$$

$$\left. - 2K_\varphi\left(\frac{L}{2} - \Delta x\right)\right\}.$$

This expression is evaluated using the definition of $K_\varphi(\Delta x)$ in Eq. 4,

$$\langle D_{NL}(\Delta x)\rangle = 2\sigma_\varphi^2\left\{1 - \exp\left[-\left(\frac{\Delta x}{\Lambda}\right)^2\right]\right\} + \frac{2\sigma_\varphi^2(\Delta x)^2}{\Lambda^2}$$

$$+ \frac{4\sigma_\varphi^2\Delta x}{L - \Delta x}\left\{\exp\left[-\left(\frac{L}{2\Lambda}\right)^2\right] - \exp\left[-\left(\frac{L/2 - \Delta x}{\Lambda}\right)^2\right]\right\} \tag{12}$$

which is valid only for $\Delta x < L$. For $\Delta x > L$, $D_{NL}(\Delta x) = 0$. Using the above equation a lower bound for the distortion function $\tilde{h}_{ST}(\Delta x)$ can be evaluated from

$$\tilde{h}_{ST}(\Delta x) = e^{-\frac{1}{2}\langle D_{NL}(\Delta x)\rangle}.$$

27

3. Interpretation of Calculations

The phase-structure functions, with and without the linear term, will now be plotted and their asympototes evaluated.

For $\Delta x \ll \Lambda$, $D_\varphi(\Delta x)$ defined in (5b) becomes:

$$D_\varphi(\Delta x) \cong \frac{2\sigma_\varphi^2 (\Delta x)^2}{\Lambda^2}$$

Any realistic phase-structure function must be quadratic for small values of its argument, since this property implies that for small Δx there is only a phase tilt. If $\varphi(x) = a x$, where a is a random variable, then from (5a), $D_\varphi(\Delta x) = E |ax - a(x - \Delta x)|^2 = \Delta x^2 \times E |a^2|$, which is quadratic in Δx. Uniform continuity of the wave front guarantees that over a small enough interval the phase must be linear, and therefore $D_\varphi(\Delta x)$ must be quadratic in Δx as $\Delta x \rightarrow 0$.

Similarly, the value of $\langle D_{NL}(\Delta x) \rangle$, Eq. 12, for small Δx is evaluated:

$$\langle D_{NL}(\Delta x) \rangle \approx \frac{4\sigma_\varphi^2 \Delta x^2}{\Lambda^2} \left[1 - e^{-\left(\frac{L}{2\Lambda}\right)^2} \right] \tag{13}$$

Thus for small Δx the nonlinear phase structure is proportional to $(\Delta x)^2$ as was the phase structure function $D_\varphi(\Delta x)$ except that the coefficient of $(\Delta x)^2$ is reduced by a factor $1 - e^{-(L/2\Lambda)^2}$. For small L, i.e., $L < \Lambda$, the factor is approximately $\left(\frac{L}{2\Lambda}\right)^2$.

To illustrate the distinction between long- and short-term phase structure functions, $D_\varphi(\Delta x)$ and $\langle D_{NL}(\Delta x) \rangle$ are plotted in Figs. 4, 5, and 6. In these plots the Δx axis is measured in units of $\frac{L}{2\Lambda}$.

28

page 29 intentionally blank
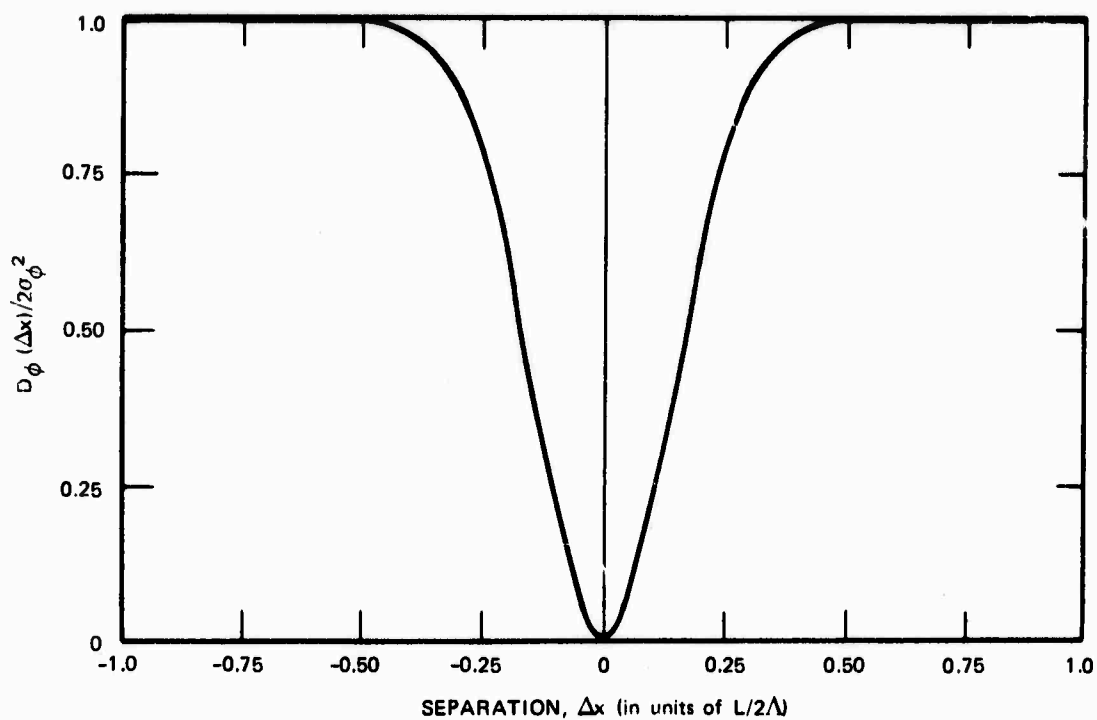
Figure 4   Normalized phase structure function
L = array length, Λ = phase correlation
distance, L/Λ = 10
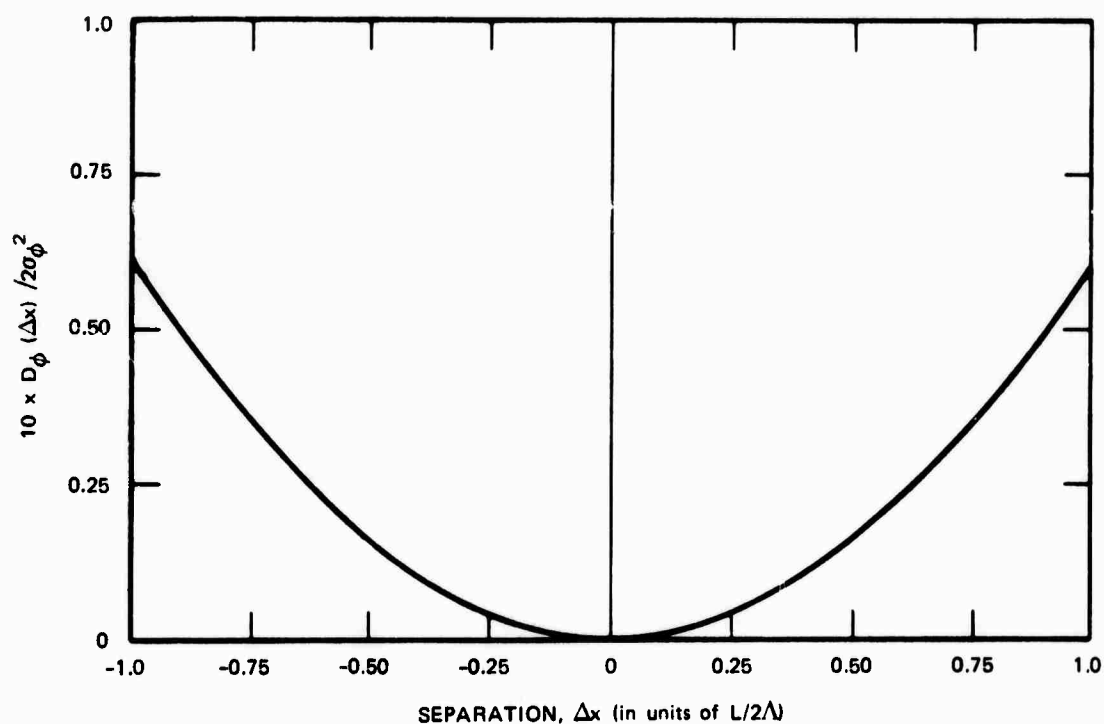
Figure 5   Normalized phase structure function
L/Λ = 1/2

30
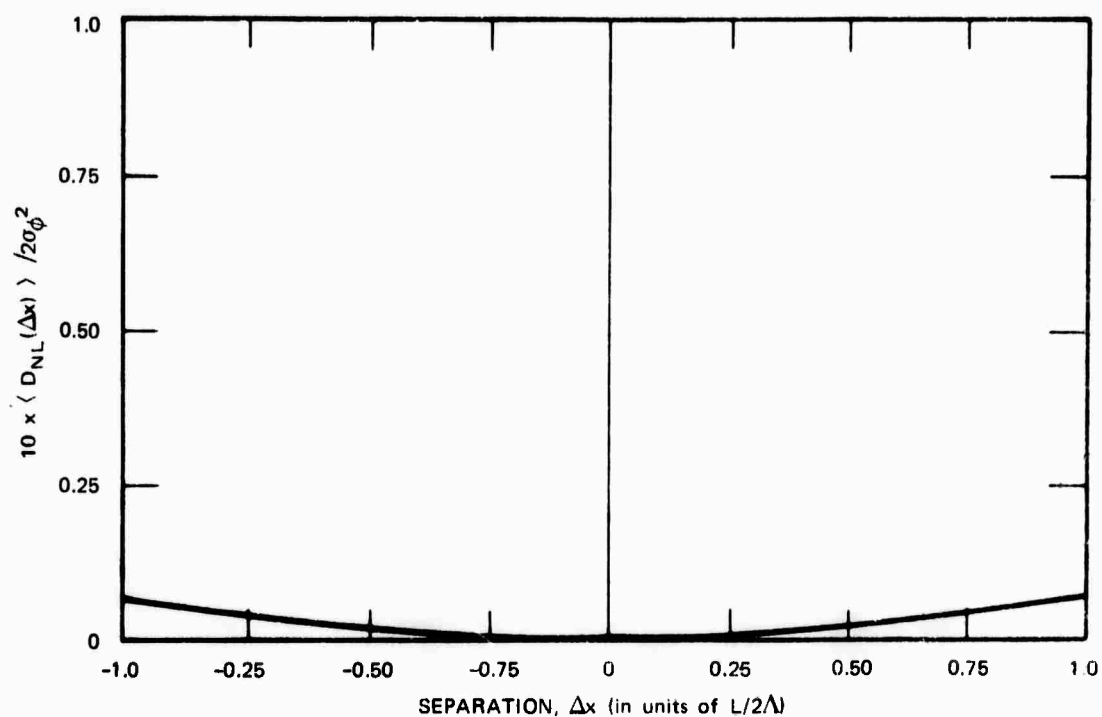
Figure 6   Normalized nonlinear phase structure function
$L/\Lambda = 1/2$
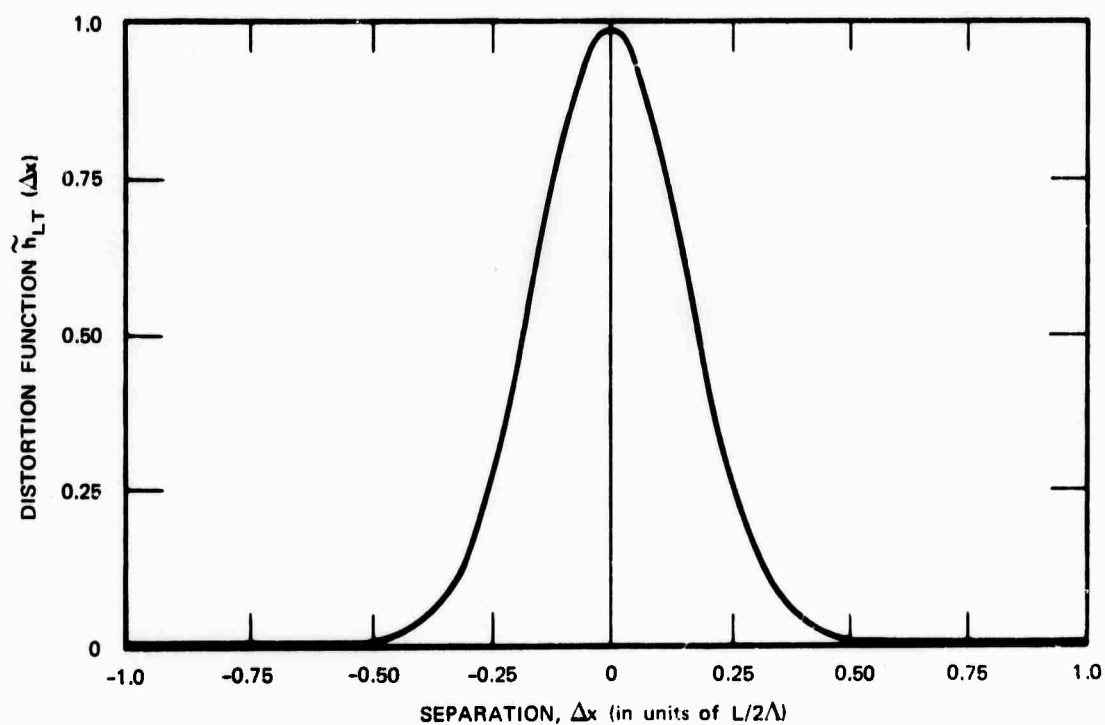
Figure 7   Long-term distortion function
$L/\Lambda = 1/2$, $\sigma_\phi = 3.0$

31

Figure 4 shows $D_\varphi(\Delta x)$ normalized to $D_\varphi(\infty) = 2\sigma_\varphi{}^2$ for $\frac{L}{\Lambda} = 10$. Figure 4 also shows $D_\varphi(\Delta x)$ except a factor of ten gain is applied to the curve and $\frac{L}{\Lambda} = 1/2$. Making $\frac{L}{\Lambda}$ smaller has the effect of expanding the horizontal axis. The value of $\frac{L}{\Lambda}$ is significant because for small $\frac{L}{\Lambda}$ the array length is much shorter than the phase correlation distance, Λ ; therefore very little distortion should occur. On the other hand more distortion is expected for $L > \Lambda$.

For $L \cong \Lambda$ the amount of distortion depends on whether the long- or short-term case is being considered. The wavefront tilt should be correlated over a distance of about Λ and therefore removing the tilt term should significantly modify the distortion function for $\frac{L}{\Lambda} < 1$. Figure 6 shows the nonlinear phase structure function $\langle D_{NL}(\Delta x)\rangle$ plotted for $L = 1/2$ and for a gain of 10 (i.e., $10 \times \langle D_{NL}(\Delta x)\rangle/D_{NL}(\infty)$). Thus, Figs. 5 and 6 permit a direct comparison of two phase structure functions.

The utility of these phase-structure functions is that they are used to evaluate the distortion functions $h_{LT}(\Delta x)$, and $\tilde{h}_{ST}(\Delta x)$, defined in Eqs. 6 and 10. Figures 7, 8, and 9 show these functions evaluated for $\sigma_{\tilde{\varphi}} = 3$ cycles. Figure 7 is $h_{LT}(\Delta x)$ for $\frac{L}{\Lambda} = 1/2$ and Fig. 8 is $\tilde{h}_{ST}(\Delta x)$ for $\frac{L}{\Lambda} = 1/2$.

The short term distortion function is not significantly attenuated for large Δx , indicating the full beam width of $\frac{\lambda}{L}$ radians would be achieved. This is about a factor of three improvement over the long-term case. Figure 9 shows the short-term distortion function for $\frac{L}{\Lambda} = 1$. In this case about 75 percent of the aperture is almost completely attenuated to zero. As expected, as L becomes comparable to Λ, removing the tilt does not improve the expected array performance significantly. This is especially true for the calculations presented here since the tilt at the mid point of the array rather than the average tilt was removed. For small $\frac{L}{\Lambda}$ the distinction between the two measures of tilt is not great, yet for large phase variance, $\sigma_\varphi{}^2$, the distinction between long- and short-term effects is pronounced as will be shown in the next section.

32
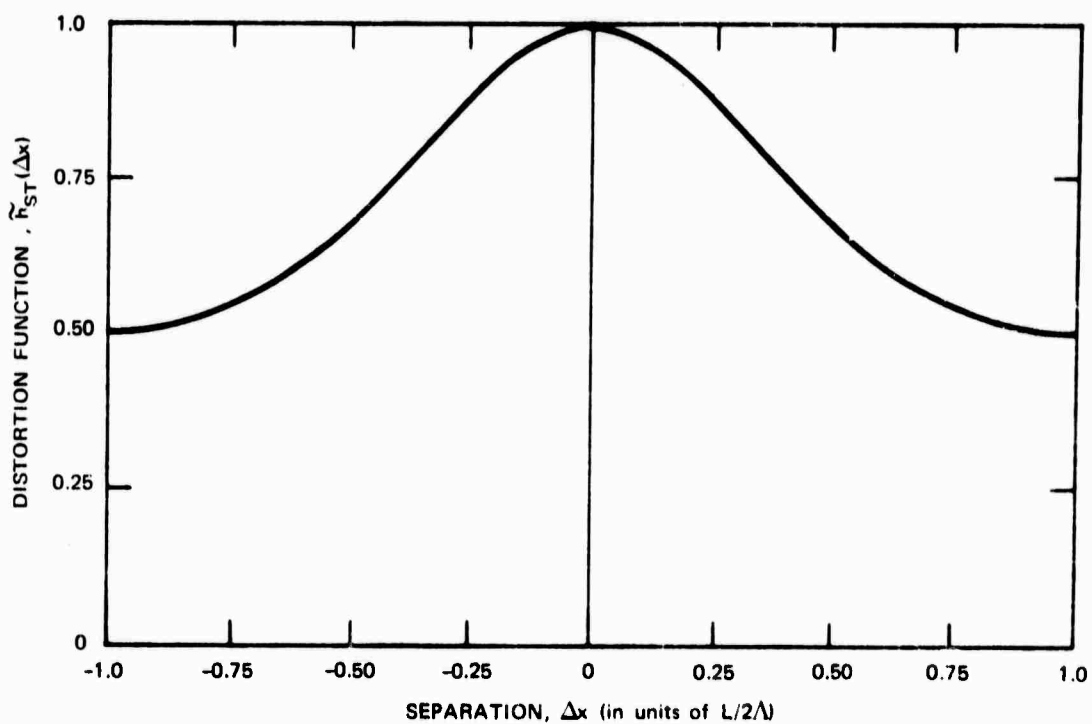
Figure 8   Short-term distortion function
$L/\Lambda = 1/2$, $\sigma_\phi = 3.0$
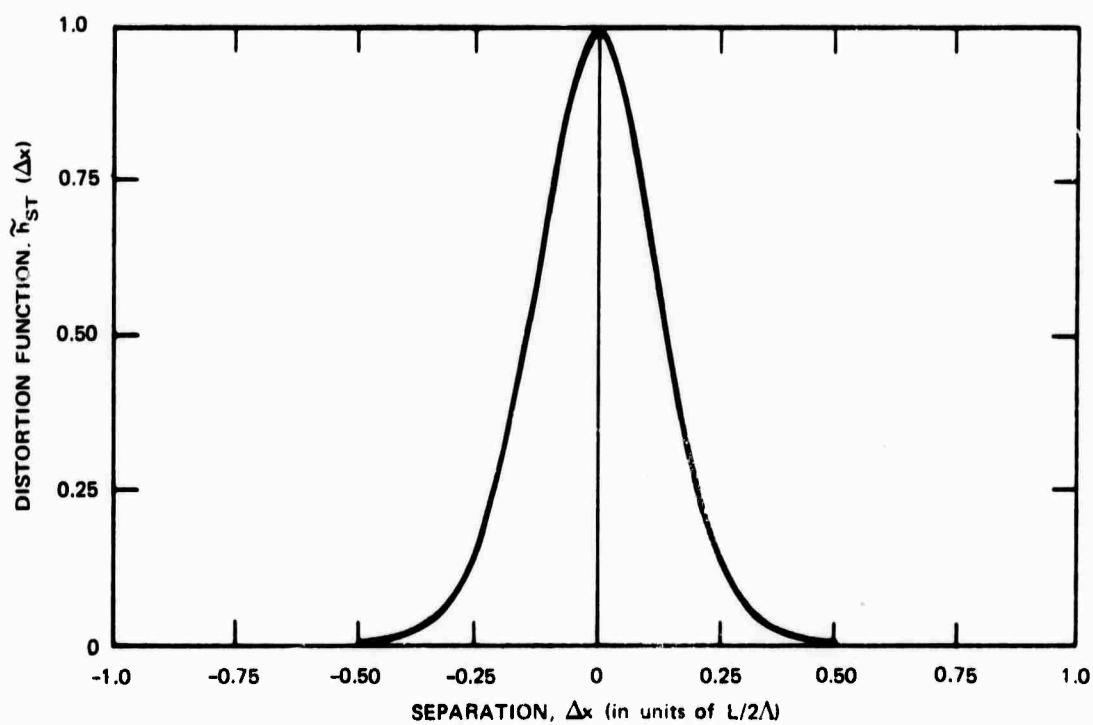
Figure 9   Short-term distortion function
$L/\Lambda = 1.0$, $\sigma_\phi = 3.0$

33

4. Evaluation for Large Rms Phase Variance

For large rms phase, $\sigma_\varphi > 2\pi$, the distortion function has no significant pedestal; therefore, the major effect of the distortion is to broaden the main lobe. The width of the main lobe is given approximately by the inverse of the effective aperture length L_e , multiplied by the wavelength λ -- i.e., by λ/L_e .

The structure function $D_\varphi(\Delta x)$ can be approximated by a quadratic term in Δx for $\Delta x < \Lambda$. However, as Δx approaches Λ the distortion function $h_{LT}(\Delta x)$ is very small. Therefore the quadratic approximation for $D_\varphi(\Delta x)$ is useful for determining the width of $h_{LT}(\Delta x)$. Thus for $\sigma_\varphi > 2\pi$

$$h_{LT}(\Delta x) \cong \exp\left[-\sigma_\varphi^2 (\Delta x/\Lambda)^2\right] \quad .$$

The same argument applies to the short-term distortion function $\widetilde{h}_{ST}(\Delta x)$. For small Δx it was found that (Eq. 13) $<D_{NL}(\Delta x)>$ could be approximated by a second-order expression from which

$$\widetilde{h}_{ST}(\Delta x) \cong \exp\left\{-2\sigma_\varphi^2 \left(\frac{\Delta x}{\Lambda}\right)^2 \left(1 - \exp\left[-(L/2\Lambda)^2\right]\right)\right\} \tag{14}$$

The effective aperture length is defined to be the width of $h(\Delta x)$ at a level $1/e$ ($\cong 10$ dB) below its peak. The approximate beam widths for the long- and short-term average cases for small $\frac{L}{2\Lambda}$ are found to be

$$\theta_{LT} \cong \frac{1}{2}\left(\frac{\lambda}{\Lambda}\right)\sigma_\varphi$$

$$\theta_{ST} \cong \frac{1}{\sqrt{2}}\left(\frac{\lambda}{\Lambda}\right)\sigma_\varphi\left(\frac{L}{2\Lambda}\right) \tag{15}$$

34

Note that the approximate beam width for the long-term case is proportional to the rms angle of arrival given by Eq. 9b,

$$\sigma_{\theta_o} = \frac{\sqrt{2}\sigma_\varphi}{2\pi} \left(\frac{\lambda}{\Lambda} \right)$$

Thus as expected the tilt term dominates the long-term average distortion.

The ideal beam width is given by λ/L ; therefore the increase in the beamwidth over the ideal case is $\frac{1}{2}\sigma_\varphi L/\Lambda$ for the long-term case and is $\frac{\sigma_\varphi}{\sqrt{2}} \left(\frac{L}{\Lambda} \right)^2$ for the short-term case. Therefore, little distortion occurs in the long-term case if

$$L < \frac{2\Lambda}{\sigma_\varphi}$$

and little distortion occurs in the short-term case if

$$L \lesssim \frac{2\Lambda}{\sqrt{\sigma_\varphi}} \tag{16}$$

Thus for large σ_φ the distinction is quite dramatic.

C. EFFECT OF IONOSPHERIC IRREGULARITIES ON A SYNTHETIC APERTURE

The spatial irregularities of the ionosphere affect a synthetic aperture in the same way that they affect a fixed array. On the other hand, temporal variations of the ionosphere do not affect the short-term averaged performance of a fixed array; but they do affect the short-

term averaged performance of a synthetic aperture. These temporal
variations may be caused by the random motion of the spatial irregu-
larities or by large-scale changes in the ionospheric structure due
to solar activity, diurnal changes, etc. A simple model for the spatial
and temporal variations of the ionosphere will be used in this section
to evaluate the relative importance of the various system and iono-
spheric parameters.

If the irregularities were stationary, or if the velocity v_a
of the moving antenna used to synthesize the aperture were very fast
so that the time to form the aperture was short relative to the time
scales of the ionospheric changes, then the performance of the synthetic
aperture would be the same as that of the fixed array as calculated in
the previous section. At the other extreme, consider the situation in
which there are no spatial phase variations [i.e., $D_\varphi(\Delta x) = 0$] , but
in which there are random temporal phase variations. In this case there
is a doppler frequency resolution limitation on the system. However,
doppler and angle of arrival are related for the synthetic aperture;
therefore the temporal phase variations would cause a loss in the
angular resolution of the aperture. Of course if the temporal phase
variations were linear (i.e., if the frequency shift were constant)
then the beam would be skewed, but a loss in angular resolution would
not occur.

The array performance is determined by the phase-structure function,
which in the time-varying case is given by

$$D_\varphi(\Delta x) = 2 [K_T(0, 0) - K_T(\Delta x, \Delta t)]$$

where $\Delta t = \Delta x / v_a$ and $K_T(\Delta x, \Delta t) \overset{\Delta}{=} E [\varphi(x, t) \varphi(x - \Delta x, t - \Delta t)]$.

If the irregularities that cause the spatial variations also cause
the temporal variations, which is physically reasonable, the spatial
and the temporal correlations would be similar in form. With this
partial justification the following analytically simple correlation
function is assumed to hold:

36

$$K_T(\Delta x, \Delta t) = \sigma_\varphi^2 \exp\left[-\left(\frac{\Delta t}{T}\right)^2 - \left(\frac{\Delta x}{\Lambda}\right)^2 \right] , \tag{17}$$

where T is the temporal correlation time. Nonstationary phase variations which could be caused by diurnal changes in the ionosphere are not included in this model. Making the substitution $\Delta t = \Delta x/v_a$, the correlation function can be rewritten as

$$K_T(\Delta x, \Delta x/v_a) = 2 \sigma_\varphi^2 \exp\left[-\left(\frac{\Delta x}{\Lambda_e}\right)^2 \right] , \tag{18}$$

where Λ_e is the "equivalent spatial correlation distance" defined by

$$\frac{1}{\Lambda_e^2} = \left(\frac{1}{v_a T}\right)^2 + \frac{1}{\Lambda^2} . \tag{19}$$

The concept of an equivalent spatial correlation distance Λ_e for a synthetic aperture is the important result of this section. The equivalent spatial correlation distance takes into account the antenna motion, and the temporal as well as the spatial variations of the ionosphere. The equivalent spatial correlation distance Λ_e is always smaller than the actual spatial correlation distance Λ. Since the quantity $1/\Lambda$ is proportional to the increase in beam width (beam spreading), the above equation simple states that the variances of the two causes of beam spreading add.

37

III. APPLICATION OF SIGNAL RESTORATION TECHNIQUES TO HF ARRAYS

The problem of restoring signals to their undistorted form has received much attention in the areas of telephone data communications and optical image processing. The approach generally taken is to find a linear time-invariant filter which operates on a distorted, noisy signal to minimize the mean-square error between the filter output and the original undistorted, noiseless signal. Least-mean-square linear filtering was originally described by Norbert Wiener;[23] a modern treatment has been given by Van Trees.[24] Applications of this technique to the restoration of incoherent optical images have been discussed theoretically by Helstrom[25] and by Slepian.[26]

The least-mean-square filter reduces to the inverse of the transfer function of the distortion function for high signal-to-noise ratios. If this inverse filter is used when the noise is not negligible, the filtering is not optimal, and in fact even further distortion can occur. Experimental evidence showing the importance of considering noise for optical applications has been given by Horner.[27] Application of inverse filtering to point-to-point HF propagation has been made by Belknap, Haggarty, and Perry.[28] They operated in a high signal-to-noise situation and were able to obtain substantial improvement in the delay resolution of wide-band signals.

Inverse filtering requires the compensation of both amplitude and phase distortion if these quantities are known. It is an already known result that if there is noise, the optimum restoring filter de-emphasizes its own effect on the amplitude in order to reduce the chance of applying a very high gain to noise. The following analysis considers the situation in which neither the amplitude nor the phase of the distortion is completely known. In this case the optimum filter again de-emphasizes restoration of the amplitude.

A. USE OF THE OPTIMUM FILTER IN OVERCOMING SIGNAL DISTORTION

The theory presented here is for temporal rather than spatial

Preceding page blank

signals, since this is the standard notation. Therefore the filters are described by transfer functions in the frequency (f) domain. An optimum filter with transfer function $H_o(f)$ will be described (see Fig. 10) which estimates an incoming signal a(t) after the latter has been distorted by a linear filter with transfer function D(f) and a noise n(t) has been added. The estimate is denoted a(t).

The signal a(t) and the noise n(t) are assumed to be stationary random processes with spectral densities $S_a(f)$ and $S_n(f)$ respectively. The signal r(t) and the input a(t) have a cross spectral density $S_{ra}(f)$, defined as the Fourier transform of the cross correlation function given by

$$K_{ra}(\tau) = E[r(t) a(t - \tau)] \quad .$$

The transfer function of the Wiener filter is given by:

$$H_o(f) = \frac{S_{ra}(f)}{S_r(f)} \quad , \tag{20}$$

where $S_r(f)$ is the spectral density of the signal r(t).

Evaluating the required spectral densities gives the well-known form of the least-mean-square restoring filter:

$$H_o(f) = \frac{E[D^*(f)] S_a(f)}{E[|D(f)|^2] S_a(f) + S_n(f)} \quad , \tag{21}$$

where $D^*(f)$ denotes the complex conjugate of D(f).

40
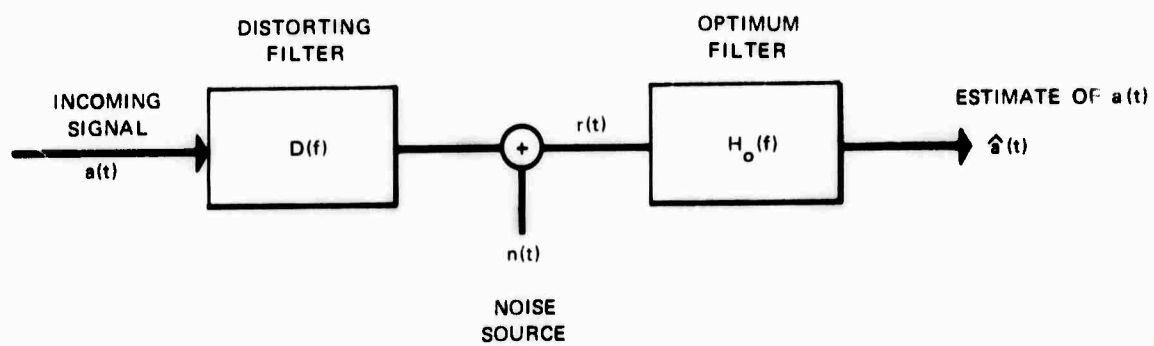
Figure 10   Use of the optimum filter in overcoming signal distortion.

If the signal spectrum is white within the band of interest, i.e., if $S_a(f) = 1$, and if the distortion function is known, the optimum filter is:

$$H_o(f) = \frac{D^*(f)}{D(f)^2 + S_n(f)} \quad . \tag{22}$$

For negligible noise this reduces to the inverse filter given by:

$$H_o(f) = \frac{1}{D(f)} \quad . \tag{23}$$

The inverse filter can have very large gains at those frequencies for which the amplitude of $D(f)$ is near zero. If the noise is not negligible, however, the effect of the noise at the filter output can be severe.

B.   EVALUATION OF THE OPTIMAL FILTER FOR TWO SPECIAL CASES

The optimal restoring filter will now be evaluated for two siutations wherein the distortion is not known exactly. In the first case it is assumed that the measurement of the distortion took place in the presence of noise. In the second case, which is a special case of multipath, it is assumed that the exact delay difference between two interfering signal paths is not known; this could be due either to inaccurate measurement or to a change in the propagation path. In many practical situations it may be possible to establish a reference signal to calibrate a propagation path, but the reference signal itself may be displaced from the data signal in time or space, so that the distortion cannot be known exactly.

42

1. Effect of Noise in the Measurement of the Distortion

Assume that the distortion is measured in the presence of zero-mean gaussian noise $n_M(t)$, which is independent of the distortion and other signals. Denote the result of the measurement as the reference distortion $D_{ref}(f)$. Assume further that the measurement was made in a finite time interval $[0, T]$. Then the reference distortion is

$$D_{ref}(f) = D(f) + N_M(f) \quad , \tag{24}$$

where

$$N_M(f) = \int_0^T n_M(t) \, e^{-j2\pi ft} dt \quad .$$

Since the noise, $N_M(f)$, is assumed to have zero mean the expected value of the distortion is

$$E[D^*(f)] = D^*_{ref}(f) \quad .$$

Since the noise, $N_M(f)$ is assumed independent of the distortion the mean square value of the distortion $D(f)$ is

$$E[|D(f)|^2] = |D_{ref}(f)|^2 + E[|N_M(f)|]^2 \quad .$$

The optimum restoring-filter transfer function is therefore [assuming $S_a(f) = 1$]

43

$$H_o(f) = \frac{D^*_{ref}(f)}{|D_{ref}(f)|^2 + E[|N_M(f)|^2] + S_n(f)} \quad .\tag{25}$$

Thus the noise encountered in the channel measurement and the noise encountered during data transmission have essentially the same effects, since they both de-emphasize the amplitude fluctuations of $H_o(f)$.

2. Effect of Changes in Multipath

The optimum restoration filter for a special case of multipath (the latter could be caused by magnetoionic splitting of rays in the ionosphere) will now be considered. Let the impulse response of the distortion consist of two random-amplitude time-displaced impulses:

$$a_1 \, \delta\left(\tau + \frac{(\tau_o + \tau_e)}{2}\right) + a_2 \, \delta\left(\tau - \frac{(\tau_o + \tau_e)}{2}\right) ,\tag{26}$$

where τ_o is a constant difference between the two modes; $\delta(\tau)$ is an impulse; a_1 and a_2 are independent gaussian random variables with means $E[a_1] \triangleq 1$ and $E[a_2]$ = a variable, and with variances σ_a^2 ; and where τ_e is another independent gaussian random variable (a delay) with zero mean and variance σ_e^2 . The time displacement is written symmetrically, since it is assumed that an overall time shift in the data is not regarded as an error.

The distortion $D(f)$ is given by

$$D(f) = a_1 e^{j \pi f (\tau_o + \tau_e)} + a_2 e^{-j \pi f (\tau_o + \tau_e)} \quad .$$

44

The mean of $D^*(f)$ is

$$E[D^*(f)] = e^{-j\pi f \tau_o} M(f) + E[a_2] e^{j\pi f \tau_o} M(f) \ .$$

$M(f)$ is the characteristic function of the probability density of τ_e and is defined as

$$M(f) \triangleq E\left[e^{-j2\pi f\tau_e}\right] \ .$$

For the gaussian random variable case assumed here,

$$M(f) = e^{-2\pi^2 \sigma_e^2 f^2} \ .$$

The mean-square value of $D(f)$ is

$$E[|D(f)|^2] = 1 + E[a_2] + 2\sigma_a^2 + 2 E[a_2] M(f) \cos 2\pi f \tau_o \ .$$

Assuming $S_a(f) = 1$, the optimum restoring filter for the special multipath case is therefore

$$H_0(f) = \frac{e^{-2\pi^2\sigma_e^2 f^2}\left(e^{-j\pi f\tau_0} + E[a_2]\, e^{j\pi f\tau_0}\right)}{1 + 2\sigma_a^2 + E[a_2^2] + 2\, E[a_2]\, e^{-2\pi^2\sigma_e^2 f^2}\cos 2\pi f\tau_0 + S_n(f)} \qquad .(27)$$

This result reduces to the known channel case if σ_e^2 and σ_a^2 are both zero. The effect of not knowing the differential delay τ_0 between the two paths is made more clear in Fig. 11. In this figure the magnitude of the restoration filter is plotted for the following parameters: $\sigma_a^2 = 0$, $S_n(f) = 0.01$, and $\sigma_e = 0.2/2\pi$. Note that for low frequencies, namely $f < 1/(2\pi\sigma_e)$, the filter is approximately an inverse filter; for high frequencies, however, the gain of the filter drops off. Thus for frequencies where the unknown variation in the differential delay of the multipath is not significant, the filter uses amplitude information; for frequencies where the unknown delay is significant the restoring filter essentially discards amplitude information and relies only on the phase.

The effect of the unknown gain of the multipath is similar to the effect of increasing the noise level. As σ_a increases, the restoring filter again places less emphasis on the amplitude.

C. APPLICATION OF SIGNAL RESTORATION TECHNIQUE TO HF BACKSCATTER SOUNDING

The term "backscatter sounding" refers to forming an image of the radio reflectivity of the ground. This process is completely analogous to taking an aerial photograph of the ground thus forming an image of the optical reflectivity of the ground. Of course, different features of the ground are prominent reflectors at the widely different frequencies involved. While backscatter sounding sometimes refers to a technique which gives the reflectivity as a function of range and radio frequency at a fixed azimuth, in this study it refers only to the reflectivity as a function of range and azimuth at a fixed frequency.

The analysis in the previous sections modeled the lateral

46
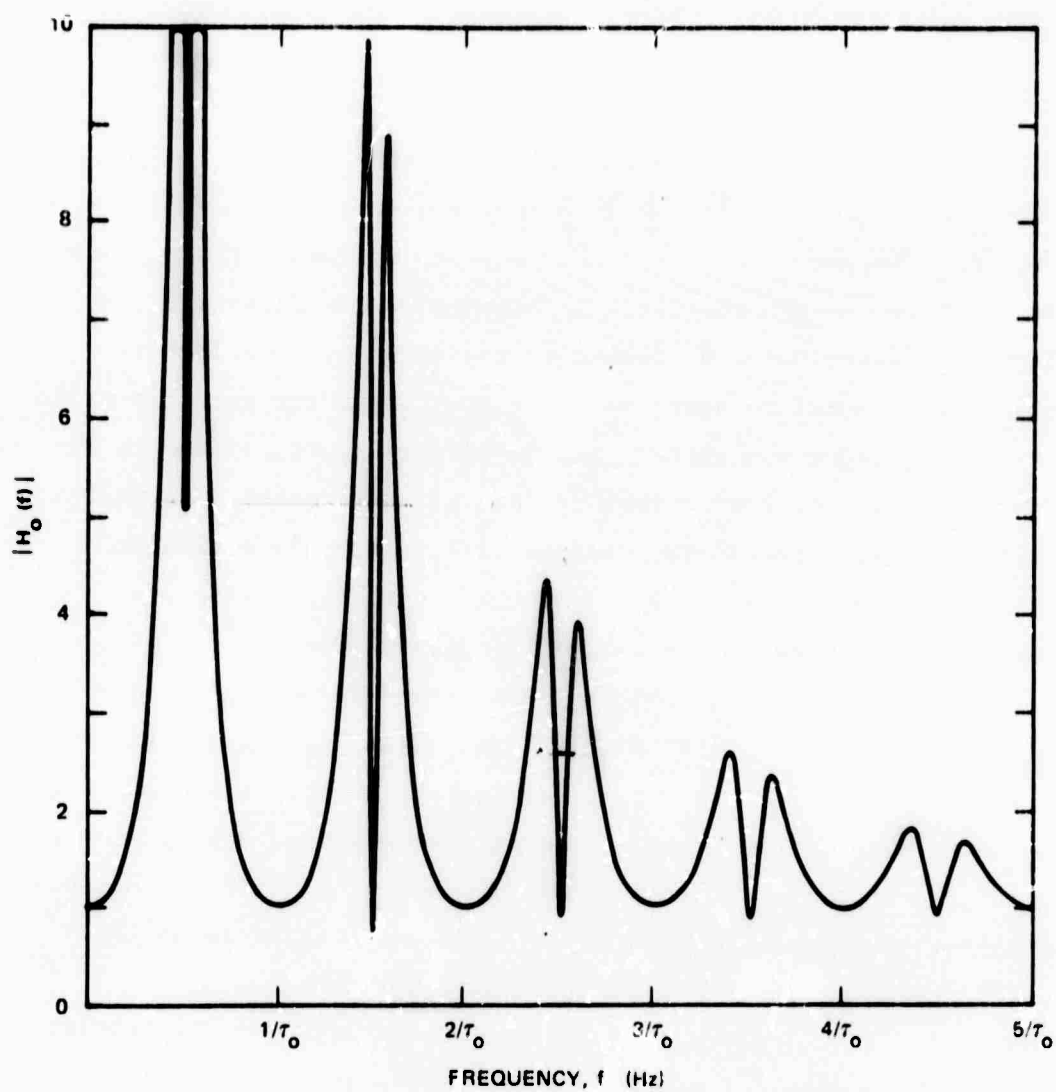
Figure 11   Amplitude of optimum filter transfer function $|H_o(f)|$.

(τ_o is delay difference between two modes.)

47

variation of the amplitude and phase of a signal but not the variation as a function of range. Experimental results relating to the range variation are not available. However because of the geometry of the ray propagation, the correlation distance in range should be greater than the lateral correlation distance.

The application of the previous analysis to backscatter imaging requires interpreting time as representing an angle, and interpreting frequency as an indicator of distance along the array. Improved angular resolution is achieved by use of a reference to calibrate the amplitude and phase vs distance along an array. Scatterers sufficiently close to the reference are optimally processed by use of an inverse filter (assuming a high signal to noise ratio). Scatterers far from the reference have an amplitude and phase which is almost uncorrelated with the reference and therefore the optimum filter uses only phase information. In the intermediate interval the optimum filter uses the amplitude information only partially. The region which can be successfully compensated by the reference is called the isoplanatic region. This region is not necessarily directly related to the three regions previously defined. The practical problem imposed by the optimum filter is that its transfer function depends on the distance of the scatterer from the image. In circuit theory this is equivalent to saying that the impulse response depends on the time of the input. A further complication is that this dependence is a function of the statistics of the amplitude correlations, which may not be precisely known.

A practical solution requires the processing filter to be spatially invariant. Thus a compromise filter which partially satisfies the requirements both close to and far away from the reference is required. In the absence of noise, consider the effect of using an inverse filter over all regions. The amplitude of the inverse filter, $1/A(f)$, can cause an unbounded error in the region where the reference and the scatterer are uncorrelated, and therefore might be useless for signal restoration.

The use of the phase-only filter is near optimal far from the reference, but suboptimal in the first region close to the reference.

48

In this first region the error is in the amplitude $A(x)$. The variance of $A(x)$ is assumed bounded and therefore it is possible for some array beam or image to be formed. Whether one should use the phase-only filter or an approximation to the inverse filter (which would use amplitude information) depends on the degree of the distortion and on how well one wants to do near and far from the reference. If the distortion is not too great, then the phase-only processing may be adequate close to the reference and the best one can do far away. If the distortion is severe, then the phase-only processing may be inadequate everywhere and the best one can do is use the inverse filter to restore signals very close to the reference.

In certain applications there may be physical reasons why the amplitude distortion is not as bad as the phase distortion. For example, in holographic imaging only phase distortion is compensated by the reference beam. Yet the quality of the reconstructed images made from light propagated through atmospheric turbulence is good (see Goodman et al.).[17] Similarly, there may be conditions for which obliquely propagated HF signals are distorted mainly in their phase characteristics rather than in their amplitude characteristics. The problem of the type of restoration filter to use is discussed again in Chapter V when an experimental comparison is made of including or excluding amplitude information.

D. CALCULATION OF THE PERFORMANCE OF AN HF APERTURE WHICH USES A PHASE REFERENCE FOR SIGNAL RESTORATION

1. Case of a Fixed Array

In the previous section it was shown that compensating for phase distortion improves the quality of distorted backscatter images. The amount of the improvement is calculated in this section based on a simple but realistic model of ionospheric irregularities. The model does not include amplitude distortion, and therefore compensation for amplitude effects is not included in the analysis.

Define $\varphi(x, y)$ as the phase difference between a signal propagated from a source at coordinate y in the source plane and the

49

local oscillator of a receiver situated at coordinate x in the receiving-array plane. These relationships have been illustrated in Fig. 1. Let the phase $\psi(x, \Delta y)$ measured at coordinate x in the receiving array plane be defined as

$$\psi(x, \Delta y) = \varphi(x, y_s) - \varphi(x, y_s - \Delta y) \quad , \tag{28}$$

where y_s is the coordinate in the source plane of a scatterer or source which is to be imaged by the array, and $y_s - \Delta y$ is the coordinate in the source plane of a reference signal.

In the previous chapter(see Eq. 6) the array performance was shown to depend on a distortion function given by

$$h_{LT}(x) = \left. \exp\left[-\tfrac{1}{2}D_\varphi(\Delta x)\right] \right|_{\Delta x = x} \quad ,$$

where phase distortion $\varphi(x)$ was the phase difference between the array and the source at coordinate x . In the present case the phase distortion is given by $\psi(x, \Delta y)$, since part of the distortion has been assumed to be cancelled by the reference. Therefore the distortion function used for computing the array performance depends on $\psi(x, \Delta y)$ rather than on $\varphi(x)$. The distortion function for the case of a reference, $h_{ref}(x)$, is therefore defined to be

$$h_{ref}(x) = \left. \exp\left[-\tfrac{1}{2}D_\psi(\Delta x)\right] \right|_{\Delta x = x} \quad , \tag{29}$$

where $D_\psi(\Delta x)$ is the phase-structure function of $\psi(x, \Delta y)$ given by

50

$$D_\psi(\Delta x) = E[|\psi(x, \Delta y) - \psi(x - \Delta x, \Delta y)|^2] \quad . \tag{30}$$

Substituting the definition of $\psi(x, \Delta y)$, Eq. (28), into the expression for $D_\psi(\Delta x)$, Eq. (30), and expanding the squared terms gives

$$D_\psi(\Delta x) = E\left[|\varphi(x, y_s) - \varphi(x, y_s - \Delta y)|^2\right]$$

$$+ E\left[|\varphi(x - \Delta x, y_s) - \varphi(x - \Delta x, y_s - \Delta y)|^2\right]$$

$$-2E\left[\{\varphi(x, y_s) - \varphi(x, y_s - \Delta y)\}\{\varphi(x - \Delta x, y_s) - \varphi(x - \Delta x, y_s - \Delta y)\}\right] \quad .$$

The correlation function of the phases of two signals transmitted from points separated by Δy and received at points separated by Δx is defined as

$$K_\varphi(\Delta x, \Delta y) = E[\varphi(x, y) \varphi(x - \Delta x, y - \Delta y)] \quad . \tag{31}$$

Using this definition, $D_\psi(\Delta x)$ can be rewritten as

$$D_\psi(\Delta x, \Delta y) = 2K_\varphi(0, 0) - 2K_\varphi(0, \Delta y) + 2K_\varphi(0, 0) - 2K_\varphi(0, \Delta y)$$

$$\tag{32}$$

$$- 2K_\varphi(\Delta x, 0) - 2K_\varphi(\Delta x, 0) + 2K_\varphi(\Delta x, -\Delta y) + 2K_\varphi(\Delta x, \Delta y) \quad .$$

The correlation function in Eq. 31 is difficult to evaluate. The difficulty in the analysis occurs if the rays of two signals cross

51

in the ionosphere as illustrated in Fig. 12. If the ionosphere is modeled as a thin screen of irregularities the crossing rays should have highly correlated phases, since the perturbations introduced by the ionosphere should be the same for both rays. If on the other hand the ionosphere is modeled as a thick screen of irregularities, then the phase correlation of the crossing rays is low. In the analysis to follow an assumption is made which corresponds to the thick-screen, low-correlation case, Fig. 12b. This assumption is made because it greatly simplifies the analysis and because it gives a lower bound on the array performance. If the crossing rays of the reference and the source are in fact more correlated than is assumed in the following model, the effect of the ionospheric distortion would be less than that predicted by the equations to be derived. This is so since a high correlation implies that the reference signal is more effective at compensating for the phase distortion than it would be for a low correlation. (See Gaskill[22] for a similar discussion of this approximation.)

The correlation function $K_\varphi(\Delta x, \Delta y)$ defined in Eq. (31) assumed here is even and symmetrical in Δx and Δy and is given by

$$K_\varphi(\Delta x, \Delta y) = \sigma_\varphi^2 \exp\left[-\frac{(\Delta x)^2 + (\Delta y)^2}{\Lambda^2}\right] . \tag{33}$$

Substituting this definition, Eq. (33), into the expression for $D_\psi(\Delta x)$, Eq. (32), it is found that

$$D_\psi(\Delta x) = 4\sigma_\varphi^2 \left\{1 - \exp\left[-\left(\frac{\Delta x}{\Lambda}\right)^2\right]\right\} \left\{1 - \exp\left[-\left(\frac{\Delta y}{\Lambda}\right)^2\right]\right\} . \tag{34}$$

This phase-structure function can be rewritten as
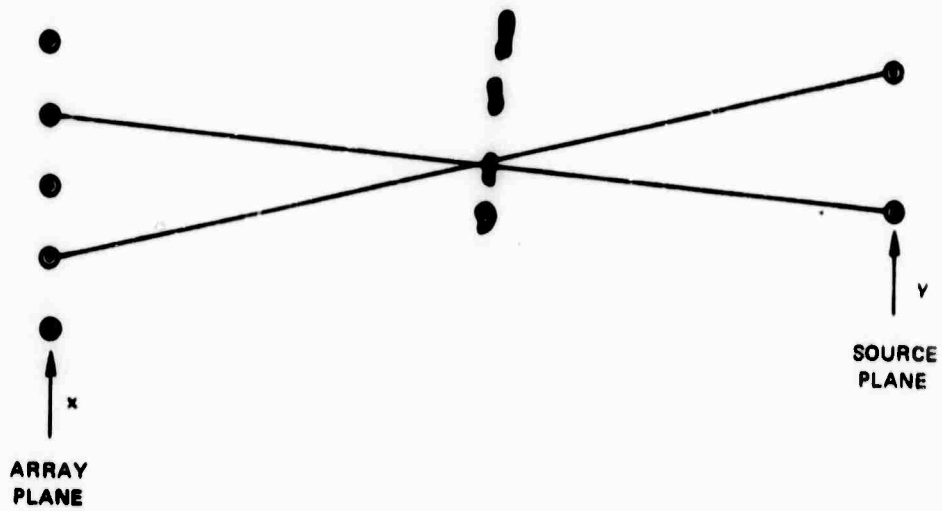
(a) IONOSPHERE MODELED AS A THIN SCREEN OF IRREGULARITIES (High Phase Correlation)

(b) IONOSPHERE MODELED AS A THICK SCREEN OF IRREGULARITIES (Low Phase Correlation)

Figure 12   Rays crossing among ionospheric irregularities.

$$D_{\psi}(\Delta x) = 2\sigma_e^2 \left\{ 1 - \exp\left[-\left(\frac{\Delta x}{\Lambda}\right)^2 \right] \right\} \quad , \tag{35}$$

where

$$\sigma_e^2 = 2\sigma_\varphi^2 \left\{ 1 - \exp\left[-\left(\frac{\Delta y}{\Lambda}\right)^2 \right] \right\} \quad . \tag{36}$$

This form of $D_{\psi}(\Delta x)$ makes it resemble the form of $D_{\varphi}(\Delta x)$ in Eq. 5b, except that an equivalent phase variance σ_e^2 is substituted for the actual phase variance σ_φ^2. In Figs. 8 and 9 it was shown that the performance of an array depends on this phase variance. Equation 36 gives an explicit expression for determining how the performance of the array depends on the separation Δy of the reference from the point to be imaged. As the point to be imaged gets closer to the reference, $\Delta y \longrightarrow 0$, the equivalent phase variance σ_e^2 approaches zero, $\sigma_e^2 \longrightarrow 0$. Thus the problem of determining the improvement in array performance afforded by a phase reference has been reduced to an already solved problem by defining an "equivalent phase variance", σ_e^2.

An approximation valid for large phase variance σ_φ^2 can be made which makes the expression for σ_e^2 easier to interpret. For $\sigma_\varphi^2 > (2\pi)^2$

$$\exp\left[-\left(\frac{\Delta y}{\Lambda}\right)^2 \right] \cong 1 - \left(\frac{\Delta y}{\Lambda}\right)^2 \quad ;$$

therefore σ_e^2, Eq. (36), can be approximated by

$$\sigma_e^2 \cong 2\sigma_\varphi^2 \left(\frac{\Delta y}{\Lambda}\right)^2 \quad . \tag{37}$$

In Chapter II it was shown that the equivalent rms phase should be less than 1/4 cycle to avoid distortion of the mean array power pattern. For the case of large rms phase, the distance Δy between the reference and the point to be imaged should be smaller than

$$\Delta y \leq \frac{2\pi\Lambda}{2\sqrt{2}\sigma_\varphi} \quad . \tag{38}$$

It was noted in Chapter II, Eq. 9b, that the rms angle of arrival σ_{θ_o} was given by

$$\sigma_{\theta_o} = \sqrt{2} \, \frac{\sigma_\varphi}{2\pi} \, \frac{\lambda}{\Lambda} \quad . $$

Using this equation the expression for resolution of Δy can be rewritten

$$\frac{\Delta y}{\lambda} \leq \frac{1}{2\sigma_{\theta_o}} \quad . \tag{39}$$

Thus the size of the region which can be imaged with little distortion, expressed in units of wave lengths, is inversely proportional to the rms angle of arrival. For example, if the rms angle of arrival σ_{θ_o} is 1/4 deg (.004 rad) which has been observed by Sweeney[1], and the wave length is 20 meters, then Δy should be less than 2.5 km.

55

2. Case of a Synthetic Aperture

It will now be shown that the use of a phase reference improves the performance of a synthetic aperture in exactly the same way it operates for the fixed aperture. Namely, the effective phase variance is reduced by an amount which depends on the separation of the reference and the source. The effective correlation distance of the phase is also reduced depending on the temporal time constants and the velocity of the antenna. An equivalent scale size is defined exactly as it was in the analysis of the synthetic aperture without the reference.

The array performance is determined by the phase-structure function of $\psi(x)$ (see Eq. 30) which is given by

$$D_\psi(\Delta x) = E[|\psi(x, \Delta y, t) - \psi(x - \Delta x, \Delta y, t - \Delta t)|^2] , \tag{40}$$

where $\quad \Delta t = \Delta x/v_a$

and $\quad \psi(x, \Delta y, t) = \varphi(x, y_s, t) - \varphi(x, y_s - \Delta y, t) .$

This definition of ψ includes temporal effects and is a straight-forward extension of the definition used in the previous section. Evaluation of this expression gives

$$D_\psi(\Delta x) = 2K_T(0, 0, 0) - 2K_T(0, \Delta y, 0) + 2K_T(\Delta x, 0, \Delta t)$$
$$- K_T(\Delta x, y, \Delta t) - K_T(\Delta x, \Delta y, \Delta t) , \tag{41}$$

where

56

$$K_T(\Delta x, \Delta y, \Delta t) = E[\varphi(x, y, t) \varphi(x - \Delta x, y - \Delta y, t - \Delta t)] \quad . \tag{42}$$

Using the same justification employed in previous sections, the correlation of the phase of two signals transmitted and received at different points at different times is assumed to be

$$K_T(\Delta x, \Delta y, \Delta t) = \sigma_\varphi^2 \exp\left[-\left(\frac{\Delta x}{\Lambda}\right)^2 - \left(\frac{\Delta y}{\Lambda}\right)^2 - \left(\frac{\Delta t}{T}\right)^2 \right] \quad . \tag{43}$$

Substitution of this correlation function into the expression for the phase difference structure function yields

$$D_\psi(\Delta x) = 2\sigma_e^2 \left[1 - e^{-\left(\frac{\Delta x}{\Lambda_e}\right)^2} \right] , \tag{44}$$

where

$$\sigma_e^2 = 2\sigma_\varphi^2 \left[1 - e^{-\left(\frac{\Delta y}{\Lambda}\right)^2} \right] , \tag{45}$$

and

$$\frac{1}{\Lambda_e^2} = \frac{1}{\Lambda^2} + \frac{1}{(v_a T)^2} \quad . \tag{46}$$

Note that the _equivalent_ irregularity scale size Λ_e is relevant only for the array coordinate Δx ; the _actual_ scale size Λ is relevant for the separation of the source and the reference, Δy .

For example, consider the situation where the spatial irregularities are very large, $\Lambda \cong \infty$, but there are temporal variations with correlation time T . In this case the equivalent correlation

57

distance Λ_e is given by $\Lambda_e = v_a T$; however, the equivalent phase variance is zero, $\sigma_e^{\;2} = 0$. Thus the array pattern is not distorted at all because the reference compensates for all of the phase variations.

The conclusion of this analysis of a synthetic aperture using a phase reference is that the results for the equivalent fixed array, without a reference, can be used if the phase variance and irregularity scale size are replaced by an equivalent phase variance and an equivalent scale size. These quantities [see Eqs. (36), (46)] depend on the velocity of the moving antenna used to synthesize the aperture, the time constant of the ionospheric phase variations, and the distance of the source from the reference.

3. Evaluation of the Analytical Results for Typical Ionospheric Parameters

The properties of signals propagated over an oblique ionospheric path are quite variable, depending on the path geometry, solar activity, and time of day. It is instructive, nevertheless, to attempt to evaluate the array performance using parameters of iono-spheric propagation which are reasonable. From this attempted evaluation, one can gain better insight as to what a realistic array perfor-mance might be.

The parameters necessary for the calculation are given in the following table:

Spatial Correlation Distance	Λ	20 km
Temporal Correlation Time	T	60 sec
Rms Phase Distortion	σ_φ	$3(2\pi)$ radians
Airplane Velocity	v_a	100 m/sec
Wave Length	λ	20 m

These parameters give an rms angle of arrival σ_{θ_o} of

58

1/4 deg which is consistent with observations made by Sweeney.[1] These parameters also give an equivalent scale size Λ_e , see Eq. 46, of 6 km. It was shown in Chapter II, Eq. 16, that if the rms phase is greater than one cycle, the aperture length is limited by the following equation in order to avoid significant distortion:

$$L < \frac{2\Lambda}{\sigma_\varphi}$$

For the parameters given above this is about 20 km for fixed aperture and about 6 km for a synthetic aperture.

If compensation for distortion is provided by a reference, then it is important to determine how far from the reference an imaging point may be and have the array power pattern essentially undistorted. In the discussion following Eq. 39 it was shown that for an rms phase angle of arrival, σ_{θ_o} , of 1/4 deg, a point to be imaged should be within 2.5 km of the reference in order to avoid distortion. Thus, for the parameters given above, the region surrounding the reference which could be imaged without distortion is quite small.

BLANK PAGE

IV. DESIGN OF THE HF SYNTHETIC-APERTURE EXPERIMENT

The purpose of the experimental program was to ascertain the
ability of an HF synthetic aperture to achieve high resolution in the
reception of ionospherically propagated signals from a distant source.
An objective of particular interest was to investigate the usefulness
of an HF synthetic aperture in detecting and resolving backscatter
signals. The latter are ionospherically propagated echoes caused by
the reflection from distant areas of HF radar signals beamed to these
areas by an oblique-incidence "sounder" (transmitter) located near the
receiving array.

In much of the experimental program, backscatter echoes from an
area about 2600 km from the synthetic aperture were studied. Localized
enhancement of the backscatter signals at two specific points was
simulated by the use of repeaters located at these points. One of the
repeaters was also used to provide compensating and reference signal
features. The ultimate and most important objective of the experimental
program was to find out to what degree of resolution signals from the
two distant repeaters could be distinguished from each other by the HF
synthetic aperture.

The experimental program was designed to identify key technical
problems, evaluate their significance, suggest solutions, demonstrate
the basic feasibility of the synthetic-aperture technique, and determine
operational and other limitations.

A. BASIC COMPONENTS OF THE EXPERIMENTAL SYSTEM

The principal components of the system used in the experimental
program were:

1. A medium-sized twin-engine aircraft equipped with
    receiving and recording equipment and flying an
    approximately north-south path near Los Banos,
    Calif. (see map, Fig. 13). This aircraft and its
    equipment constituted the HF synthetic aperture.

Preceding page blank

SYNTHETIC-APERTURE
FLIGHT PATH

CW TRANSMITTER
SITE:
BEAR MOUNTAIN

LOS BAÑOS

BACKSCATTER
TRANSMITTER:
LOST HILLS

FORWARD-PROPAGATION
TRANSMITTER SITE AND
BACKSCATTER REPEATER:
BEARDEN, ARKANSAS
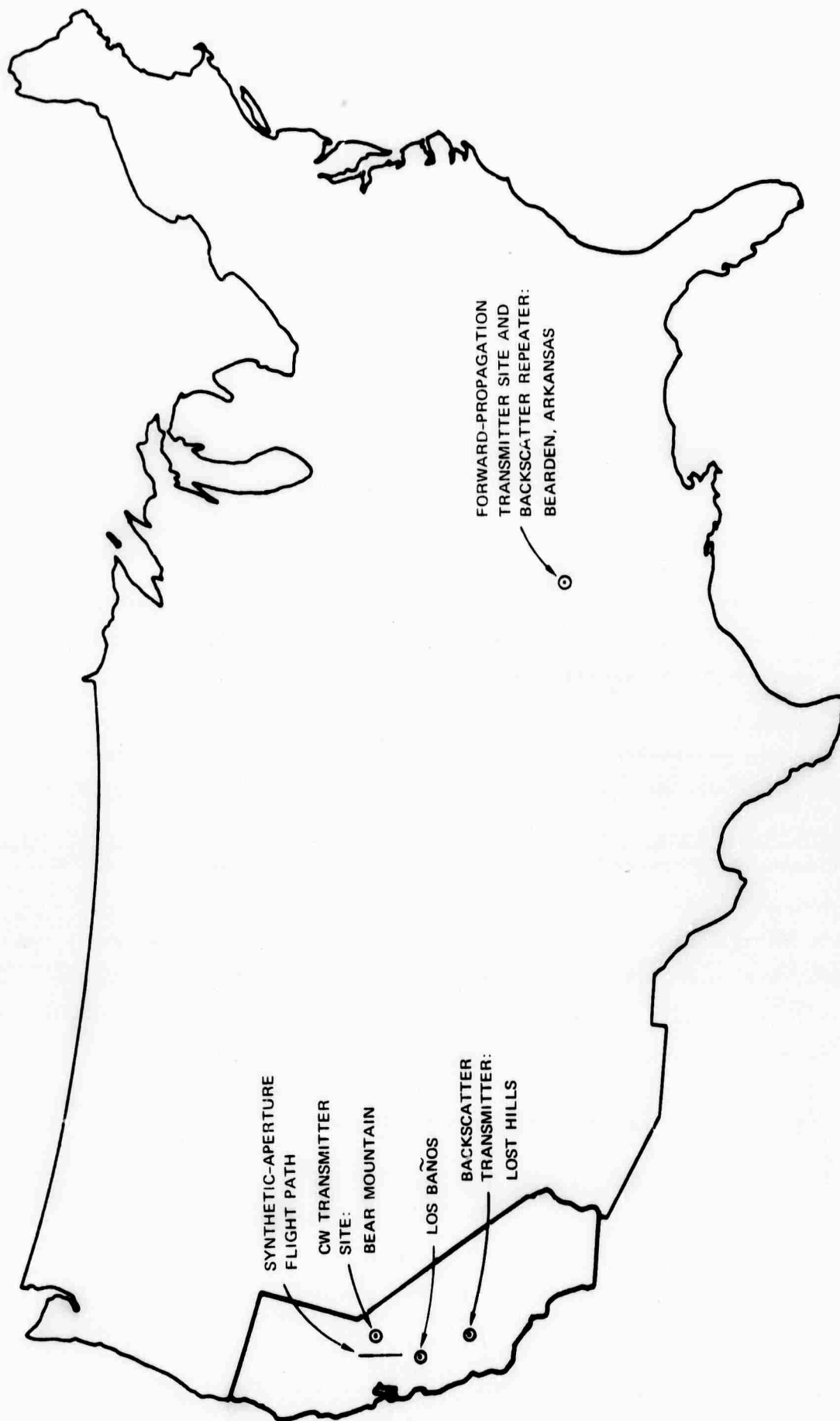
Figure 13   Map indicating locations of transmitter, repeaters, and synthetic-aperture flight path.

2. Two CW transmitters near the flight path which provided airplane tracking signals.

3. A CW transmitting source at Bearden, Ark., approximately 2600 km from Los Banos for use in the "forward-propagation" experiment.

4. Two repeaters (one fixed, one portable) at Bearden.

5. A high-power, narrow-beam transmitter at Lost Hills, for use as an "oblique-incidence ionospheric sounder" in the backscatter experiments.

6. A ground-based digital computing facility used for off-line signal processing.

These system components were utilized in the experimental program now to be described.

B. PRINCIPAL FEATURES OF THE EXPERIMENTAL PROGRAM

The essential steps in the experimental program were:

1. Verification of airplane tracking subsystem performance.

2. Measurement of beam width achievable with the synthetic aperture when it was receiving a CW signal transmitted from Bearden (the CW forward-propagation experiment). In this test compensation was applied for deviations of the airplane from a linear flight path by the use of the airplane tracking data.

3. Demonstration of feasibility of obtaining two-dimensional backscatter data (range vs cross range) without compensating for ionospheric distortion or deviations of the airplane from a linear flight path.

4. Investigation of the use of an HF repeater at Bearden to provide a reference signal in compensating for airplane flight path deviations and ionospheric distortion, for the purpose of obtaining extremely high azimuthal resolution in backscatter mapping.

C. SYSTEM DESIGN

A 100 km aperture was synthesized near Los Banos in the San Joaquin Valley of California (see map, Fig. 14). The aperture used a DC-3

63
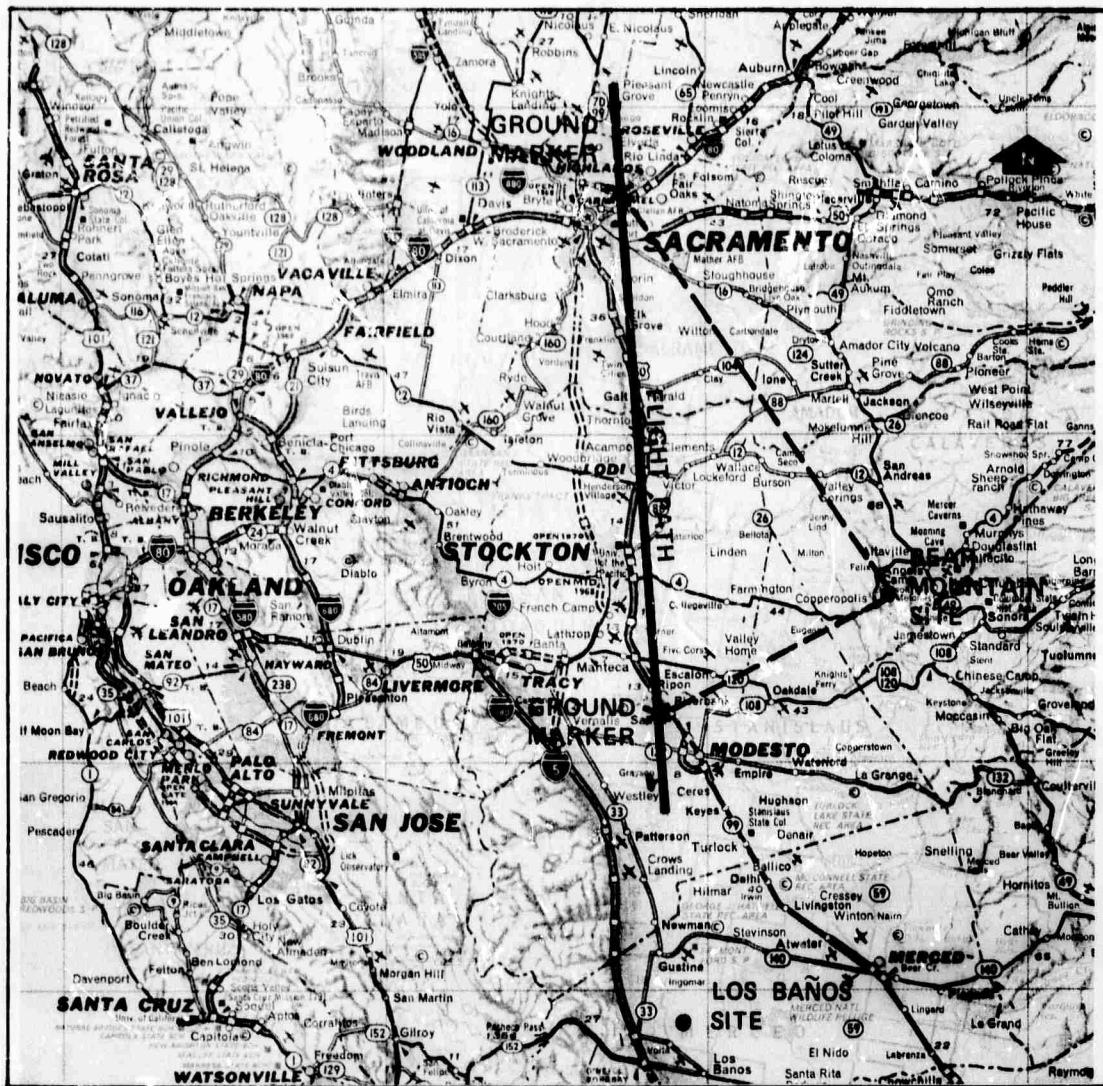
Figure 14   Detail map showing flight path in relation to Los Baños and to location of CW tracking transmitters.

64

aircraft which flew at approximately 180 mph (80 m/sec) for about 20 minutes per flight. The airplane was equipped with a horizontal and a vertical tubular aluminum antenna. A complete swept-frequency CW (SFCW) receiving system plus an analog recorder were installed in the craft. The signal was a linear FM sweep, centered near 20 MHz. The sweep was repeated every second, covering a 600 kHz band width at the rate of 1.0 MHz/sec. This sweep provides delay resolution of about 3 μsec. The flight geometry and signal design resulted in a potential range and cross-range resolution of about 500 m in the backscatter observation area and guaranteed freedom from array grating lobes (multiple side lobes) within the area illuminated by the backscatter sounding transmitter. The latter was located at Lost Hills, Calif., at a distance of approximately 200 km south cf the synthetic receiving aperture. This equipment can transmit a full 30 kW in a 4 deg beam width, using the SFCW signal described above. A detailed description of the equipment components is given in Appendix A.

Compensation for ionospheric and aircraft-motion effects was provided by measurements made on a signal returned from the fixed repeater in Bearden. The repeater is a receiver and transmitter combination with separate antennas and is used to rebroadcast signals in the frequency band of interest. The amplitude and phase of this strong signal were used in this experiment to compensate for distortion of the backscatter signals.

In order to separate the distorting effects of the ionosphere from those caused by aircraft motion, it is necessary to know the airplane flight path with high accuracy. To meet this requirement two CW transmitters were located on the ground within line of sight of the flight path; their signals were received and recorded on the plane. (See signal diagram, Fig. 15.) In addition, a precision differential aneroid altimeter was mounted in the plane and its output recorded. An aerial camera mounted on the aircraft provided aerial photographs from which the aircraft position coordinates were determined by photogrammetric reduction at the beginning and end of each flight.

Use was made of the ionospheric sounding capability of the Stanford

65

FLIGHT PATH

DOPPLER
TRANSMISSION (CW)

BACKSCATTER
SIGNAL

DOPPLER
TRANSMISSION
(CW)

CALIBRATION
SIGNAL

LOS BAÑOS
RECEIVER AND
DOPPLER TRANSMITTER
SITE

BACKSCATTER
SIGNAL

SFCW TRANSMISSION

LOST HILLS
TRANSMITTER
SITE
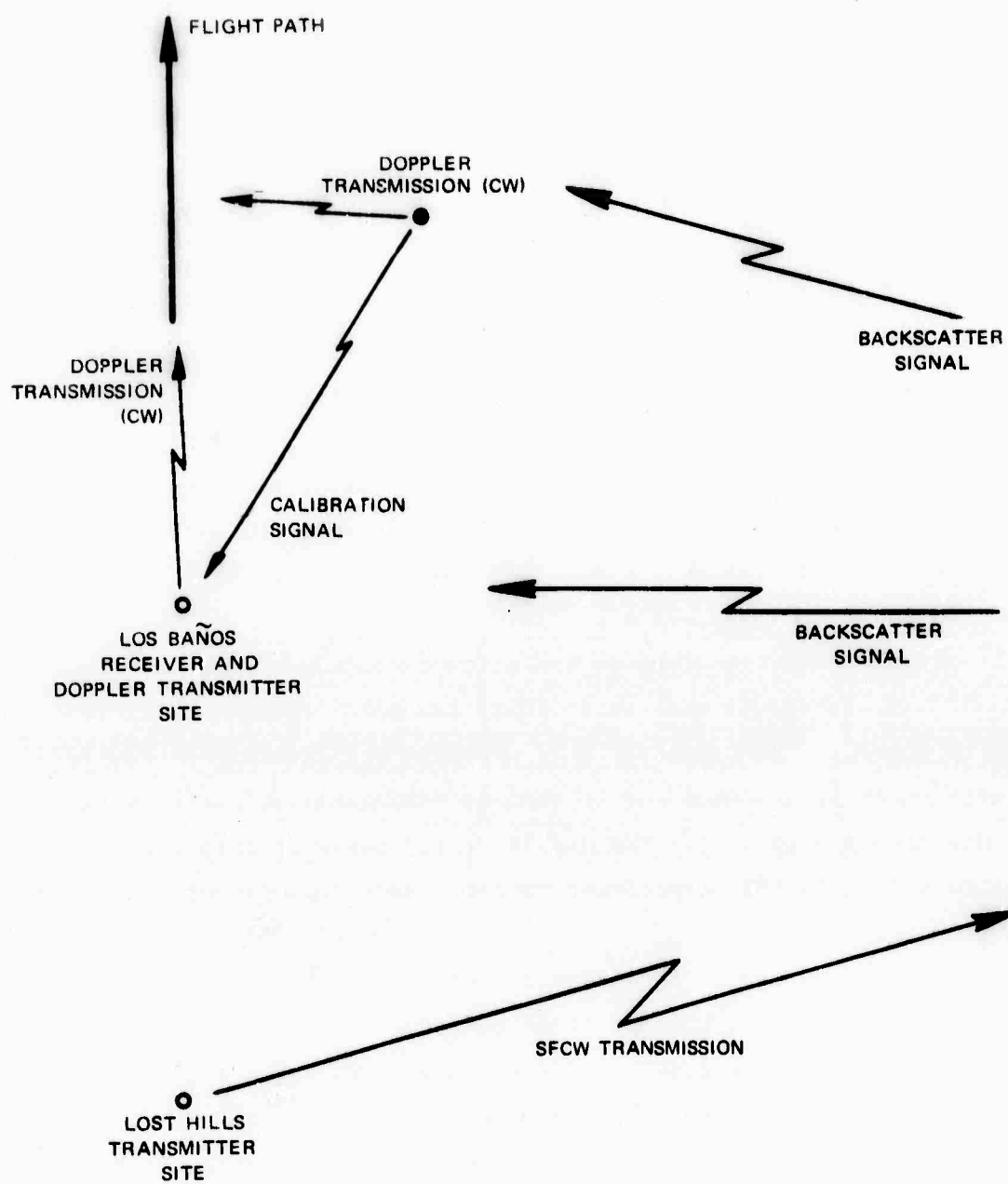
Figure 15   Diagram of signals for synthetic-aperture experiment.

66

Radioscience Laboratory, whose equipment includes the SFCW generator and repeaters in Bearden, Arkansas, plus a wide-aperture linear receiving array and processing equipment at Los Banos. Thus it was natural to make Los Banos the control center for the operational aspect of the experiment.

As already noted, the forward-propagation experiment used CW signals transmitted from Bearden. The operating frequency of the CW signal had to be selected to make sure that only a single ionospheric propagating mode was used. This mode was the one-hop lower ray of the F layer. Compensation for airplane motion was essential to the forward-propagation experiment and was provided by the method already described. The CW measurements were made independently of the backscatter measurements, although much of the equipment was the same.

D. SYSTEM PARAMETERS

1. Backscatter Experiment

The backscatter system parameters were determined from value tradeoffs among considerations of achieving a small cross range resolution cell (defined as range times azimuth), reasonable aircraft velocities, and processor complexity. A range resolution of 2 or 3 μsec can be achieved reasonably often without dispersion compensation. An aircraft velocity of 180 miles/hr seemed reasonable. The ground resolution cell was therefore established to be about 500 m in range and 500 m in azimuth at a range of 2600 km. A square resolution cell appeared appropriate for the purpose of mapping, since increasing resolution in only one dimension does not seem necessarily to improve the interpretability of the map. It should be possible to extend the resolution of the system by including some dispersion compensation and using a faster aircraft and longer flight paths. However, the 500 m X 500 m resolution is an improvement of more than an order of magnitude as compared with that achievable in the present state of the art, and appears to be good enough to obtain usable ground maps and ionospheric data.

A range resolution of 500 m corresponds to a time-delay resolution of about 3 μsec. This in turn requires at least a 0.3 MHz

67

band width. The azimuthal resolution of 500 m (ΔA) corresponds to a flight path of about $L = \frac{\lambda R}{\Delta A} = 100$ km for $\lambda = 15$ m , R = 2600 km ; or an angular resolution of 1.5×10^{-4} radians for a half minute of arc. An improvement in angular resolution by a factor of two could be achieved by installing the backscatter transmitter in the airplane; however this would greatly complicate the design.

With the system band width determined at about 0.5 MHz and the synthetic aperture length determined at 100 km ($\cong$ 60 miles), the next issue to consider was the type of pulses to be used, and their period. SFCW was chosen for good range resolution and high average signal energy. The pulse repetition frequency (PRF) and the duty cycle of the pulses are determined by three factors:

1. The sweep rate.
2. The energy desired per pulse.
3. The spacing of the array grating lobes.

The array grating lobes are secondary lobes due to spatial aliasing which occur when the elements of an array are spaced by more than a fourth of a wave length. For the experimental system, as much energy as possible was desired, and the grating lobes should be spaced by at least 10 deg, since the available transmitting antenna had a 4 deg beam width. This result requires about 1000 pulses for the synthetic array (equivalent to 1000 array elements in a stationary array). If the aircraft velocity is 180 mph and the signal length is one-half second, the sweep rate required is 1 MHz/sec. The nominal parameters of the system are summarized in Table 1.

Another important parameter of the system is the degree of phase coherence required. The timing and frequency standards at the transmitting site and in the aircraft must be synchronized, and all oscillators must be phase-locked to these standards.

The basic requirement for the frequency standard is that its phase should drift by only an insignificant amount in the 20 minutes it takes the aircraft to fly the aperture. The exact meaning of

TABLE 1

PARAMETERS OF BACKSCATTER EXPERIMENT

Aperture length	80 km
Approximate wave length λ	15 m (center frequency 20 MHz)
Pulse length	0.5 sec
PRF	1 pps
Signal coding	SFCW
Band width	0.5 MHz
Range resolution	3 μsec ($\cong$ 500 m)
Azimuthal resolution	1.5×10^{-4} radian $\cong$ 0.5 minute of arc
Lateral resolution in far field (2600 km)	500 m
Grating-lobe spacing	$\pm$ 10 deg
Sweep rate	1 MHz/sec
Airplane velocity	80 m/sec
Flight-path duration	17 min (1000 sec)
Transmitted power	30 kW
Transmitted beam width	4 deg .

69

"insignificant" depends on the nature of the phase drift. No signal distortion results if the phase drift is linear; if the drift is a quadratic, it should be less than one radian. If the drift is periodic or completely random, a more careful analysis is required. Long-term stability of a cesium-beam frequency standard is specified to be a drift in frequency of less than one part in 10^{11}. The short-term drift of such a standard, measured over 1000 seconds, is specified to be less than 2×10^{-12}, which at 20 MHz is about 14 deg. The short-term stability is therefore sufficient for the synthetic-aperture experiment. However, it is to be noted that a less stable standard would not necessarily be sufficient.

The dynamic range of the entire system is quite high because of the two-dimensional Fourier-transform processing described in Section F. The conversion from demodulated SFCW to range information (a one-dimensional Fourier transform) is equivalent to passing the signal through a bank of 2 Hz filters. The increase in ratio of signal voltage to noise is equal to the square root of the ratio of the receiver pass-band to the analysis passband. This band width ratio is 6000/2, giving a signal-to-noise ratio increase of better than 30 dB. The formation of a beam by the aperture improves the voltage signal-to-noise ratio by the square root of the number of synthetic elements (or equivalently by the square root of the number of pulses integrated). The design is for a 1000-element array; therefore the improvement is 30 dB. The 40 dB signal-to-noise ratio of the receiver and analog recorder bring the overall system signal-to-noise ratio to 100 dB.

This signal-to-noise ratio is only relevant to the strongest backscatter signal, which is generally that from the fixed repeater. The system dynamic range is much larger than the range of backscatter intensities which one might want to image in a feasibility experiment, and is also much greater than the self noise due to side lobes. The latter arises as follows: Phase errors vs frequency (in the SFCW) introduce range side lobes, while phase errors in the synthetic aperture give angular side lobes. The side lobes cause backscatter returns at different ranges and angles (cross ranges), with the result that they

70

mutually interfere. The effect is similar to that of noise, and has often been called "self noise". (See Evans and Hagfors[29] for a review.) The design goal is to keep the amplitudes of the side lobes 30 dB or more below the peak amplitude of the main lobe. Thus, at the least, large variations in the backscatter intensity should be visible.

2. Forward-Propagation Experiment

The parameters for the CW forward-propagation experiment were established by the parameters of the backscatter experiment. The only new parameter of interest is the stability of the clock at Bearden. It was not expected that apertures longer than 20 km would be synthesized in this portion of the experimental program; therefore, the stability requirement on the standard is not as great as it is for the backscatter experiments. A crystal frequency standard was used which had a specified stability of 10^{-10} for averaging times of 1 sec to 1 hour. Over the 200 sec the airplane requires to fly a 20 km path, the phase error on a 20 MHz signal is about 130 deg. Since most of this error is expected to consist of a drift which does not distort the array beams but only skews them in angle, this phase error was judged acceptable.

E. FLIGHT-PATH ACCURACY AND MEASUREMENT

Unknown deviation from a straight line in the aircraft flight path degrades the performance of the synthetic array. A random error of a radar wave length (15 m) from pulse to pulse would make it essentially impossible to process the data in such a way as to obtain an effective narrow beam width. A sinusoidal flight-path variation causing a phase change of 6 deg (0.25 m) can produce a single "error" side lobe about 26 dB (0.05) down from the level of the main lobe. A random phase error with rms value 6 deg can produce a hash side lobe level about 60 dB down $(0.05/\sqrt{2000})$. Because the structure of the phase variation cannot be specified, it is necessary to set as a design goal the tolerance which guarantees a good main lobe width and side lobe level. Thus a 6 deg tolerance is specified, corresponding to a lateral distance of

71

$\Delta x \simeq \frac{\lambda}{60} = 25$ cm, or a nominal flight-path accuracy of one foot. The height accuracy required is not as severe because the angle of arrival of the ray will be about 10 deg from the horizontal. The height requirement is therefore 1/sin(10 deg) or about 5 ft.

It is not required that the flight path be linear to this accuracy, but rather that the flight path be measured to this accuracy. The phase variations, if known, are removed during the digital processing stage.

Two techniques for measuring the flight path were employed. One makes use of an aerial camera mounted on the aircraft. This camera, providing about 5 ft of resolution in ground track, was used to establish the starting reference for the CW tracking system.

The second system employed an aneroid altimeter and two CW transmitters, one located in line with and the other perpendicular to the flight path as shown in Fig. 14. These signals were received in the aircraft and recorded on analog magnetic tape. The recorded signals were digitized at a later time and processed by a small general-purpose digital computer to obtain the coordinates of the airplane as a function of time. The CW signals were in the HF band above the critical frequency of the ionosphere.

The orientation and altitude of the flight path were determined by several considerations. The altitude had to be set to guarantee a line-of-sight path to Los Banos (a CW tracking station) but not to Lost Hills (in order to suppress the direct SFCW signal from the latter). The compromise arrived at an altitude of 6000 ft. This altitude was also satisfactory for the aerial photography.

The flight-path orientation was set to pass over flat land and in line with Los Banos, so that the CW signal from Los Banos could be used directly to measure ground speed. The path could not be too close to Los Banos because large changes in the strength of the CW signal would then result as the plane flew the path. Nor could the path be too far from Los Banos, because the CW signal would then be too weak because of propagation loss and shielding from the earth.

72

F.   DIGITAL SIGNAL PROCESSING

Digital data processing was used to make a two-dimensional backscatter map from the sequence of demodulated SFCW received signals which were produced by the synthetic-aperture experiments. The recorded signals were bandpass filtered and then sampled at a 5 kHz rate. The samples were converted from analog to digital form (A/D) and were recorded on digital tape using a Sigma 5 computer. 4096 samples were stored in one tape record each second. (904 samples were discarded every second. These correspond to the interval when the transmitter was off.) A total of 1024 records were made, which corresponded to about 17 minutes of data. At an average aircraft velocity of 80 m/sec, these data represented a coherent synthetic aperture about 80 km in length. The details of the signal process are presented in Appendix B.

The data group for each sounding pulse represented an element in the equivalent stationary array. Each demodulated SFCW signal was Fourier-transformed to produce information on amplitude and phase vs delay.

The second part of the computer signal processing took one range bin at a time and combined the data for each synthetic element, i.e., amplitude and phase vs distance, to form a record of amplitude vs angle. The processing was a Fourier transform in most cases. However, a more general form of coherent addition had to be used in some cases and is explained more fully in Appendix B.

Because the aircraft velocity variations were not insignificant, the spacing of the equivalent stationary array elements was not uniform. Aircraft tracking data were available, and have been used in some cases to compensate for the longitudinal variation in the equivalent array-element position. This compensation is a function of the cross range from the reference to the point to be imaged, however, and therefore further complicates the coherent summing operation.

The Fourier-transform processing was implemented on an IBM 360/67 computer and was designed to be as flexible as possible. It is possible to use less than the 1024 equivalent elements available, or to compute a partial backscatter map.

73

The program output was made available in several forms. One form of output was on magnetic tape which can be read by the Sigma 5 computer. Thus the output data are now stored on tape and can be replotted in any format. The principal Sigma 5 display was three-dimensional and was drawn by a computer-controlled plotter.

The digital processing for the CW data from the forward-propagation experiment was much simpler than the processing for the backscatter data. At the A/D conversion process, the amplitude and phase of the CW signal at one-second intervals were measured and recorded on tape. A second program, written for the Sigma 5, was analogous to the beam-forming program for the backscatter; it essentially executes a Fourier transform. Aircraft tracking data were incorporated into the beam-forming program (see Appendix B).

V. <u>RESULTS</u>

In Chapter IV, the principal features of the experimental program were outlined. The results are described below.

A. VERIFICATION OF AIRPLANE TRACKING SUBSYSTEM PERFORMANCE

The airplane tracking subsystem, used in the CW forward-propagation measurements, proved to be quite accurate. On four different flights a comparison was made between the location of the airplane at the ground markers at the ends of the flight path (which are separated by about 60 km) as measured by the radio system, and as measured by the photogrammetry. The flights used for the tracking verification were Flights 2N, 2S, and 3N on 22 April 1.69, and Flight 3S on 26 April. Detailed data are presented in Table 2 at the end of this chapter.

The location errors were found to be 20, 25, 35, and 60 m, respectively, for the above flights. Thus the long-term average error was quite small.

A plot of the lateral deviations of the plane from a straight line that represents a mean-square best fit for position data for the entire flight path is shown in Fig. 16 for Flight 3N made on 22 April 1969. To aid in evaluating the effect on antenna performance, the rms deviation of the position data from straight-line segments is determined. The curve is divided into 32 segments of 32 seconds each, 16 segments of 64 seconds each, and so on to two segments of 512 seconds each. For each of these segments a mean-square best fit straight line is determined. The rms deviation of the curve from the straight line is then measured. The minimum, average, and maximum rms deviations for the group of segments of each length is plotted in Fig. 17. These numbers can be used to determine whether it might be possible to use a certain length time interval in forming a synthetic aperture if compensation for the plane motion were not used. However, it appears that even with a lax requirement such as 0.2 λ for rms variations from a straight line, an aperture of less than 3 km might be the maximum possible at

75
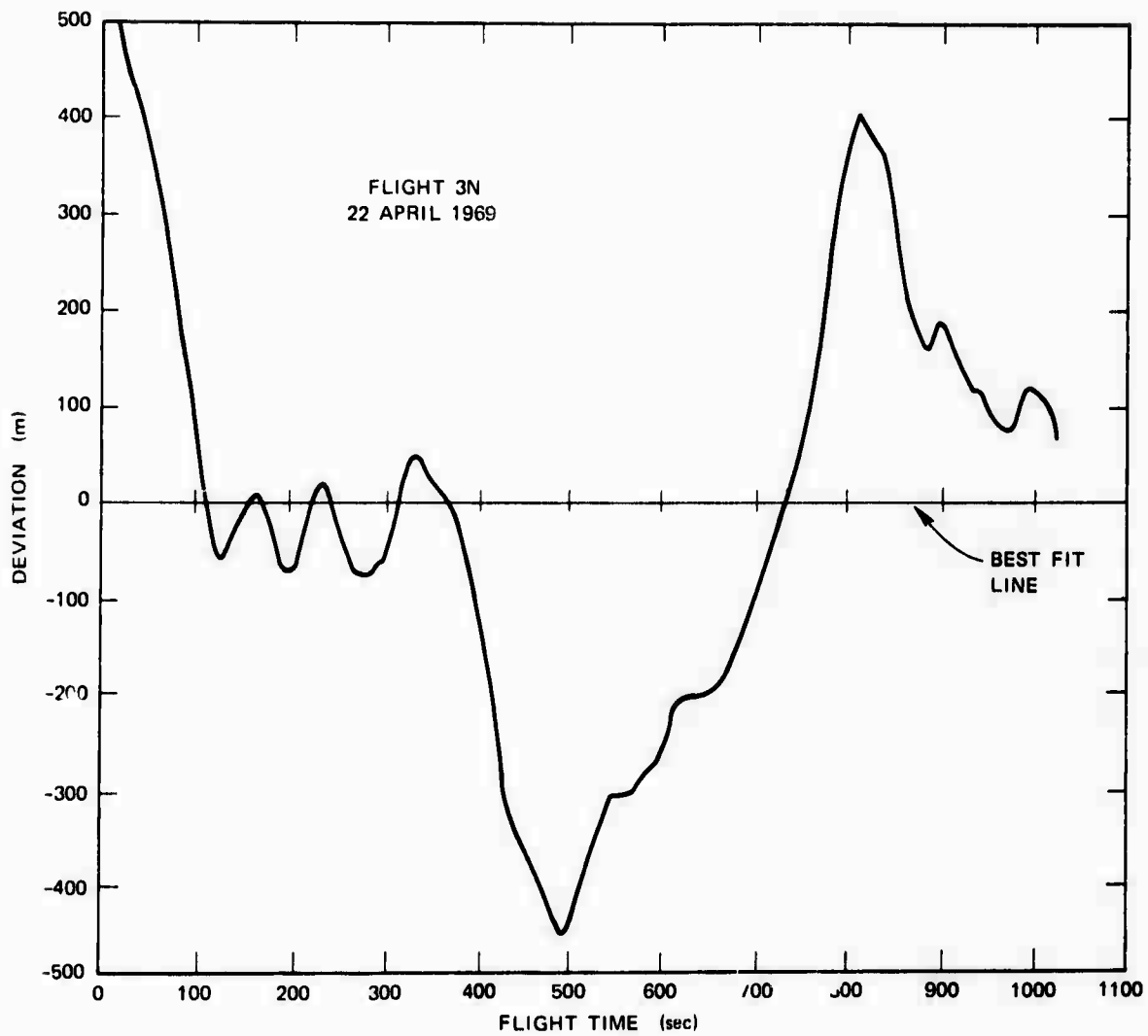
Figure 16   Deviations of flight path from straight line that represents mean—
square best fit for position data taken over entire flight path.
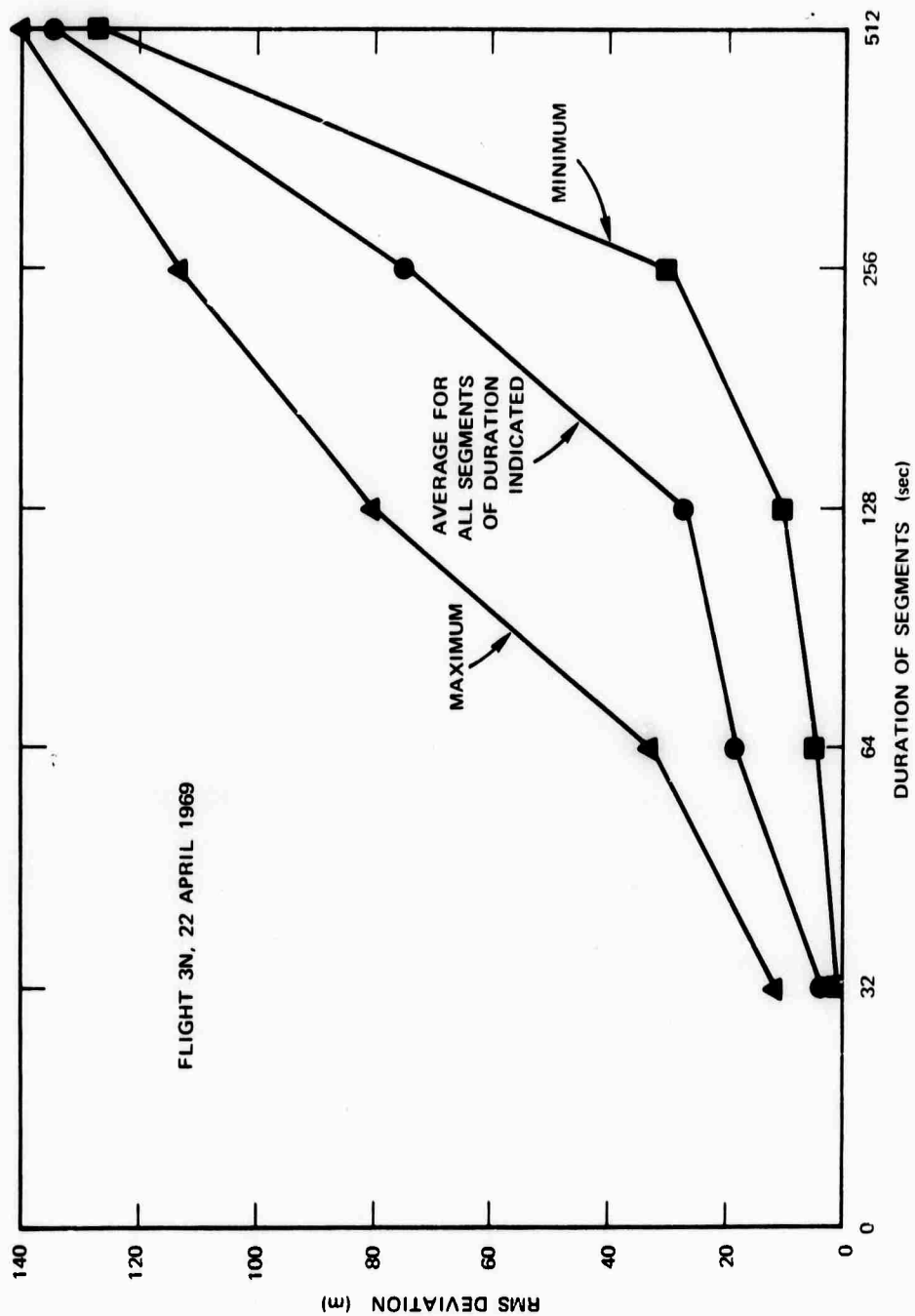
Figure 17   Rms deviations of flight path from a series of straight lines representing mean-square best fits for position data taken over various segments of flight path.   Same flight as Fig 16.

77

$\lambda = 20$ m if compensation for flight-path deviations were not applied.

B. CW FORWARD-PROPAGATION MEASUREMENTS

The frequency spectrum of the CW signals transmitted on a one-hop F-mode (lower ray) from Bearden, Arkansas and received either at Los Banos or in the airplane were calculated by Fourier-transforming the data in time intervals of certain lengths. The frequency spectrum determined from the data received at the fixed Los Banos site give an indication of the temporal variations of the ionosphere. These temporal variations limit the processing time which can be used, or equivalently the frequency resolution which can be obtained. The frequency spectra determined from the data received in the airplane give an indication of the spatial and temporal variations of the ionosphere. The forward motion of the plane produces a synthetic aperture, so that the frequency spectrum is equivalent to an angular spectrum, as was described in Chapter II. Thus the temporal and spatial ionospheric variations limit the angular resolution that can be achieved by the synthetic aperture. The experimental results determine what these limitations are for favorable ionospheric conditions and give an indication of the relative importance of the temporal versus the spatial variations of the ionosphere.

It is essential in these CW measurements that random deviations of the airplane from a straight course be compensated for in order that variations induced in the data by these deviations not be confused with variations induced by ionospheric irregularities.

About 1300 sec of data from run 1S on 24 April 1969 (see Table 2) were analyzed. On this day the geomagnetic activity was quiet. (See Table 3 at end of chapter.) The CW frequency for this run was 23.3 MHz. The data from the horizontal antenna of the airplane and from Los Banos were processed in time intervals of 32, 64, 128, and 256 seconds. In almost all cases the 32 sec frequency spectra were nearly ideal. The typical and best frequency spectra for the signal received at Los Banos for 64, 128, and 256 sec processing intervals are shown in Figs. 18, 19 and 20 respectively. The theoretical 3 dB frequency resolution is

78
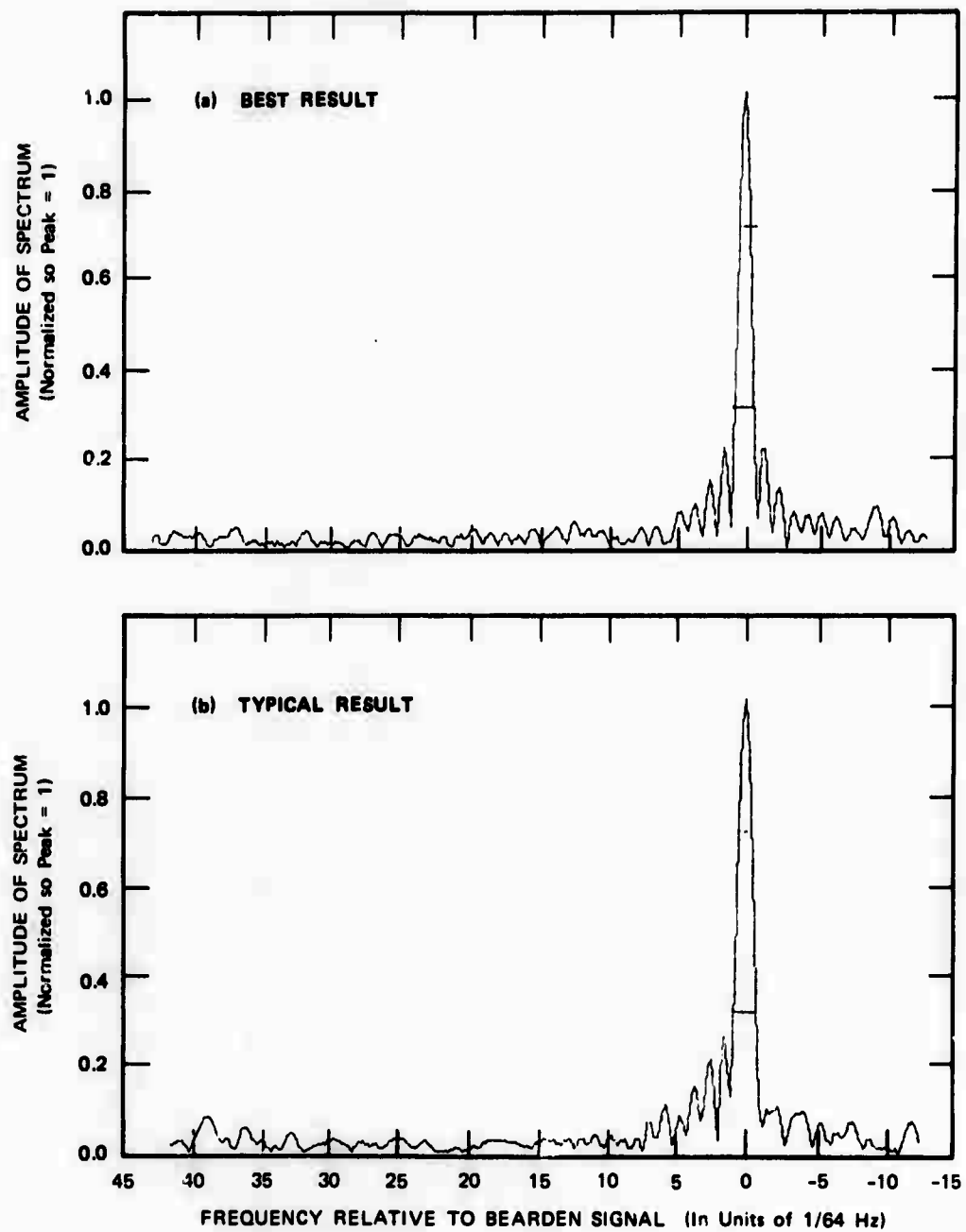
Figure 18   Frequency spectrum of forward-propagated CW signal
received at Los Baños––64 sec processing time.
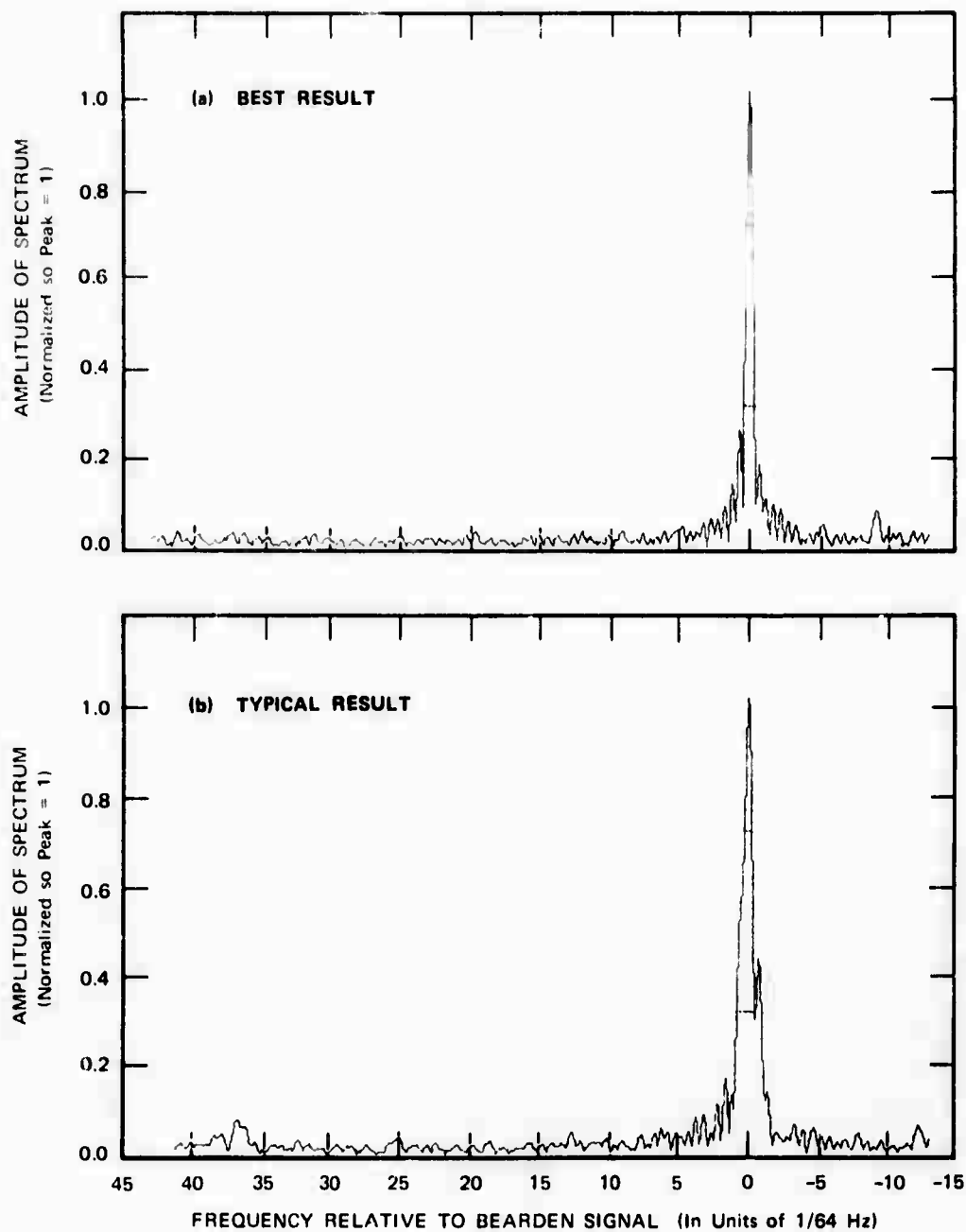
Figure 19   Frequency spectrum of forward-propagated CW signal
received at Los Baños--128 sec processing time.
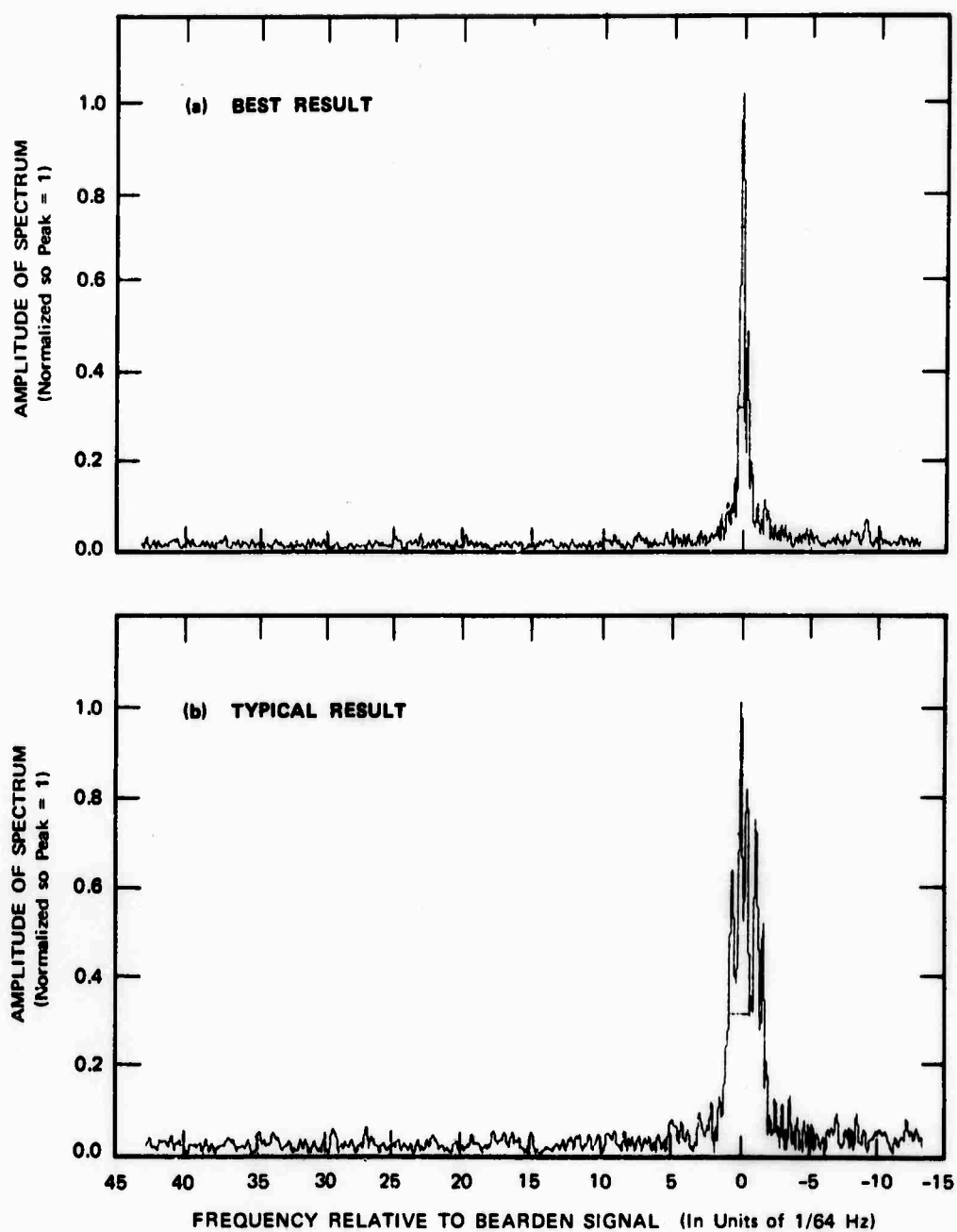
Figure 20   Frequency spectrum of forward-propagated CW signal
received at Los Baños—256 sec processing time.

81

$1/T_f$, where T_f is the processing time. Thus for the 128 sec processing time the 3 dB width of the frequency spectrum is about 0.008 Hz.

The typical and best frequency spectra (or equivalent angular spectra) for the signal received _in the airplane_ for 64 and 128 sec processing intervals are shown in Fig. 21 and 22 respectively. The nominal airplane velocity was 75 m/sec and the wave length was about 14 m. Thus the 128 sec processing time gives an angular resolution of $14/(128 \times 75) = 0.0014$ radians or about 0.08 deg. The equivalent aperture length is 9.6 km, which is longer by a factor of four than the Los Banos phased array.

The results for this data are summarized in the following table.

SUMMARY OF CW RESULTS

	Processing time (sec)		
	64	128	256
Los Banos receiver	20/27	7/13	1/5
Airplane receiver	12/21	2/10	0/5

Numerator = number of cases for which nearly ideal
frequency (angular) resolution was achieved.
Denominator = total number of cases.

Additional measurements were also made for Flights 2S and 2N on 22 April 1969, 1S on 24 April 1969, and for 3S on 26 April 1969. The results for these other flights are essentially the same as those shown in the above table for Flight 1S on 24 April 1969. The airplane speeds for all the above runs were between 56 and 88 m/sec. The results did not appear to depend in a direct way on the airplane speed.

These results are interpreted as indicating that the theoretical ideal beam width of a 5 km aperture was achieved in about 50 per cent

82

page 83 intentionally blank
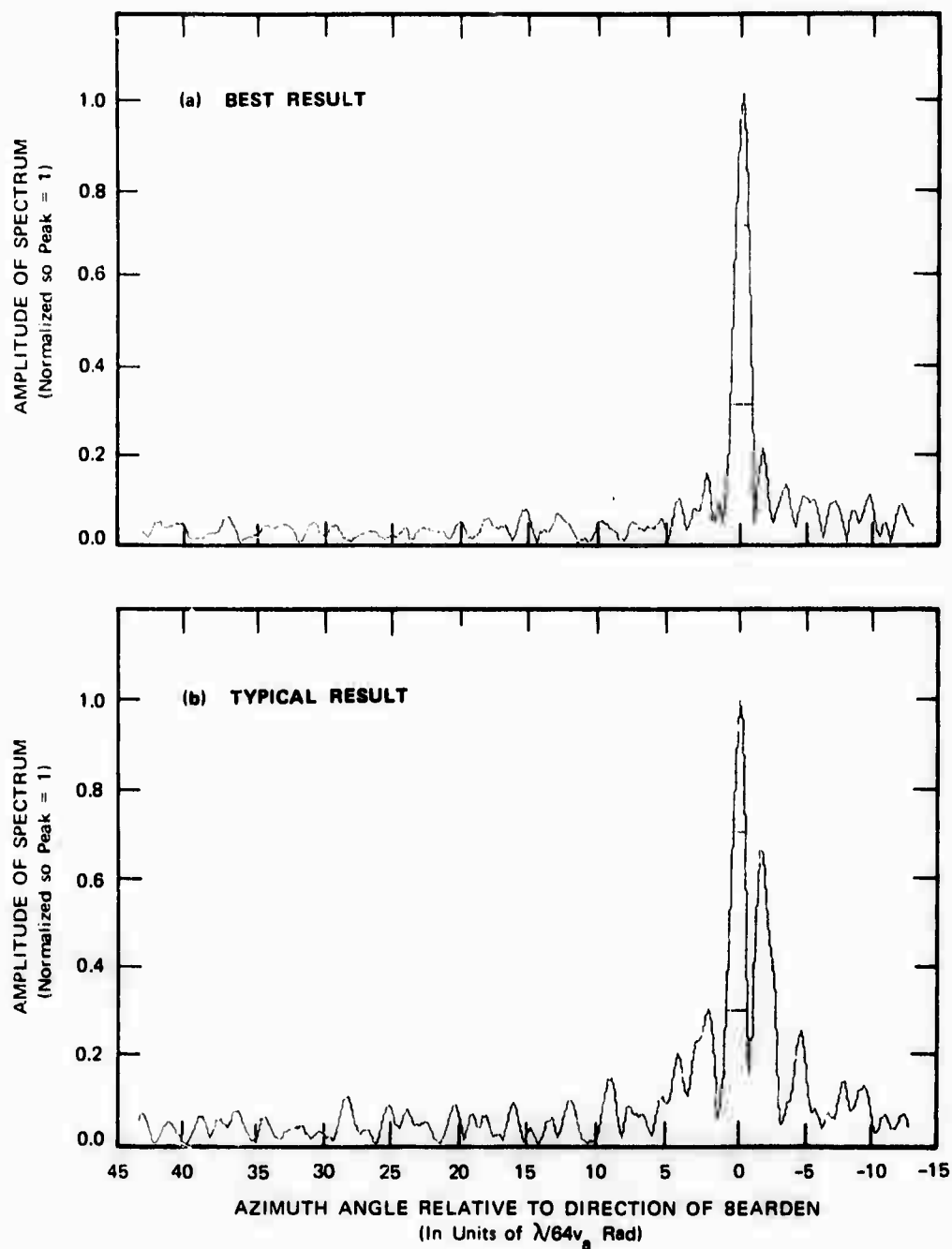
Figure 21   Angular spectrum of forward-propagated CW signal received in airplane--
64 sec processing time, equivalent to 5 km aperture.

The angular spectrum is equivalent to the frequency spectrum.
$1/64$ Hz represents $\lambda/(64\ v_a)$ radians or about 0.16 deg for
the parameters of the test.

84
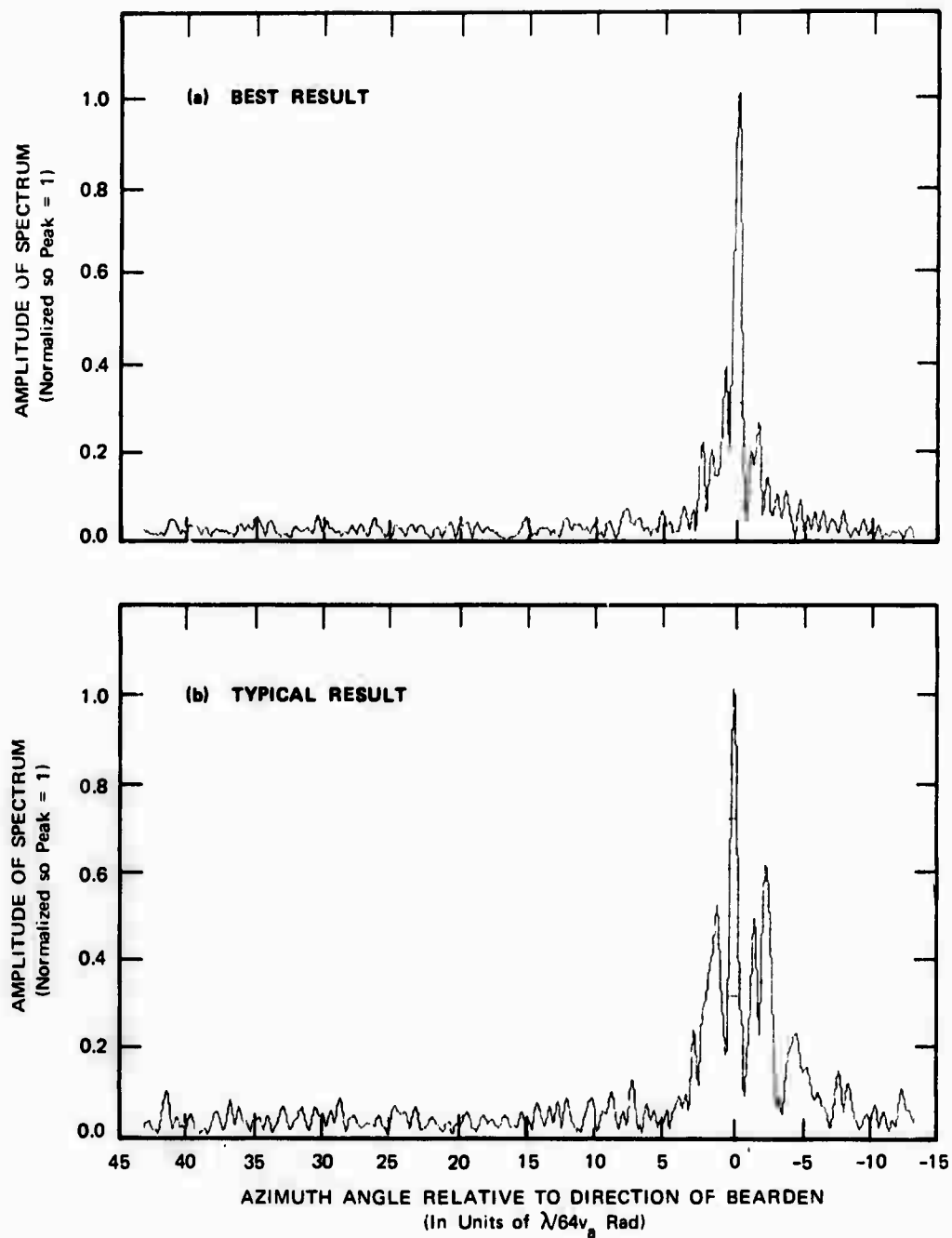
Figure 22   Angular spectrum of forward-propagated CW signal received in airplane--
128 sec processing time, equivalent to 10 km aperture.

of the cases tested, while the theoretical ideal beam width of a 10 km aperture was achieved in about 20 per cent of the cases tested.

Although the frequency spread of the data received in the airplane is not quite as narrow as that received at the fixed site, the time variations of the ionosphere appear to be a significant factor in limiting the beam width achieved by the synthetic aperture. It is unlikely that the aircraft flight-path deviations are the cause of the frequency spread. It was shown by checking the tracking data with the photogrammetry results that the long-term tracking error was exceptionally small. The ability to form an almost ideal frequency spectrum for short intervals (32 sec) most of the time indicates that the short-term tracking error is also small. Clearly the above argument does not constitute a proof that flight-path deviations are accurately measured, since a much more thorough test of the tracking system would be required in order to reach a firm conclusion. The difference between fixed and airborne data is associated with spatial distortion in the received signal caused by irregularities in the ionosphere. These differences are not great and it is not really possible to deduce any characteristics of these irregularities except to establish a lower bound on their effect.

The implications of the above results are far reaching. A synthetic aperture, coping with temporal and spatial variations, was able to achieve the nearly ideal beam width of a 10 km array part of the time. This implies that a fixed array, not having to cope with the temporal ionospheric variations which are significant, should do even better. Thus it is expected that a 10 km fixed array operating under similar favorable one-hop modes would perform nearly ideally a large part of the time.

To illustrate the importance of the airplane tracking (for the DC-3 used) array patterns were computed without the benefit of the tracking data. The 3 km array produced good results about 50 per cent of the time, and the 6 km array about 10 per cent. This inferior result was to be expected from an inspection of the airplane tracking data, which showed significant flight path fluctuations for intervals longer than

86

30 sec. However, even this result is of practical importance, since it indicates that apertures of intermediate size (1 to 3 km) can be synthesized without the benefit of a complicated airplane tracking system. Of course, the length which can be synthesized depends on the flight characteristics of the airplane used.

C. BACKSCATTER MEASUREMENTS MADE WITHOUT COMPENSATION FOR FLIGHT-PATH DEVIATIONS OR IONOSPHERIC VARIATIONS

Backscatter measurements were made by transmitting an SFCW signal once per second from Lost Hills and receiving the signal in the airplane. On the particular run to be discussed here, backscatter from the areas near Bearden, Arkansas (2600 km) was seen as well as an enhancement at a much closer range (1600 km). In addition, a fixed repeater located at Bearden was used to return a large signal as if it were a huge scatterer of HF energy.

As described in Chapter IV, the signal processing is a two-step process. The first step transforms the demodulated SFCW signal into amplitude and phase vs delay for each equivalent synthetic element. The second step then transforms the data at each delay to give amplitude vs azimuth or cross range.

A backscatter image of the Bearden repeater is shown in Fig. 23a. This image was made without compensation for airplane or ionospheric variations. Thirty-two equivalent elements were used, which spanned an aperture of about 2.5 km. The theoretical 3 dB beam width of an aperture of this length at the frequency used is about 0.4 deg, which is approximately what is obtained in this record. The data are from Flight 4S, 26 April 1969, and were made using a sweep rate of 250 kHz/sec and a center frequency of 15.6 MHz. An ionogram taken on the Bearden-Los Banos path on 26 April near the time of the test is shown in Fig. 24, and indicates that at a range of 2600 km there is a complicated signal mode structure at 15.6 MHz. At the shorter range of 1600 km where some backscatter was observed it is believed that only a one-hop F mode existed.

A backscatter record using 64 elements from the same set of data is

87
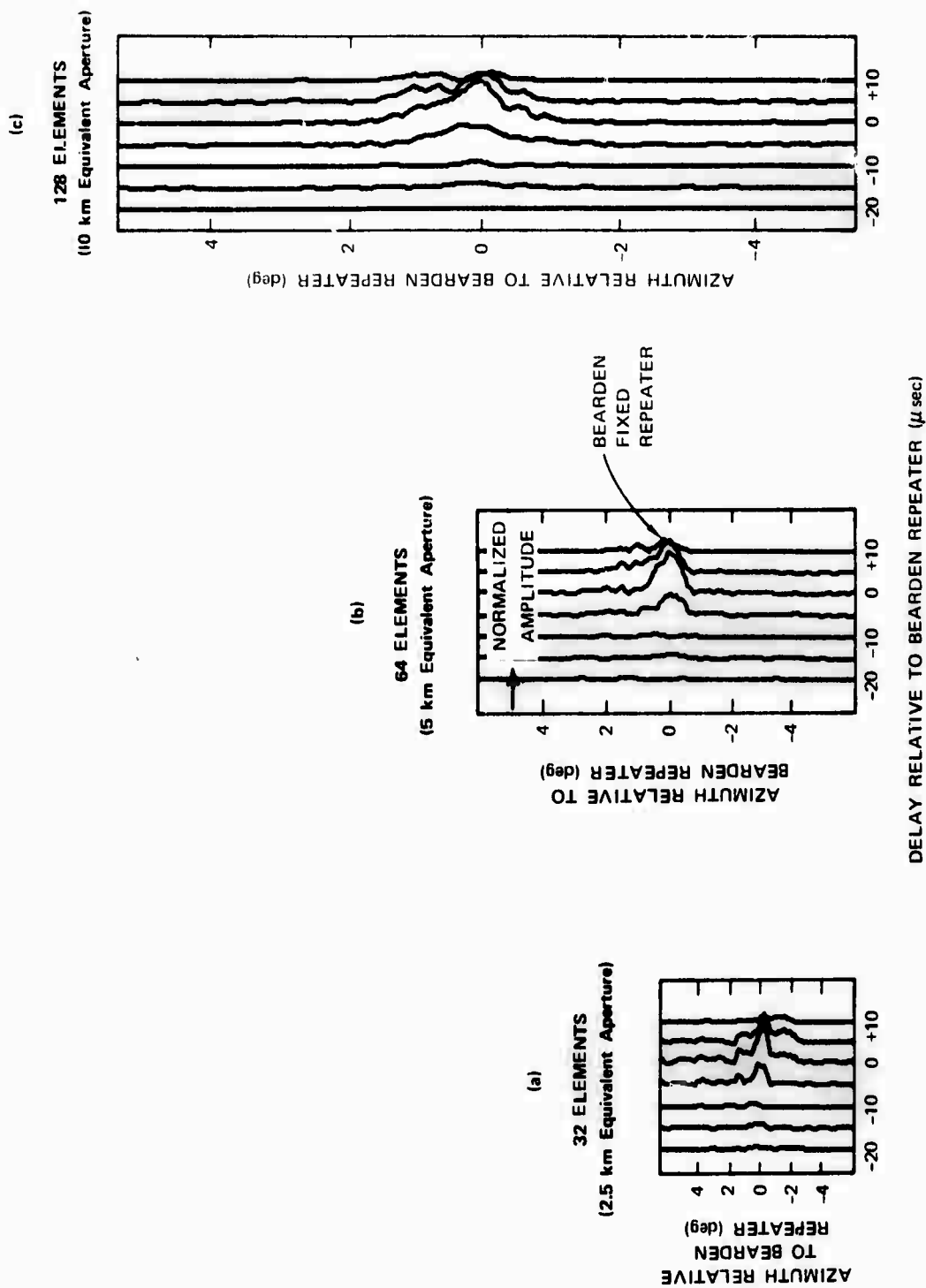
Figure 23 Backscatter map: Normalized amplitude vs delay and azimuth.

No compensation for airplane or ionospheric distortion. Record shows signal from fixed repeater at Bearden, which is at a range of 2600 km from the synthetic aperture.
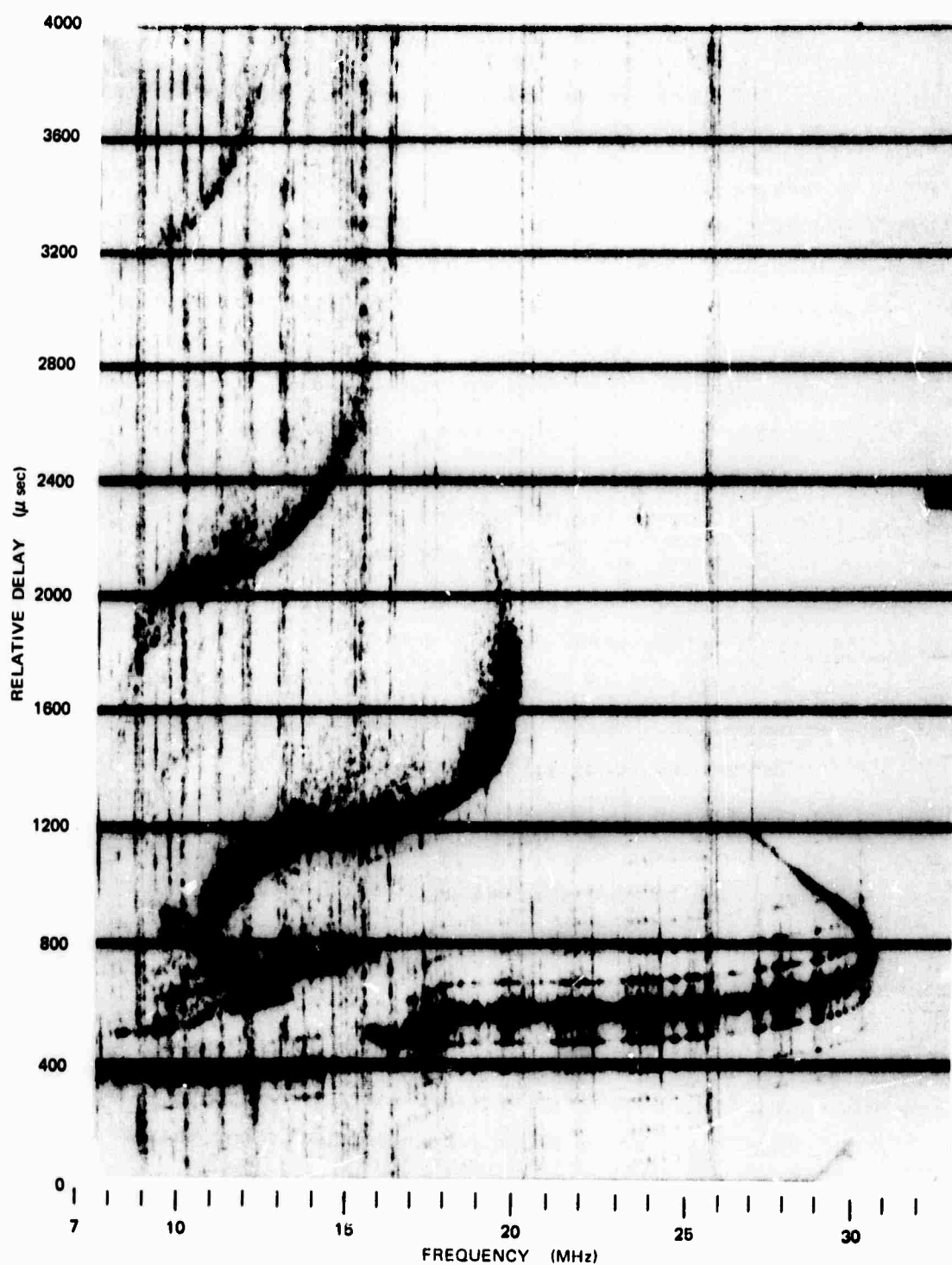
Figure 24   Ionogram, Bearden to Los Baños, 26 April 1969, 22:45 GMT.

89

shown in Fig. 23b. The equivalent aperture is 5 km long, which yields a 0.2 deg theoretical beam width. Figure 23c is again from the same data but using 128 equivalent elements spanning 10 km, which requires more than 2 min of flight time. Note that increasing the aperture did not improve the angular resolution, indicating that either airplane motion or ionospheric irregularities were limiting the performance. Based on the results of the CW experiment described in the last section the airplane deviations are most probably the source of the problem.

Backscatter data at a much closer range (1600 km) were also processed to see if the enhancement observed at that range would be confined in azimuth if imaged by the synthetic aperture. Figure 25 is a record showing the result of the processing when 32 equivalent elements were used and airplane or ionospheric compensation was not employed. (Note: Airplane tracking data were not available on this particular run.) The record in Fig. 25 shows a 3-dimensional display of amplitude squared (i.e., power or intensity) vs delay and azimuth and indicates that the enhancement was confined in azimuth. The third coordinate (squared amplitude) was made easier to read by doubling the number of delay increments. The latter was accomplished by interpolating a new line between each of the original pairs of lines. The effect is similar to that achieved by the averaging inherent in a cathode ray tube (CRT) displays. The averaging by the CRT is due to the finite dot size of the cathode ray beam.

The records presented in this section indicate that during favorable ionospheric conditions a synthetic aperture using a DC-3 airplane to fly a reasonably linear path, and without compensation for any distortion effects, can image backscatter with azimuthal resolution comparable with that achieved by the world's largest HF ground arrays.

D.   BACKSCATTER MEASUREMENTS MADE USING FIXED REPEATER SIGNAL TO COMPENSATE FOR AIRPLANE AND IONOSPHERIC VARIATIONS

In this series of tests the synthetic aperture was focused on backscatter signals from the area surrounding Bearden, Arkansas. Delay (range) resolution was provided by the wide-band SFCW signal.

90
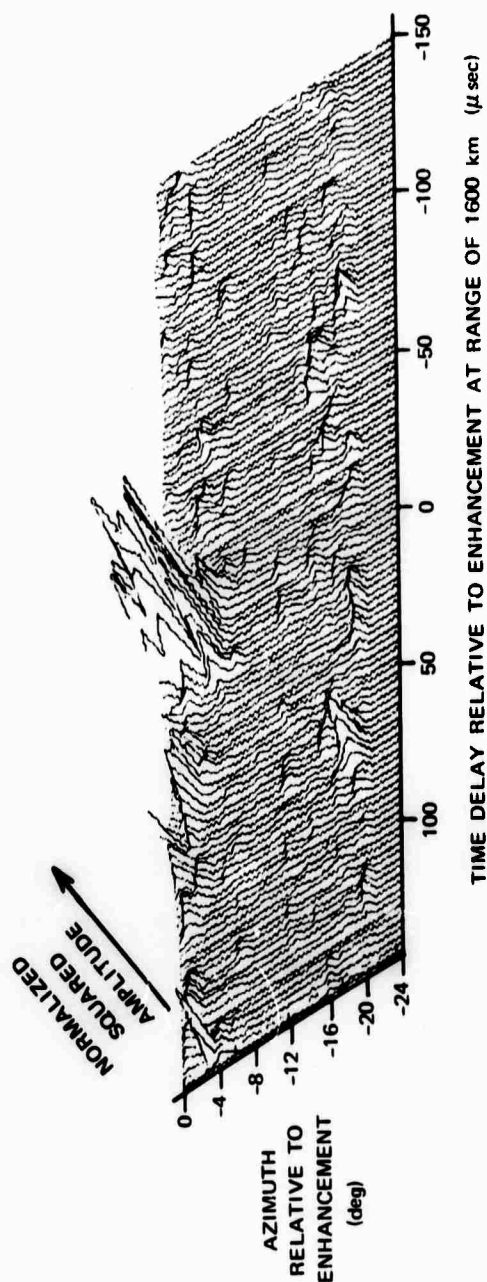
Figure 25 Backscatter map of normalized squared amplitude vs delay and azimuth, showing enhancement at 1600 km.

2.5 km synthetic aperture. No compensation for airplane or ionospheric distortion.

91

1. <u>Use of a Portable Repeater With Low Gain Antenna</u>

Besides the fixed repeater used for airplane flight-path and ionospheric compensation, a second repeater--the portable one described in Chapter III and in Appendix A--was used to simulate a large backscatter return from several locations in the area. Several runs were digitized and at least partially processed to see if the signal from the portable repeater could be seen with the synthetic aperture. For Flight 1N on 25 April 1969, the repeater was about 50 km north of Bearden; but no indication could be found on any of the records at any stage of the processing. Several other runs were processed from different days, with the portable repeater at different locations using its own whip antenna. Again, no indication of the repeater on any of the records was found.

When operated in a special mode, however, the portable repeater was detected at the Los Banos site, thus verifying that the repeater was operating. In this special mode the portable repeater could offset its output signal in frequency. This offset had the effect of isolating the repeater return from the backscatter return. The portable repeater signal could then be detected much more easily without the interference from the backscatter clutter.

In the normal mode of the portable repeater, the average level of the ground backscatter was apparently obscuring the portable repeater return. The signal from the fixed repeater was only about 20 dB above the backscatter measured in the delay domain (i.e., after SFCW processing). The high gain of the Log Periodic Antenna (LPA) used by the fixed repeater had two advantages over the whip used by the portable repeater. The high gain on receiving helped reject other signals. Thus the full 10 W was used by the SFCW signal. Secondly, the high gain on transmit increased the effective radiated power. The LPA was mounted about 100 ft above the ground, which could significantly reduce signal attenuation due to shielding by trees. The ambient noise was not a problem, since it was well below the backscatter level.

The sketch in Fig. 26 shows two locations, denoted Sites 1 and 2, where the portable repeater was situated for the tests to be

92
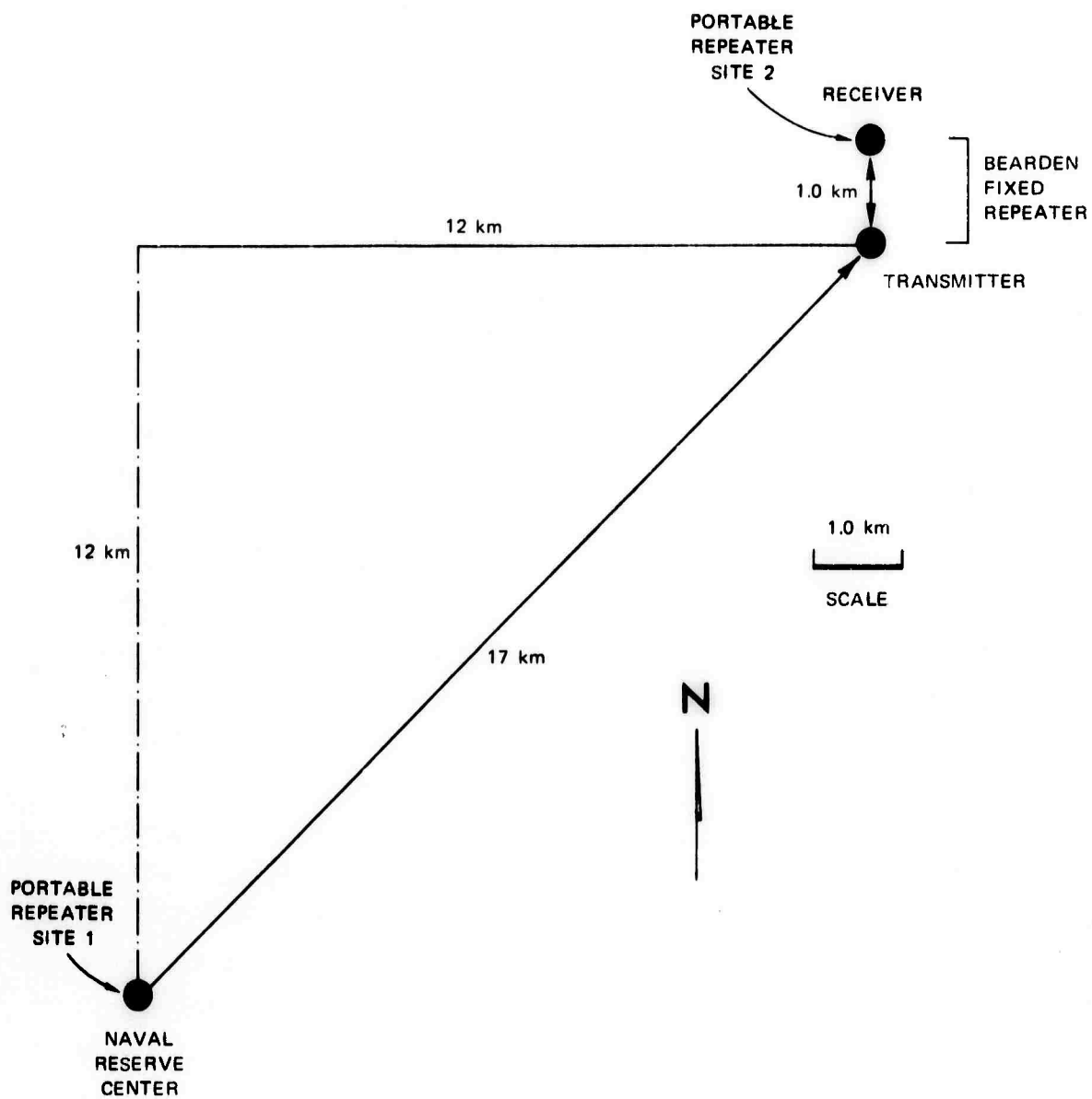
Figure 26   Sketch showing two locations at which portable repeater operated.

described below. Site 1 is at a Naval Reserve Station located at Harrell Field, 17 km southwest of the transmitting site of the fixed repeater. Site 2 is at the location of the receiving antenna of the fixed array, 1 km north of the transmitting antenna. At this location the portable repeater shared a high-gain LPA with the fixed repeater in a manner described in Appendix A.

A strange result occurred for Flight 3N on 26 April 1969, when the portable repeater was operated at Site 1, the Naval Reserve Center. This is seen by observing the amplitude vs delay of signals at a sequence of equivalent elements shown in Fig. 27. This record is the result of the first stage of processing, called delay processing in Appendix B. The amplitudes shown are normalized so the value of the peak of the repeated signal is unity. The pulses appear to have a distortion which tends to spread the signal only on the lower side. This one-sided distortion was never seen on any other records. At Site 1 the portable repeater was closer to the airplane than the fixed repeater, but the 63 μsec internal delay (see Appendix A) of the portable repeater would make it appear farther away than it really is. These two effects tend to offset each other and it is conceivable that the seeming one-sided distortion was, in fact, the signal from the portable repeater. The beam-forming program was run with these data; however, the entire distorted pulse came out at the same azimuth, not separated as it should have been. It is possible that some portion of the system was detuned or that an interaction occurred between the two repeaters causing the one-sided distortion.

2. Use of Portable Repeater With High Gain Antenna

For Flight 3N on 22 April 1969, the portable repeater was at Site 2, the receiver site for the fixed repeater (see Fig. 26). Because the portable repeater shared the high gain LPA located there with the fixed repeater, the returns from each repeater were about equal in strength. Even though both repeaters are at the same range from the airplane, the portable repeater appears farther away because of its internal 63 μsec delay, which compares with a 5 μsec delay in the fixed

94
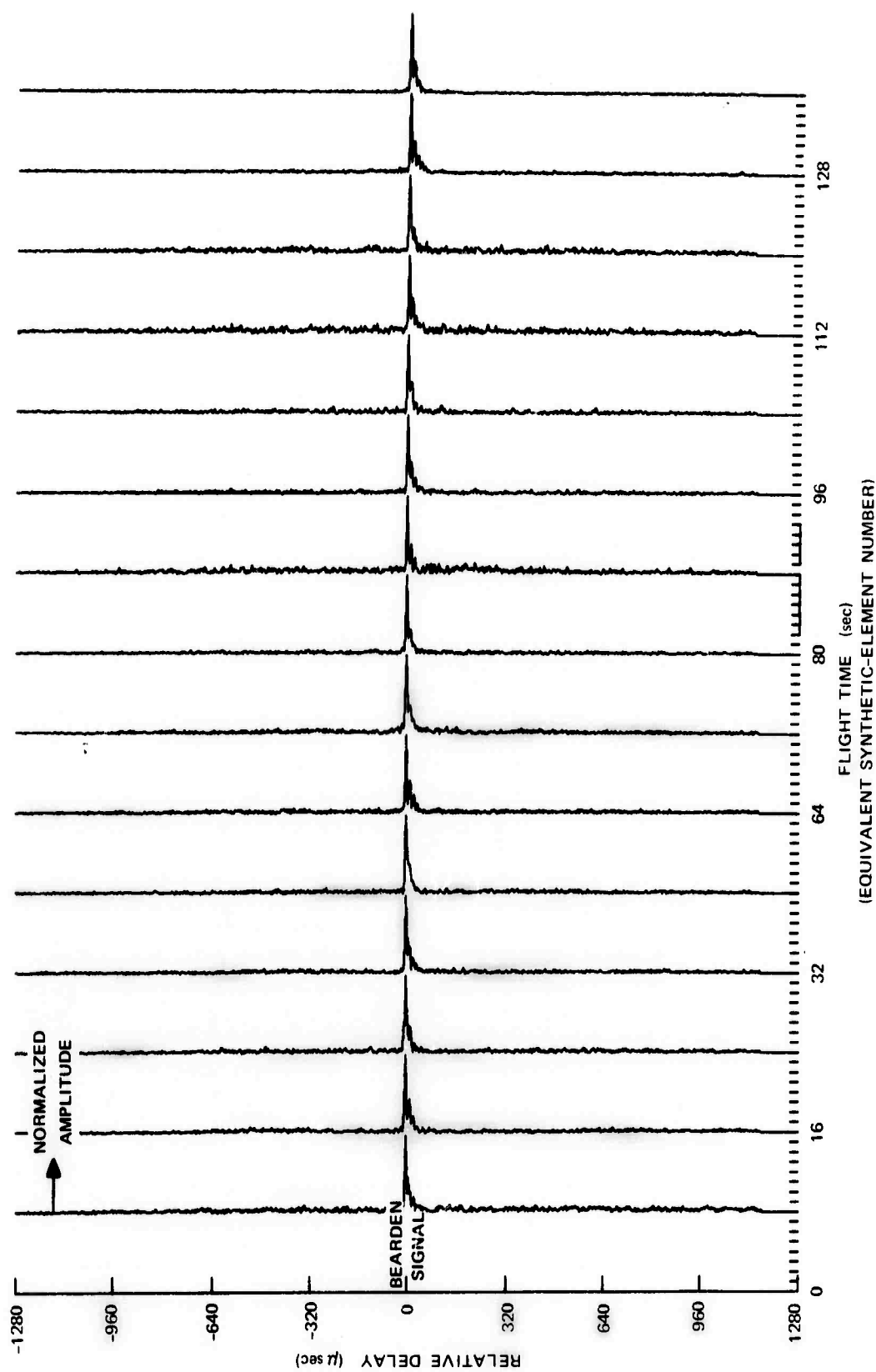
Figure 27   Normalized amplitude vs relative delay for a sequence of equivalent elements of the synthetic aperture (Flight 3N on 26 April 1969).

These data show the fixed repeater signal originating 2600 km to the east. The portable repeater was operating at Site 1 (see Fig. 25); but its signal is not positively identifiable on the record.

repeater. The normalized amplitude vs delay for a sequence of equivalent elements is shown in Fig. 28. The amplitudes are normalized so that the peak of the signal from the fixed repeater (positioned at relative delay = 0) would be unity for each equivalent element.

The data for this record were made with a sweep rate of 1.0 MHz per second and over a band 23.0 to 23.6 MHz. This band width and the fact that 2048 samples (of the 5000 taken every second) were used in the delay processing for each equivalent element gives a theoretical 3 dB delay resolution of about 2.5 μsec. This delay resolution is equivalent to a theoretical 3 dB range resolution of about 375 meters. The actual range resolution, which is poorer due to side lobe weighting and dispersion, is about 500 meters.

One feature of Fig. 28 deserves special attention. The level of the backscatter appears to vary from second to second. Because the amplitude of the repeater is normalized to unity for each second, the observed level variation is really that of the repeater. The backscatter signal level is an average over a wide interval of range and azimuth, and should therefore be much less variable than a signal originating from a single point.

An ionogram taken on the Bearden-Los Banos path is shown in Fig. 29 and indicates that at 23 MHz a one hop mode existed from Los Banos to Bearden. As indicated in Table 3, the geomagnetic activity on 26 April 1969 was quiet.

3. Backscatter Data Taken With 12 km Synthetic Aperture

The same data that were used for Fig. 28, taken on Flight 3N on 22 April 1969, were then processed by the beam-forming program to make a backscatter image of delay vs azimuth or cross range. The term cross range refers to a coordinate perpendicular to the range or delay coordinate and is approximately equal to the angle coordinate in radians times the range. The data in the following description was made using 128 equivalent elements spanning about 12 km. At a center frequency of 23 MHz this aperture gives an angular resolution of 0.084 deg, or a cross-range resolution (at 2600 km) of about (0.084 $\times$ 2,600,000/60) = 2800 m.

96
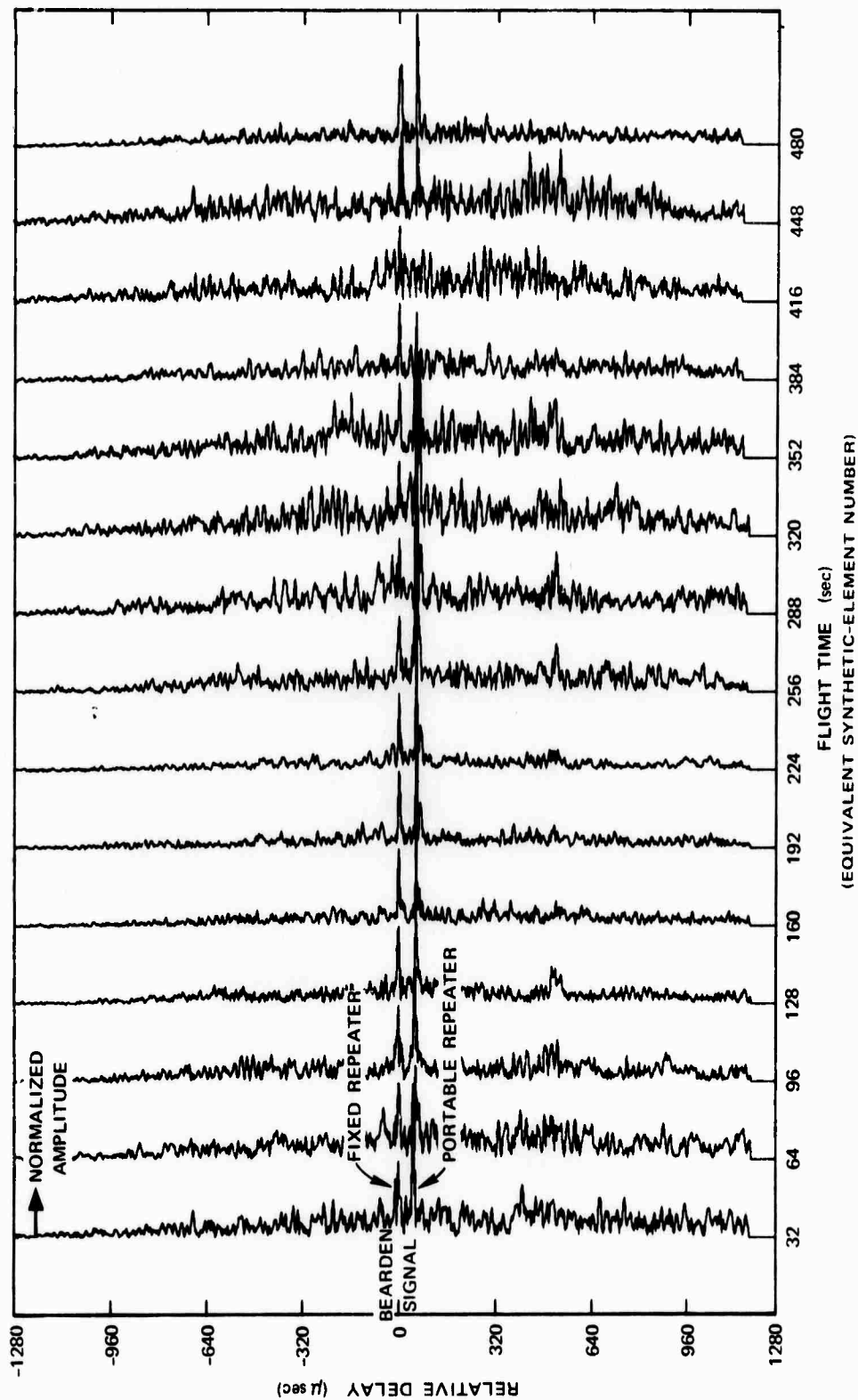
Figure 28   Normalized amplitude vs relative delay for sequence of equivalent elements of the synthetic aperture (Flight 3N on 22 April 1969).

These data show signals from the fixed repeater (at 0 relative delay) and from the portable repeater. The latter was at Site 2, at the same range as the fixed repeater. The apparent delay difference of 58 μ sec is caused by a difference in internal delays of the two repeaters.

97
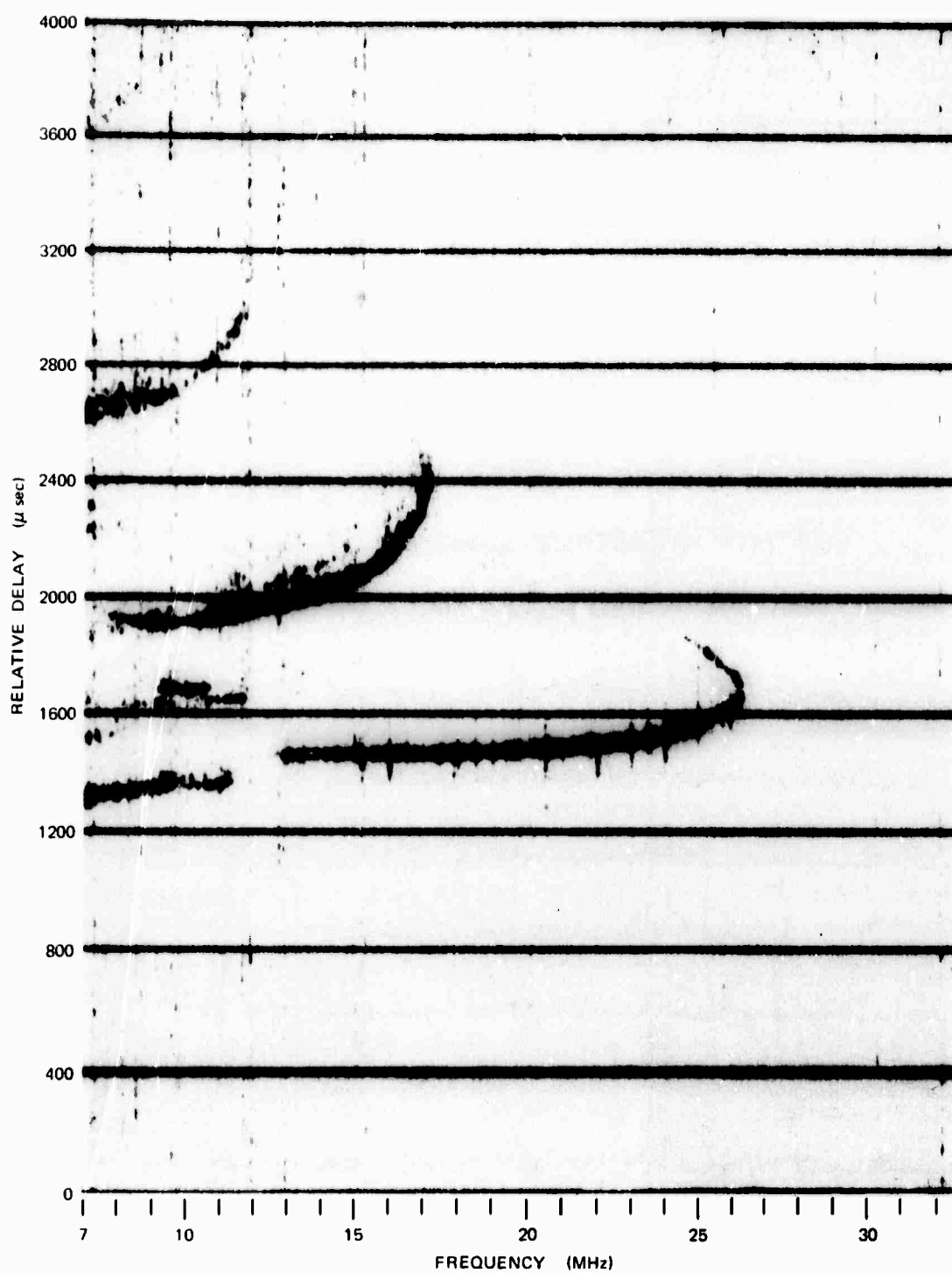
Figure 29   Ionogram, Bearden to Los Baños, 22 April 1969, 22:34 GMT.

Figure 30 shows the squared amplitude vs delay and cross range for these data, in which the signal from the fixed repeater was used as a reference to compensate for amplitude and phase distortion arising from airplane motion and ionospheric irregularities. In situations such as this, where the repeater is used as a reference, it is not necessary to compensate separately for nonlinear airplane motion, since the repeater signal compensates for both airplane and ionospheric effects simultaneously. Figure 30a shows the squared amplitude normalized so the peak of the fixed repeater is unity. Figure 30b shows the same squared amplitude multiplied by 10 and then truncated to unity. The 10 dB gain makes it possible to see small features in the record.

The portable repeater is readily seen on this record. Although it is at the same range as the fixed repeater, it appears at a larger delay because its internal delay is much greater than that of the fixed repeater. As already noted, the portable repeater internal delay, due to the inherent nature of its design as explained in Appendix A, is about 63 μsec, while the delay of the fixed repeater due primarily to long cable runs is about 5 μsec. The delay difference is 58 μsec, which is clearly identified on the record.

As shown on Fig. 26, the portable repeater, which was located at Site 2 for this test, was 1000 m north of the transmitting antenna of the fixed repeater. Because the cross-range resolution of the 12 km synthetic aperture is only 2800 m, the two repeaters appear in Fig. 30 to originate at the same cross range. Thus they are not resolvable in cross range. The side lobes in delay and cross range of both repeaters are seen in Fig. 30b. These are larger than they would be in an ideal case because of distortion in the propagating medium or in the recording process.

4. Backscatter Data Taken With 70 km Synthetic Aperture

The next data to be displayed are from the same basic data (Flight 3N 22 April 1969), except that all of the available synthetic aperture was used. On this particular run there were 768 equivalent elements spanning an aperture of 70 km. This gives a theoretical

99
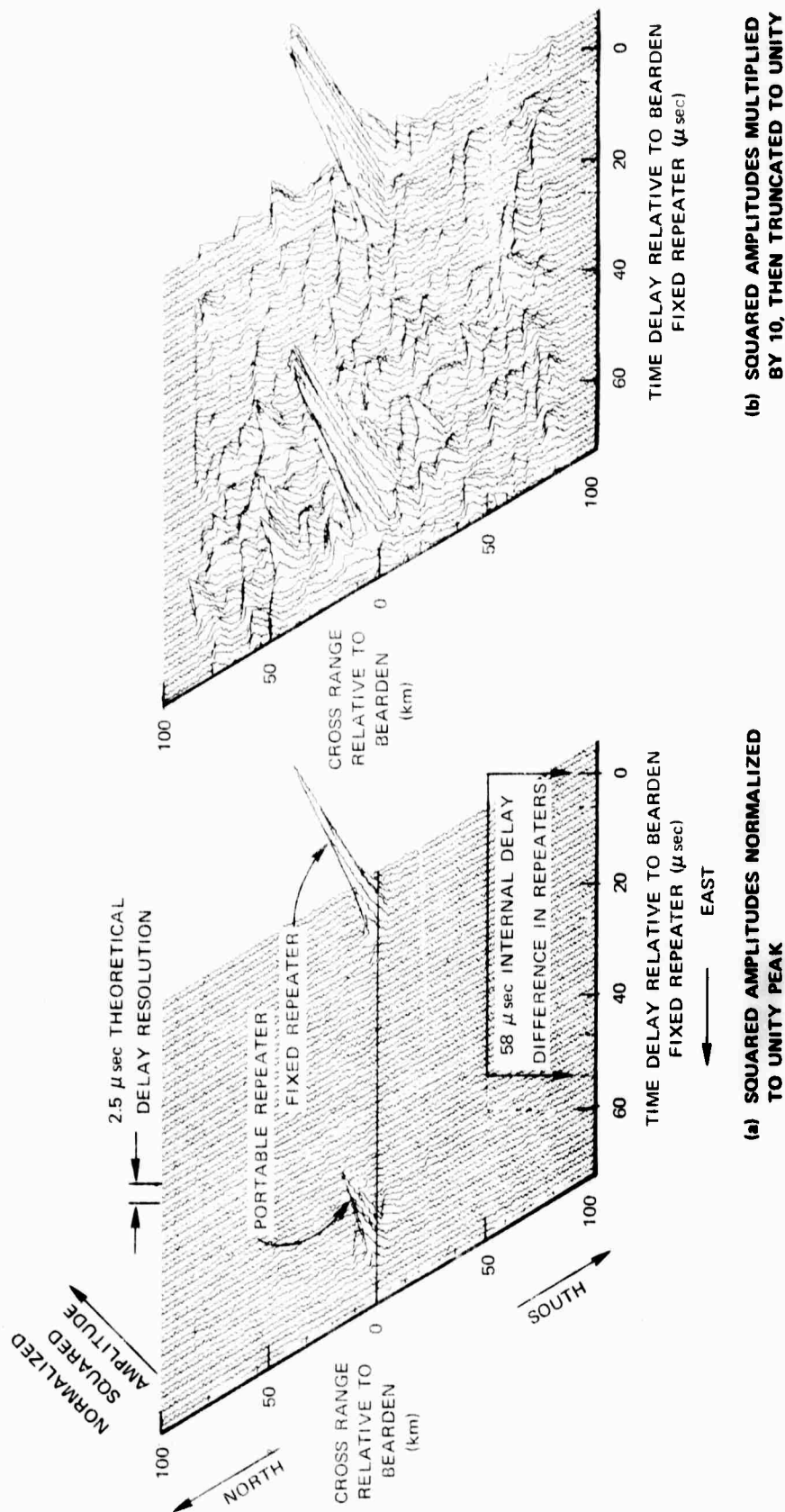
Figure 30   Backscatter map of normalized squared amplitude vs delay and cross range for flight 3N on 22 April 1969 (same flight as Fig. 28) using 12 km synthetic aperture.

Record was made using fixed repeater as reference to compensate for amplitude and phase distortion of ionosphere, and for flight-path deviations. Record shows that the portable repeater was not resolved in cross range.

100

angular resolution of 0.014 deg or a cross-range resolution of 470 m.
As discussed in Chapter II, there are situations when amplitude and
phase compensation for distortion is appropriate and other situations
when only phase compensation should be used. Results of both types of
compensation are illustrated here. As in the previous example, the use
of the repeater as a reference means that distortion due to flight path
deviations as well as ionospheric effects are compensated.

Figure 31 is a backscatter map showing both repeaters, in
which normalized squared amplitude is plotted vs delay and cross range.
Compensation was provided by only the phase measured from the signal
from the fixed repeater. Figure 31a shows the display normalized so the
peak of the fixed repeater is unity. Figure 31b shows the same squared
amplitude multiplied by 50 and then truncated to unity.

The first observation is that the achieved cross-range
resolution is worse by about a factor of 2 than it would be in an un-
distorted case. The resolution of the record in cross range is not
quite sufficient to resolve the signals from the two repeaters in that
dimension. The second observation is that the cross-range side lobes
are quite high, but the range side lobes from both repeaters are not
visible.

The next record is a result of applying amplitude and phase
compensation, using the fixed repeater as a reference. Figure 32 is
the backscatter map for this case. Again Fig. 32a shows amplitude
normalized to unity peak, while Fig. 32b shows amplitude multiplied by
50, then truncated to unity. On Fig. 32 the two repeaters are resolved
in cross range, indicating that the 470 m ideal cross-range resolution
was achieved for this case.

5.   Discussion of Delay and Cross Range Side Lobes

The delay side lobes are readily seen on Fig. 32. The
delay side lobes never seem to be less than 20 dB below the peak of the
main lobe, while the delay side lobes nearest the main lobe are only
10 dB down.

The azimuthal or cross range side lobes are even larger than

101
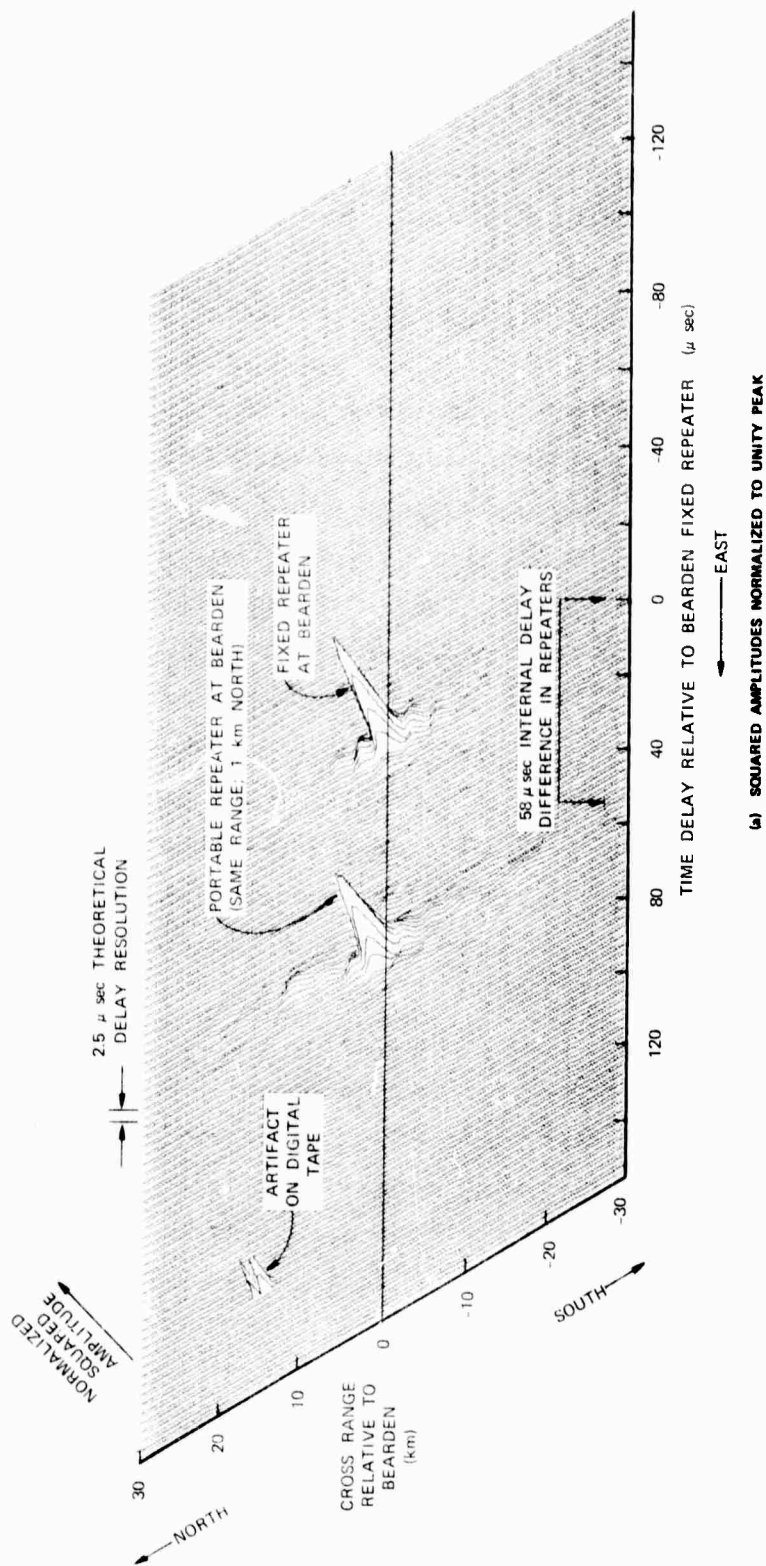
Figure 31 Backscatter map of normalized squared amplitude vs delay and cross range, using same data as Fig. 30 but with a 70 km synthetic aperture.

Fixed repeater at Bearden used to compensate for phase distortion only. Record shows the two repeaters not quite resolved in cross range.

TIME DELAY RELATIVE TO BEARDEN FIXED REPEATER (μ sec)

(b) SQUARED AMPLITUDES MULTIPLIED BY 50, THEN TRUNCATED TO UNITY

CROSS RANGE
RELATIVE TO
BEARDEN
(km)
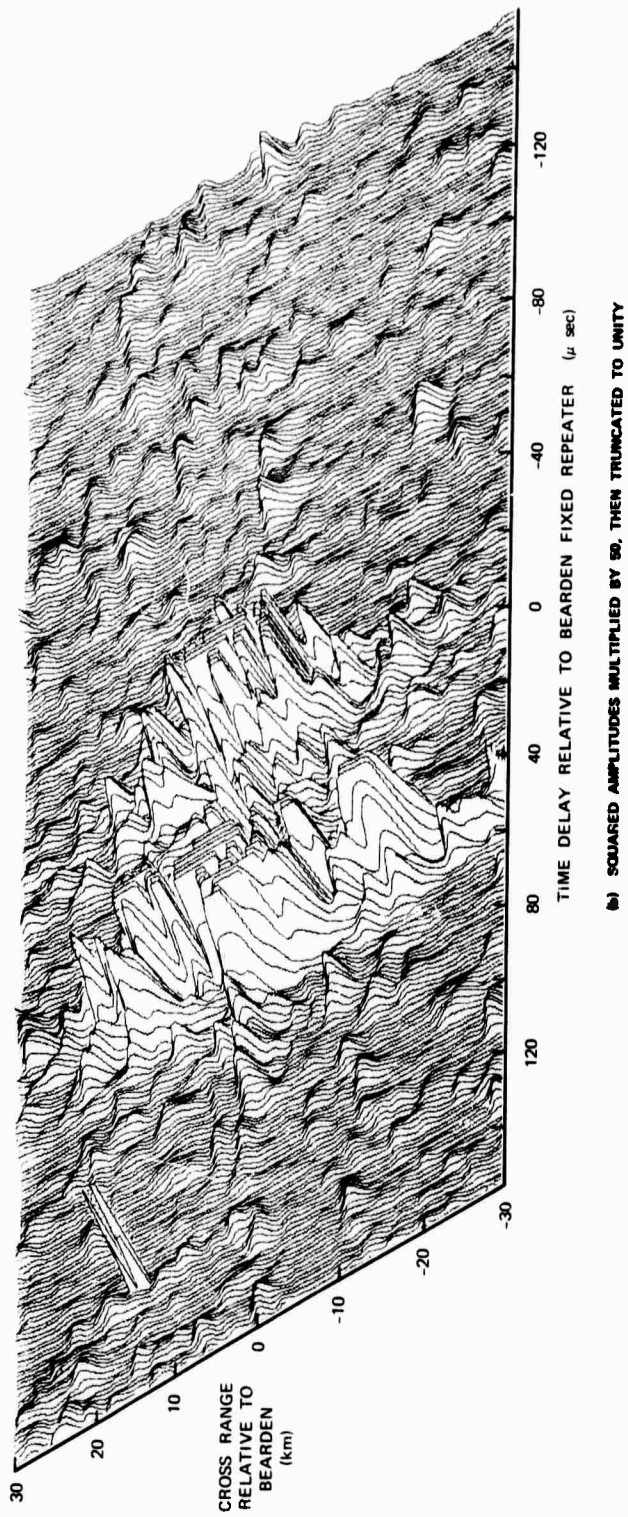
Figure 31 (Concluded)
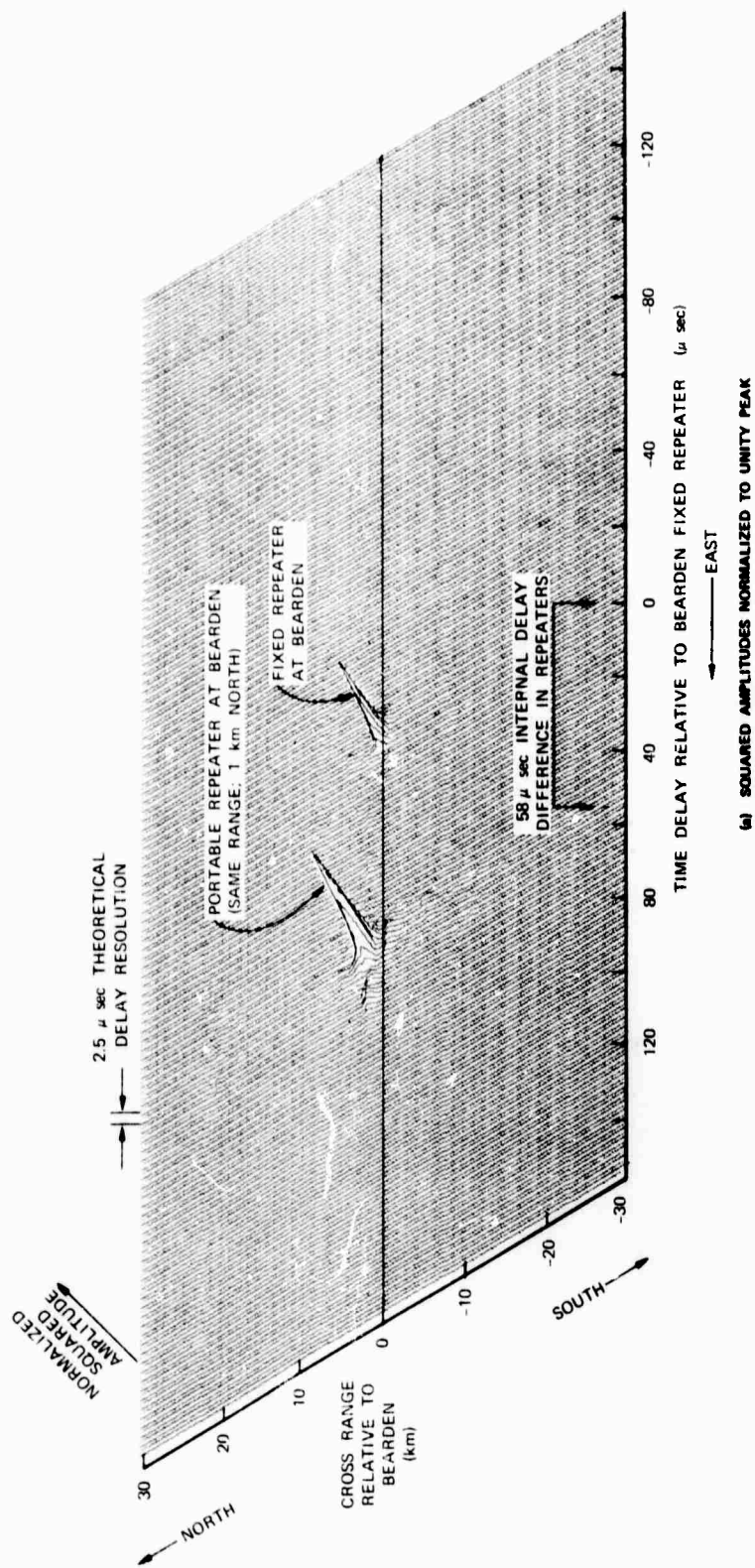
Figure 32 Backscatter map made with 70 km synthetic aperture, using same data as in Fig. 31, but using compensation for amplitude and phase distortion caused by ionosphere and by flight-path deviations.

Record shows fixed and portable repeaters, which were separated by 1000 m, resolved in cross range.

104

CROSS RANGE
RELATIVE TO
BEARDEN
(km)

TIME DELAY RELATIVE TO BEARDEN FIXED REPEATER (μ sec)

(b) SQUARED AMPLITUDES MULTIPLIED BY 50, THEN TRUNCATED TO UNITY
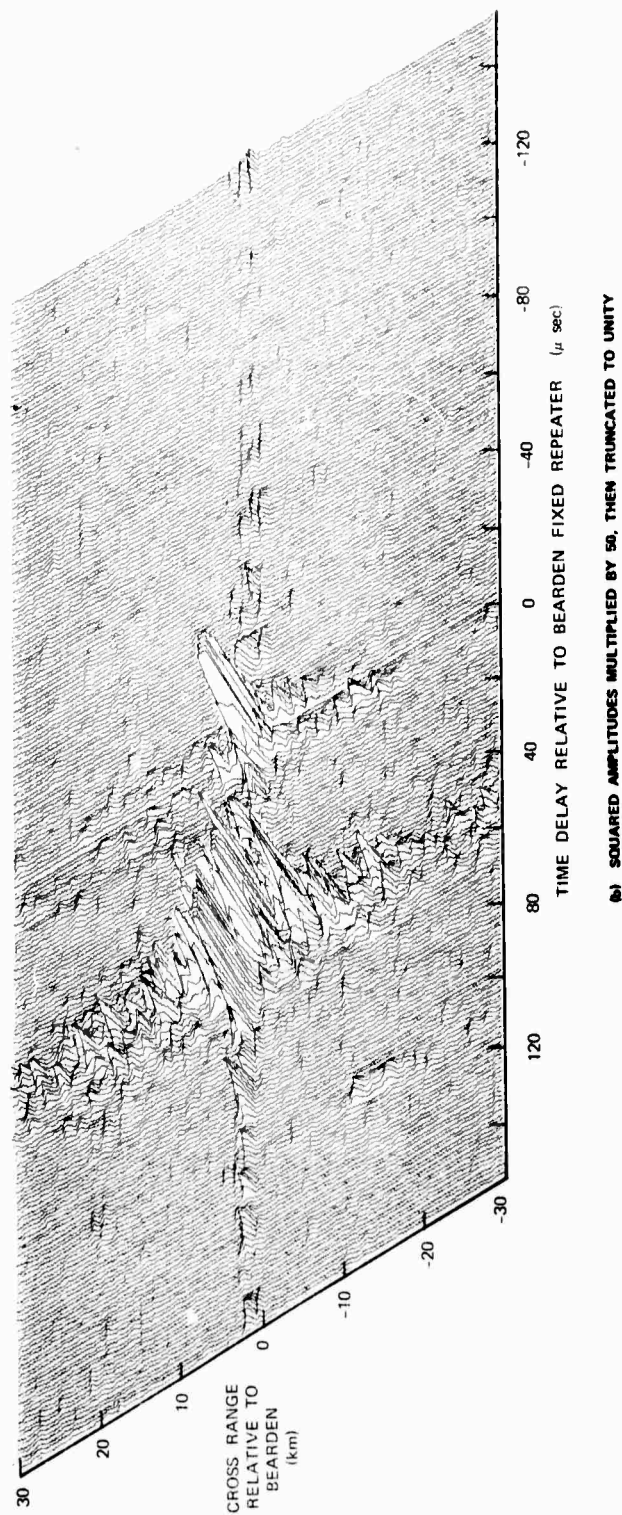
Figure 32   (Concluded)

the delay side lobes. Of course, the cross-range side lobes of the fixed repeater at the range increment for which the compensation is made are ideal--i.e., 30 dB down. The cross-range side lobes of the fixed repeater at nearby delays are only down by about 15 dB; however, they do drop off quickly with increasing angle. The cross-range side lobes of the portable repeater are very large. The side lobes near the main lobes are down only by 10 dB, and at 32 angular cells from the main lobe (about 15 km), the side lobes are only about 15 dB down.

The large delay side lobes may be due to imperfections in the SFCW signal. Ionospheric variations are generally negligible over periods less than the one second of the sweep. Another possible cause is fast jitter introduced by the tape recorder. The cross-range side lobes of the fixed repeater could be caused by phase differences within the pulse due to magnetoionic splitting; or perhaps this effect too could be due to tape jitter. The poor side lobes of the portable repeater compared to those of the fixed repeater is a significant finding and is attributed to ionospheric fluctuation differences in the two closely spaced paths.

The large angular side lobes of the portable repeater are an indication that the region which can be imaged is not very large. In Chapter III (see Eq. 36) it was shown that the phase reference reduced the effective variance of the phase by an amount:

$$2 \left[1 - \exp \left[-\left(\frac{\Delta y}{\Lambda}\right)^2 \right] \right] \ ,$$

where Δy is the distance from the reference, and Λ is the correlation distance of the phase. For small Δy, this factor grows as $(\Delta y)^2$, implying that if the phase distortion causes poor side lobes at a distance of only 1 km from the reference, then at 2 km from the reference the side lobes would be four times as prominent (measured as squared amplitude). Thus it is expected that at distances as little as 3 or 5 km from the reference, backscatter would be very distorted.

106

The large side lobes are on the range and angular axis while
off these axis the side lobes are much smaller (more than 20 dB down).
In general the off-axis side-lobe level is given by the product of the
side-lobe level on each axis. If the on-axis lobes are down by 15 dB
then the off-axis lobes should be down by 30 dB. This is a crude
estimate but, as is readily seen, appears to be approximately true.

The general nature of the backscatter is significantly
different between the records shown in Fig. 31, where only phase
compensation was used, and in Fig. 32, where both amplitude and phase
compensation were used. The background level of the backscatter appears
to be <u>higher</u> in Fig. 31 than in Fig. 32, probably due to the fact that
the processed repeater signals are <u>lower</u> in amplitude. The spreading
in cross range and the loss in amplitude of the repeater returns is a
result of the amplitude distortion, which is not compensated for in
Fig. 31. It is further noted that the side lobe level of the portable
repeater is high in Fig. 31, but that delay side lobes of both repeaters
which are visible in Fig. 32 are not visible in Fig. 31. This indicates
that the backscatter signals from the ground are masking these delay
side lobes in Fig. 31.

If the backscatter were coherent with the repeater, the
relative amplitude of the repeaters and the backscatter would be the
same for both kinds of processing. But for the data presented here it
appears that the backscatter is so distorted that changing the form of
processing does not alter its characteristics appreciably. One possible
problem could be the self noise[29] mentioned in Chapter III. In this
case, the side lobes in delay and cross range of scatterers far removed
from the repeaters could be combining to give a noise-like interference.

For this particular set of data it was concluded that
amplitude and phase compensation is superior to phase compensation
alone. It is therefore believed that most of the background features
of the backscatter record are a result of smearing of backscatter re-
turns over a wide interval of delays and cross ranges. A possible ex-
ception is the enhancement seen in the lower left-hand quadrant (positive
delay, negative cross range). This enhancement is above the general

107

noise-like backscatter and does not seem to be associated with delay
or cross range side lobes.

TABLE 2

SUMMARY OF EXPERIMENT LOG

DATE	PASS	START TIME (GMT)	ENDING TIME	TYPE	FREQUENCY* MHz	CLOCK DELAY msec	FIXED REPEATER	PORTABLE REPEATER	REMARKS	IONOSPHERIC CONDITIONS
4/14	1N								Scratched	
	1S								Scratched	
4/15	1N	12:34		SFCW	22.5-23.1	+13	On	Cemetery	Considerable interference	
	1S	13:10		SFCW	22.5-23.1	+13	On	Cemetery		
	2N	14:19		CW	25.7				Poor tracking	
	2S	14:56		CW	25.7				Poor tracking, 12 mph northerly wind	
4/17	1N			SFCW			On		test	
	1S			SFCW			On		test	
4/18	1N	11:33	14:41	SFCW	22.0-22.6	+13	On	Gravel pit	sunny, hazy	Wait 2 hrs at Sacramento Metro Airport for Ionospheric conditions to improve
	1S	14:18		SFCW	21.0-21.6	+13	On	Gravel pit	Good Backscatter	
	2N	15:01	15:29	SFCW	21.0-21.6	+13	On	Gravel pit	Better Backscatter/ some air turbulence	
	2S	15:39	16:03	SFCW	21.0-21.6	+13	On	Gravel pit	Best Backscatter	
4/21	1N	22:01	22:25	SFCW	23.0-23.6	+13.5			OK	
	1S	22:46	23:15	CW	23.3				OK	
4/22	1N	22:07	22:21	SFCW	23.0-23.6	+14	On	Cemetery		Wait 3 hrs Los Banos Airport for Ionosphere
	1S	22:40	23:09	SFCW	22.2-22.4	0	On	Cemetery	Air turbulence go to 7000' to avoid turbulence	
	2N	23:27	23:51	CW	24.470					
	2S	00:00	00:31	CW	24.470				Author took over as pilot for this run	
	3N	00:41	01:03	SFCW	23.0-23.6	+14	On	Receiver Site	moderate light, partially cloudy	
4/24	1N	18:23	18:52	SFCW		+14	On		(rain on day before), too many clouds	
	1S	22:25	22:51	CW	23.260				(new co-pilot for one day), 7000', SFCW generator at Lost Hills down, land Sacramento Metro	
	2N	23:21	23:48	***	21.0-24.0	-1/2				
	2S			SFCW			On		Scratched, Lost Hills SFCW down	
4/25	1N	23:48	00:16	SFCW	21.1-21.7	+14	On	Sheridan	Clear weather, clean backscatter	
	1S	00:23	00:46	SFCW	22.3-22.5	-10	On	Sheridan	Lost Hills at 82° (rather than 86°)	
	2N								Bearden Transmitter down--abort	
4/26	1N	18:54	19:23	SFCW	22.1-22.7	+14	On	NRC**	Ran out of tape before 2nd photo	Good ionospheric conditions
	1S	19:42	20:10	SFCW	22.3-22.5	-10	On	NRC		
	2N	20:34	21:01	SFCW	20.5-20.7	-2	On		Transmitter at 82°	
	2S	21:20	?	SFCW	20.3-20.9	+11	On	NRC		
	3N	22:10	?	SFCW	24.3-24.9	+14	On	NRC	Strong Repeater Visible	
	3S	23:36	00:00	CW	25.330					
	4N	00:25	?	SFCW	17.1-17.6		On		Remove Matching network and bandpass filter (interference on tracking signal)	
	4S	01:04	01:27	SFCW	15.5-15.7	-6.5	On			
	5N								False Start	
	6N	01:58	02:21	***	18.0-27.0	+8.1			Poor light for photo	

* 0.6 MHz Band width indicates 1.0 MHz/sec sweep rate
  0.2 MHz Band width indicates .250 MHz/sec sweep rate

** Naval Reserve Center (NRC)

*** SFCW from Bearden (Ionogram)

TABLE 3

SUMMARY OF GEOMAGNETIC ACTIVITY INDEX (K_p)

April 1969

DAY	STATE	TIME INTERVAL (GMT)		
		15 - 18	18 - 21	21 - 00
15		3-	2+	2+
16		3+	3	4
17	D	4-	4-	4-
18		2-	1+	2-
19	QQ	1+	0+	1+
20	Q	1+	1	3-
21	QQ	0+	1-	1+
22		3	2-	1
23	QQ	2-	1+	1+
24	Q	1	2	2-
25	Q	2-	2-	2-
26	QQ	1	2	2

D ∼ Disturbed

Q ∼ Quiet

QQ ∼ Very Quiet

VI. CONCLUSION

A. SUMMARY OF RESULTS

1. Analytical Results

An analysis of the performance of an HF synthetic aperture was given in Chapter II. The effect of ionospherically induced spatial and temporal variations of the phase of a received signal was determined. Using a simple but physically meaningful model of the phase distortion it was possible to relate the performance of a synthetic aperture to the performance of a fixed aperture by a simple procedure. It was assumed that the phase distortion is a zero-mean gaussian stationary random process with a correlation function

$$K_\varphi(\Delta x) = \sigma_\varphi^2 \exp\left[-\left(\frac{\Delta x}{\Lambda}\right)^2\right] \quad , \tag{4}$$

where σ_φ^2 is the phase variance and Λ is the correlation distance of the phase distortion. It was shown that if the rms phase σ_φ is greater than 1 cycle, the approximate beam width is limited to about that achieved by an array of length $2\,\Lambda/\sigma_\varphi^{1/2}$. The analysis of the array distortion took into account the fact that the wave front tilt does not contribute to increasing the beam width or side lobe level for the short-term case. An analysis was also made to determine the effect of the temporal variations of the phase distortion and the forward motion of the airplane which formed the synthetic aperture. It was found that if the temporal correlation time is defined as T , an equivalent spatial correlation distance Λ_e could be defined by

$$\frac{1}{\Lambda_e^2} = \frac{1}{\Lambda^2} + \frac{1}{(v_a T)^2} \quad , \tag{19}$$

111

where v_a is the velocity of the airplane.

The quantity $1/\Lambda$ is proportional to the rms increase in beam width (beam spreading). Therefore the above equation simply states that the variances of the two causes of beam spreading (spatial and temporal variations of the phase distortion) add.

In Chapter III an analysis was made of restoration techniques for HF synthetic apertures. It was found that the optimum restoring filter would compensate for amplitude **and** phase if the reference signal and the information bearing signal were distorted in exactly the same way. As the point to be imaged moves further from the reference, the distortions suffered by each become uncorrelated with one another, and the optimum filter de-emphasizes the amplitude information. Whether a practical spatially-invariant filter would utilize amplitude information or not depends on the degree and type of distortion. It was found analytically that the improvement in array performance afforded by a phase reference could be determined by defining an equivalent phase variance $\sigma_e^{\,2}$ by

$$\sigma_e^{\,2} = 2\,\sigma_\varphi^{\,2} \left\{ 1 - \exp\left[-\left(\frac{\Delta y}{\Lambda}\right)^2\right]\right\} , \qquad (36)$$

where Δy is the separation of the point to be imaged from the reference. Thus the problem of an array using a reference was reduced to the previously solved problem of an array without a reference. In Chapter III, Eq. (39), it was shown that a small amount of distortion would occur if Δy was restricted by

$$\Delta y \leq \lambda \left(\frac{1}{2\,\sigma_{\theta_o}}\right) ,$$

112

where σ_{θ_o} is the rms angle of arrival. Thus the size of the region which can be imaged is inversely proportional to the rms angle of arrival σ_{θ_o} . For a wave length $\lambda = 20$ m , and an rms angle of arrival $\sigma_{\theta_o} = 1/4$ deg, the separation Δy should be less than 2.5 km. This is a stringent restriction.

2. Experimental Results

The experimental program was organized into 4 principal steps:

a. Verification of airplane-tracking subsystem performance.

b. Measurement of beam width achievable with the synthetic aperture when receiving a CW signal transmitted from Bearden (CW forward-propagation experiment). In this test, compensation for deviations of the airplane from a linear flight path was applied by the use of airplane tracking data.

c. Demonstration of the feasibility of obtaining two-dimensional backscatter data (range vs cross range) without compensating for ionospheric distortion or deviations of the airplane from a linear flight path.

d. Investigation of the use of an HF repeater at Bearden to provide a reference signal in compensating for airplane flight-path deviations and ionospheric distortion, for the purpose of obtaining extremely high azimuthal resolution in backscatter mapping.

The experimental results were obtained using the F layer of the ionosphere to propagate a one-hop signal. The particular path used was an east-west midlatitude path which generally has favorable conditions. The data were taken during a period of low magnetic activity, and in general the ionosphere was undisturbed.

a. Airplane Tracking

The airplane tracking system proved to be quite accurate. A comparison was made between locations determined by the radio tracking

113

system and locations determined by photogrammetry at the ends of the
flight path (separated by about 60 km). On the four flights tested the
location error was less than 60 m.

     b.   <u>CW Forward-Propagation Measurements</u>

        The frequency spectra of CW signals transmitted from
Bearden and received at either Los Banos or in the airplane were calcu-
lated by Fourier-transforming the data in time intervals of certain
lengths. The forward motion of the plane produces a synthetic aperture,
so that the frequency spectrum of the signal received in the plane is
equivalent to an angular spectrum. It is essential in these CW measure-
ments that the deviations of the airplane from a straight course be
compensated for.

        For the data received at the <u>fixed</u> receiver in Los Banos
it was found that processing times as long as 256 sec could be used to
obtain an 0.004 Hz frequency resolution only a small fraction of the
time. Processing times of 128 sec could be used about 50 per cent of
the time, and processing times of 64 seconds about 80 per cent of the
time. By comparison, the signal received <u>in the airplane</u> could be
processed for 64 sec, giving a 5 km aperture, to yield an 0.008 Hz
frequency resolution (or equivalently a 1/6 deg azimuthal angular
resolution at 23 MHz) about 50 per cent of the time. It was found that
a synthetic aperture 10 km long could be used to form an azimuthal beam
about 1/12 deg wide for about 20 per cent of the cases tested.

        Thus it seemed that the spatial as well as the temporal
variations of the ionosphere limited the resolution of the signal
received in the airplane.

     c.   <u>Backscatter Measurements Made Without Compensation for
Flight-Path Deviations or Ionospheric Variations</u>

        Backscatter measurements were made by transmitting a
SFCW signal once per second from Lost Hills and receiving the backscat-
ter signal in the airplane. A fixed repeater at Bearden at a range of
2600 km, which simulated a ground backscatter return, plus a natural

backscatter enhancement at a range of 1600 km were imaged. It was found possible to obtain a 0.4 deg beam width at 15.6 MHz using a 2.5 km synthetic aperture.

        d.   <u>Backscatter Measurements Using a Repeater Signal to</u>
            <u>Compensate for Flight-Path Deviations and Ionospheric</u>
            <u>Variations</u>

In these studies, the fixed repeater at Bearden was used not only to simulate a large ground backscatter return, but also to furnish a reference signal for use in compensating for airplane flight-path deviations and ionospherically induced distortions. In addition, a portable repeater was installed at Bearden at a site 1000 m north of the transmitting site of the fixed repeater. The portable repeater was used to simulate a large backscatter return and thus to determine the effectiveness of the compensation system in permitting high-resolution discrimination by the synthetic aperture as between signals from the two simulated backscatter sources.

The major test employed a synthetic aperture which was 70 km long and required about 13 minutes to form. Using <u>only</u> the phase information from the fixed repeater to implement the compensation, the beam width obtained was about 0.02 deg, which is larger by a factor of two than it would be in an ideal case. However, using amplitude <u>and</u> phase information from the repeater, a beam width of 0.01 deg was achieved, as shown in Fig. 32. The cross resolution of the 0.01 deg beam was about 470 m. Thus the fixed repeater and the portable repeater were resolvable in cross range (azimuth). However, the cross-range side lobes of the portable repeater signal were much higher than they would be in an ideal distortionless case. Since the distortion increases rapidly as the point to be imaged moves further from the reference, it is not expected that a point more than 3 to 5 km from the reference could be imaged without distortion.

B.   CONCLUSIONS

There are three possible methods of operation of an HF synthetic

aperture which have been developed and for which separate although related conclusions are drawn. These methods are:

1. Operation without compensation for airplane flight-path deviations from a straight line or for ionospheric distortion.

2. Operation with compensation for flight-path deviations by means of an airplane tracking system, but not for ionospheric distortion.

3. Operation using an HF repeater to provide a reference signal to compensate for both flight-path deviations and ionospheric distortion.

1. No Compensation

In the first type of operation, for which no compensation of any kind was used, it was found experimentally that a synthetic aperture 3 km long could be used to form an azimuthal beam about 0.4 deg in width (at 23 MHz). This was achieved about 50 per cent of the time. The result was verified using both the CW forward-propagation measurements and the backscatter measurements. One of the important parameters of these tests was the type of aircraft used to synthesize the aperture. In the tests reported here a medium sized airplane, a twin-engine DC-3, was used for the test. The airplane flew at a speed of about 80 m/sec (180 miles per hr). Deviations of the course of the plane from a straight line appear to be the limiting factor in the system performance even with the aid of a trained navigator, and even when detailed ground maps and a telescope are used to determine with great precision the location of the plane. The 2.5 km aperture that was successfully synthesized without any compensation is comparable in length with the phased array operated by the Stanford Radioscience Laboratory at Los Banos, which is believed to be the world's longest HF array.

2. Flight-Path Compensation

In the second method of operation, in which airplane deviations were compensated for, it was found that an aperture 10 km long could be

116

used about 20 per cent of the time to form an azimuthal beam of approximately 1/12 deg (at 23 MHz). This was verified using the CW forward-propagation measurements. Measurements were made of the same CW signal as received in the aircraft and as received at a fixed antenna at Los Banos. A comparison of results obtained for the fixed and the airborne measurements indicated that spatial and temporal variations of the phase distortion were limiting the performance of the synthetic aperture. Apparently, better results could be obtained by flying faster. A fixed aperture, which is the theoretical equivalent of an infinite flying speed, should be able to perform even better than the experiment-ally realized synthetic aperture. A fixed aperture of 10 km in length should be able to achieve narrow beam widths without significant distortion a large fraction of the time.

3.   Flight-Path and Ionospheric Compensation

In the third method of operation, in which an HF repeater was used to compensate for flight-path deviations and ionospheric distor-tion, it was found experimentally that much increased azimuthal resolu-tion could be achieved in the region near the reference. A 70 km syn-thetic aperture was able to obtain a cross-range resolution of about 500 m at a range of 2600 km. A second repeater 1000 m away which was used to verify the cross-range resolution appeared to have very large side lobes. Since the improvement in performance afforded by the refer-ence signal diminishes rapidly as the distance between the point to be imaged and the reference increases, it is expected that the region which can be imaged is less than 3 to 5 km.

One is forced to conclude, therefore, that the use of a reference signal can indeed make it possible to obtain extremely high cross-range (azimuthal) resolution, but that this resolution can be achieved only in a region very close to the reference point.

4.   Overall Conclusions

The investigation reported here clearly shows that aperture synthesis techniques can be used for

117

signals propagated via the F layer of the ionosphere. The principal advantages of using aperture synthesis are (1) that the receiving equipment is by its very nature portable, and (2) that apertures much longer than any ever built for use at HF are easily implemented. The analytical and experimental program have helped to delineate the fundamental limitations in implementing aperture synthesis at HF.

It should be noted that the conclusions which are drawn from the experimental program are for a particular set of ionospheric conditions which are generally regarded as quite favorable. These conditions included a midlatitude east-west path which is known from other studies to have favorable properties such as small pulse spreading due to magnetoionic splitting, and small azimuthal spreading. The data were taken during a period of low magnetic activity and in general the ionosphere was undisturbed. Another important qualification is that only one-hop F-layer propagation was tried. Presumably multi-hop signals would sustain severe distortion because of the intermediate ground reflection, which would make aperture synthesis difficult. On the other hand, one-hop E-layer propagation might have produced far superior results; however, this mode is not available for the 2600 km path used in this study.

Under the conditions outlined above, it has been shown experimentally, that the use of suitable compensation for ionospheric distortion, employing a reference signal close to the backscatter-imaged area, permits extremely high azimuth resolution with synthetic apertures on the order of 70 km in length. This technique has two significant disadvantages, however. First, high azimuthal resolution can be achieved only in a very small region surrounding the reference, about ± 3 km in extent. Second, it may be impractical to provide such a reference near the region to be imaged. Based on the analysis presented herein, these same restrictions apply to extremely long fixed apertures as well.

It is concluded that aperture-synthesis techniques are particularly attractive for apertures of between 1 and 1C km in length. For the shorter apertures, 1 to 3 km, it should be possible to obtain

118

full benefit of the aperture by using a medium-sized airplane and simple processing techniques which would not compensate for course deviations of the plane from a straight line. Longer apertures, 6 to 10 km, could be used effectively at least part of the time, if compensation for course variations over a time interval of 60 to 100 seconds could be provided.

C. RECOMMENDATIONS FOR FUTURE WORK

The research that has been described herein leads to the following suggestions for further study in the field.

1. Other Forms of Compensation

If temporal variations in the ionosphere are the limiting source of error, a compensation for only these variations could be used. The phase of the transmitted SFCW signal could be modified in accordance with changes measured from a single-mode, one-hop CW signal propagated over the same path. The source of the CW signal would have to be phase-stable, and the signal would have to be propagated by only a single mode. The use of the National Bureau of Standards broadcasts of frequency standards on Station WWV, Colorado, might be useful in certain regions.

A slightly more complicated version of the same idea is to receive at the transmitter site and in the airplane a CW signal transmitted from a point near the region to be imaged. The phase of the received CW signal could be used to compensate both the transmissions and the SFCW backscatter in real time as it is recorded in the plane. Thus both the transmit and the receive paths would be compensated. The processing involved is a two-dimensional Fourier transform, since both geometrical effects and flight-path variations are accounted for. The use of CW transmitters as references rather than broadband repeaters is appealing from a practical standpoint. With CW transmitters, the use of multiple reference signals becomes much more feasible than with a single reference. This would extend the region that can be compensated. (See Goodman and Gaskill[30] for a discussion of multiple references for

119

holography.) With multiple references it should also be possible to
account for changing ionospheric tilts, which would greatly extend the
region that could be mapped. For example, with two references it should
be possible to measure not only the phase but also the slope (rate of
change in space) of the phase.

2. Use of Faster and More Stable Airplanes

A small jet airplane with a high wing loading ratio (gross
weight/wing area) could fly at speeds of over 700 mi/hr, which is about
four times the speed of the DC-3 used in the experiment, and would be
much more immune to the effects of atmospheric turbulence and winds. A
radio or inertial navigation system might also be used to measure the
flight path and compensate the data in real time as it is recorded.
Even without the navigation system, the more stable plane might be able
to synthesize apertures as long as 25 km without the necessity for
flight-path compensation of the data.

3. Use of Optical Processing vs Airborne Computer Processing

The scope of the present project did not warrant the use of
optical data-processing techniques because of the complication this
would introduce. Furthermore, the digital processing of data permitted
considerable flexibility in compensating for geometrical effects and
flight path variations. However, other means of compensation might be
possible which would make the two-dimensional Fourier-transforming
properties of optical lenses usable. This would be ideal for processing
large quantities of data. The possibility of using a medium-sized
general purpose computer instead of optical processing should not be
overlooked, however, since the cost of optical equipment may be compar-
able with that of the computer. If costs are comparable, the possibility
of making real-time images with the computer becomes attractive. The
computer could be airborne, or the data could be relayed via a radio
link.

120

4. Use of Longer Synthetic Apertures, Wider Band Widths, Higher Frequencies, and Shorter Ranges

By using a 200 km synthetic aperture, a 20 MHz center frequency, and a 5 MHz band width, a resolution of 0.2 _minute_ of arc (5×10^{-5} radian) and 200 nanoseconds could be attained, at least theoretically. At a range of 1000 km the resolution cell on the ground would be roughly 50 m by 50 m. The use of such a large aperture and band width would definitely require very careful compensation. Antennas which are circularly polarized and which therefore excite only one magnetoionic mode would be extremely beneficial. The mathematical analysis of HF synthetic apertures indicates that the size of the region around the reference which can be successfully imaged depended on the correlation distance and the rms phase perturbations, but not in a direct way on the size of the aperture. Even if the region which could be imaged were only ± 3 km in extent, a map with 120 by 120 resolution cells could be made.

5. Use of Incoherent Processing Techniques

Incoherent processing for the purpose of measuring the angular distribution of received energy refers to a technique which does not require a high degree of phase stability in the received signal. There are two principal types of incoherent processing.

The first type is analogous to conventional optical imaging. It is used in radio astronomy to measure the location and size of radio stars. The basic principle is to measure the _average_ amplitude and phase of the product of two signals received at two points. The Fourier transform of this average amplitude and phase vs receiver separation yields the angular energy distribution of the incident incoherent signal. The key to the process lies in the averaging. An incoherent technique for an HF synthetic aperture has been proposed by Shearman.[4] Although Shearman uses coherent transmissions to obtain backscatter energy, he averages the data over long periods of time, and assumes that the ionosphere introduces the necessary signal incoherence to make the processing work. The long average such as an hour might be required for each

121

spacing; therefore in the Shearman method a modest map with only 100 elements could possibly take days to measure.

The second type of incoherent processing uses the delay resolution of the signal. It therefore discards radio frequency phase at the outset (after delay resolution is obtained), by using envelope detection. The basic principle is that the angle of arrival of the signal determines the relative time of arrival on individually spaced receivers. The accuracy of the method depends on the pulse width (i.e., the signal band width) and on the separation of the receivers. (Conventional phase processing depends on the wave length and thus on the frequency.) The incoherent processing would have an accuracy much poorer than the coherent processing by a factor equal to the ratio of the signal band width to the center frequency. While the performance is thus much worse, the system design for incoherent processing is in principle much easier, since the phase of the signals does not have to be preserved. Thus it becomes feasible to use receiver separations of tens of miles. The use of the second type of incoherent processing may be well suited for direction finding (DF) but appears to have many severe disadvantages for imaging. The major problem is that it would appear to be sensitive only to very large changes in the reflectivity of the surface that it was imaging. This would be similar to the self noise problem discussed in Chapter III except much more severe.

The use of multiplicative processing whereby the outputs of antenna elements are correlated with each other also has application to the situation where there are only a few points to be imaged. Cross-product terms inherent in the nonlinear process would make the application to imaging inappropriate.

6. Use of Other Ionospheric Modes and Conditions

The distance the HF signal propagates could affect its coherence properties. The longer the signal path the less deep into the ionosphere the ray tends to go. The experiment reported here used a midlatitude east-west signal propagation path, which provides very favorable ionospheric conditions. A path differently oriented might

122

encounter effects of the auroral or equatorial zones. The high ionospheric activity of these zones, especially the auroral zone during or following solar disturbances, would certainly limit the performance of any HF aperture. From the opposite point of view, however, the sensitivity of HF signals to the ionospheric variations and the highly portable character of the synthetic aperture make the latter an attractive means of studying large-scale disturbances in these normally hard-to-reach areas of the globe.

Meteors and sporadic E can distort ionospheric signals and therefore would affect synthetic-aperture performance. Should meteors prove to be important at certain HF frequencies care could be taken to operate only at periods of low meteoric activity, such as the evening hours. The presence of sporadic E is readily detectable on oblique ionograms and could therefore be avoided by selection of a suitable operating frequency if it also proved to be a problem.

The use of the E layer for ionospheric propagation could offer significant improvement in performance. One-hop E can generally propagate up to distances of 1500 km, which is sufficient for many applications. The E layer is known for its exceptional temporal stability, which suggests that it may preserve the spatial phase coherence of HF signals as well. The importance of further large-aperture experiments designed to utilize the one-hop E mode cannot be over-emphasized.

7.   Applications to Direction Finding (DF)

Thus far the synthetic-aperture technique has been described as a way of improving the quality of backscatter records. As pointed out in the Introduction, the main attraction of HF synthetic apertures is the elimination of the huge size of physical structures otherwise required to achieve narrow beam widths. At frequencies in the 2 to 3 MHz range, the argument is even more compelling. Yet this is the frequency range of the radio equipment carried by many small ships. This frequency range propagates via the E layer in most circumstances, both day and night. The Coast Guard or other sea-rescue organizations might find the synthetic-aperture technique extremely helpful in their mission

123

of locating ships in distress.

In view of the above considerations, the possibility of using
the synthetic aperture to measure the direction of arrival of unknown
signals will now be discussed. Direction finding (DF) is a major
problem in many situations such as sea rescue. A downed plane or a
disabled ship may be able to transmit a CW signal on some emergency
band. A relatively short synthetic aperture, about 1000 m long, would
be able to obtain high precision without the usual site errors caused
by the large metal structures of ship-mounted DF systems. An aperture
of about a 1000 m would require only about 10 seconds to fly. Thus the
stability requirement on the unknown transmission would be very low,
and would be satisfied by almost all unmodulated signals.

Since only modest apertures are required, the synthetic
aperture for land-based operations could be implemented in a truck. At
highway speeds (65 mi/hr), a 10 sec integration time would give about
a 300 m aperture. Thus the portability of the truck would make it
possible to synthesize an array whose performance would compare favorably
with that of a fixed array the length of three football fields. Of
course, the availability of suitably oriented, reasonably straight roads
might limit the size of the aperture achievable by a truck to a more
modest size.

Appendix A

DESCRIPTION OF EQUIPMENT COMPONENTS

A. BACKSCATTER-SIGNAL TRANSMITTER AT LOST HILLS

The backscatter-signal transmitter consisted of a cesium-beam clock, a swept frequency CW generator, three 10 kW power amplifiers, and a narrow-beam antenna array.

The cesium-beam clock was a portable time and frequency standard (Hewlett Packard 5061A) of exceptional short- and long-term stability. Three of these clocks were used in the experiment (transmitter, airborne receiver, CW tracking transmitter). The long-term stability is less than one part in 10^{11}. The outputs of the clock include: one pulse once per second with a 50 nsec rise time; a 100 kHz sine wave; a 1.0 MHz sine wave; and a 24-hour clock face with a second hand which moves incrementally once per second. This last feature is extermely useful in synchronizing start times at the distant sites.

The SFCW generator was a Barry Research LSG-6, which has flexible sweep rates and flexible start and stop frequencies. The output was swept at a 1 MHz/sec rate, once every second, across a 600 kHz band. The start time of each sweep is determined by a one-pulse-per-second (1 pps) signal from the cesium-beam standard. All signals in the generator are derived from a 1 MHz sine wave, which is also from the cesium-beam standard. A description of the principles of operation of the generator has been written by Fenwick and Barry.[31]

It is essential that the SFCW signal be exactly the same from sweep to sweep. In particular, the phase of the signal must be the same. The SFCW units did not meet this requirement for all possible sweep rates and starting and ending frequencies. However, the requirement was met for the 1 MHz/sec and 250 kHz/sec sweep rates when the starting frequencies are an integral multiple of 100 kHz.

The power amplifiers were Collins 208 U-10 transmitters, with an auto-tuning feature. Because of the fast sweep rate used, and the relatively narrow band swept, the units were operated on a fixed tuning

125

basis. After stagger-tuning the output section, the 3 dB band width of the transmitters was about 400 kHz. There was therefore some amplitude variation in the output signal. The variation was symmetrical, so that its effect on the final processed signal was to reduce range side lobes.

The three amplifiers fed an 18-element array. The elements were ITT Folded Tilted Monopoles (FTM) with 12 m spacing, giving a total aperture of about 204 m. A reflector screen provided unidirectional radiation eastward. Although the array is capable of beam steering, it was operated in the direction of Bearden, Arkansas (see Fig. 13). The three amplifiers fed the 18 elements in a symmetrical power taper in order to reduce the angular side lobes of the array.

B. AIRPLANE

A twin engine, medium sized airplane (DC-3) was fitted with two tubular antennas and a gasoline generator for ac power. The plane had to be large enough to hold several racks of equipment, a large aerial camera, and six people including two pilots. Heavy weight was desirable to reduce the effect of short-time wind fluctuations, since the plane should fly a straight course. A fast aircraft was desirable to reduce the effect of temporal variation of the ionosphere. The DC-3 was reasonably priced for rental ($195/hr), met all of the requirements except speed, and was available. Its speed was about 180 miles/hr (80 m/sec), which means it required about 20 minutes to fly the prescribed flight path (i.e., to implement the synthetic aperture).

Only a limited amount of 100 V 400 Hz power was available in the airplane. Therefore, in order to provide power to the electronic equipment, a small gasoline generator was installed in the tail section of the plane. Precautions approved by the FAA were taken to reduce fire hazard. The generator provided 2 kW of 120 V power at (60 ± 1) Hz. An averaging electromechanical voltage stabilizer was used, which did not introduce distortion in the 60 Hz signal.

The plane was ground- and flight-tested to determine if aircraft-generated radio noise was a problem. After a faulty generator was

replaced, the aircraft-generated radio noise was less than the ambient radio noise. The use of additional static precipitators was found not to be necessary, due perhaps to the prevailing dry weather conditions.

The two HF antennas installed on the airplane for the experiment consisted of 12 ft lengths of 1½ in. aluminum tubing. One of these tubular antennas was mounted vertically near the vertical stabilizer; the other antenna was extended horizontally from the tail. Figure 33 is a photograph of the airplane exterior showing the antennas. A ground test at 20 MHz with a field strength meter at a radius of 150 ft revealed that the vertical stabilizer of the airplane did not appreciably affect the vertical pipe antenna, although the engine mounts and the forward section of the fusalage did. A bandpass filter (20-26 MHz) and an impedance matching network (VSWR about 2:1) were used. Because of the strong influence of the metal airplane body, it was not expected that the vertical and horizontal pipe antennas would be orthogonally polarized. It was expected only that the two antennas would be differently polarized. This was in fact demonstrated to be the case in tests conducted during flight. This circumstance made it possible to determine if signal-amplitude variations were due to polarization effects.

Braodbanding the antennas on the airplane proved difficult. Several configurations of the common wire-type antennas were tested, but proved unsatisfactory. The tubular antennas were impedance-matched over the 20-26 MHz band without difficulty in a test setup, but proved to be a problem when mounted on the airplane. Trial-and-error adjustments of the impedance matching network finally gave a VSWR within 2:1 from 21:1 to 25.7 MHz.

The electronic equipment was strapped securely on foam rubber pads with nylon bands secured to the aircraft frame to reduce vibration and minimize the hazard of equipment breaking loose in flight.

C.   AIRBORNE RECEIVING EQUIPMENT

The airborne receiving equipment included a cesium-beam clock, an HF receiver, and an SFCW generator. A simplified block diagram showing

127
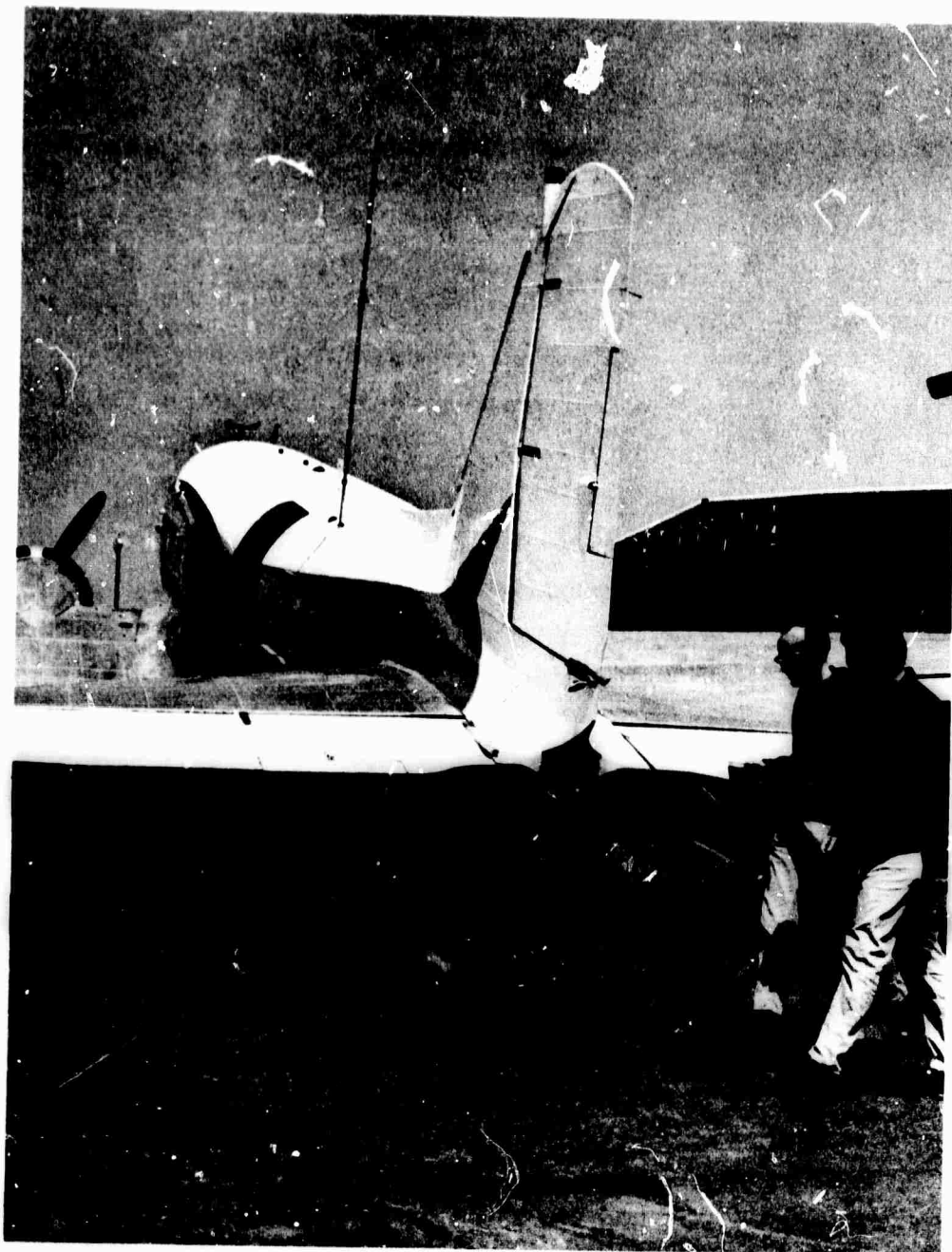
Figure 33   Airplane used in synthetic aperture experiment, showing horizontal and vertical tubular antennas.

their relationship is shown in Fig. 34. The clock and the generator were exactly the same as the clock and generator used at the transmitter. The SFCW generator was also swept at a one MHz rate, once per second. Its start and stop frequencies were set 18 MHz higher than those of the transmitted signal. Demodulation occurred when the received signal and the local SFCW were mixed on a hot-carrier-diode balanced-mixer. The difference frequency of 18 MHz was selected by the receiver.

The receiver was a Collins 75S-3. Its internal injection oscillators were disconnected, and in their place injection signals were synthesized by the LSG-6 driver unit which uses the 1 MHz signal from the cesium-beam clock. The receiver band width of 6 kHz was determined by a mechanical filter in the IF (intermediate frequency) section. The output signal was close to 1 V peak-to-peak (p-p) in the band 2 to 8 kHz. The dynamic range of the receiver was about 40 dB. The receiver was linear over this range.

A detailed block diagram of the airborne receiving equipment is shown in Fig. 35

The time of the 1 pps signal of the clock is digitally adjustable by a precise amount. This adjustment, known as setting the clock delay, has the effect of changing the final output frequency of the backscattered signals. In the experiment the demodulated output signal due to the repeater at Bearden was set to be at 4 kHz. This frequency chosen so that the desired backscatter ranges would fall within the 6 kHz pass band of the receiver and make the sampling operation more convenient.

D.   AIRPLANE-TRACKING SUBSYSTEM

The airplane-tracking subsystem included two ground stations for transmitting CW signals; receiving equipment in the plane; and a digital computer (XDS Sigma 5) for off-line processing of the recorded data. The CW signals were in the 20 to 26 MHz band in order to use available antennas and transmitters and receivers. One transmitter, located at Los Banos, was in a van which housed the processing equipment for the Stanford 2.5 km HF array. As shown previously in Fig. 13,

129

VERTICAL
ANTENNA

HORIZONTAL
ANTENNA

TRACKING
RECEIVER

RECEIVER
No. 1

RECEIVER
No. 2

TO LOCAL
OSCILLATORS

CESIUM-BEAM
FREQUENCY
STANDARD

SFCW
GENERATOR
AND
SYNTHESIZER

1 PPS
50 kHz

ANALOG
TAPE
RECORDER

ALTIMETER

Figure 34   Simplified block diagram of receiving equipment.
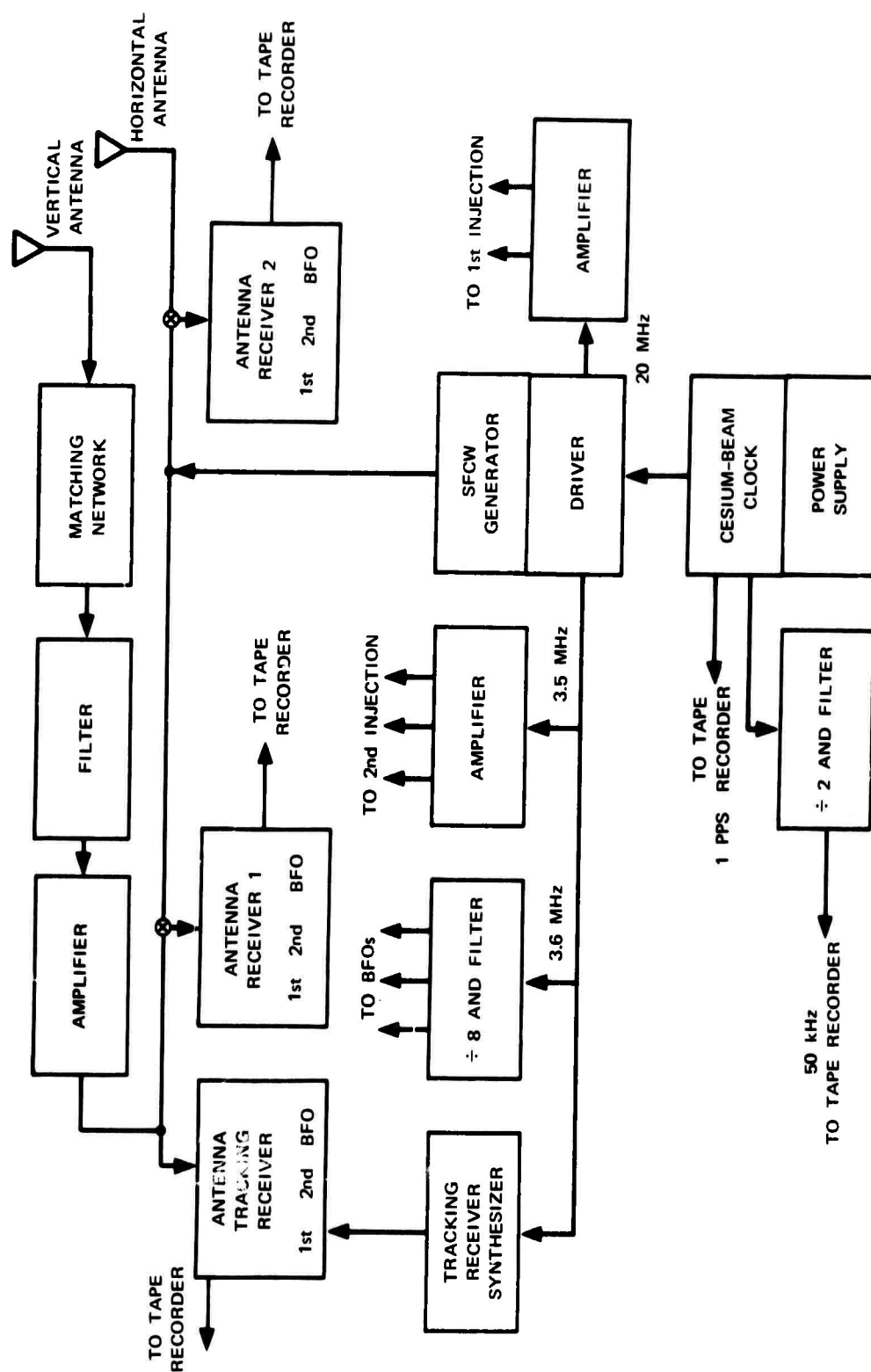
Figure 35   Detailed block diagram of receiving equipment.

131

this Los Banos site is situated so that the flight path if extended
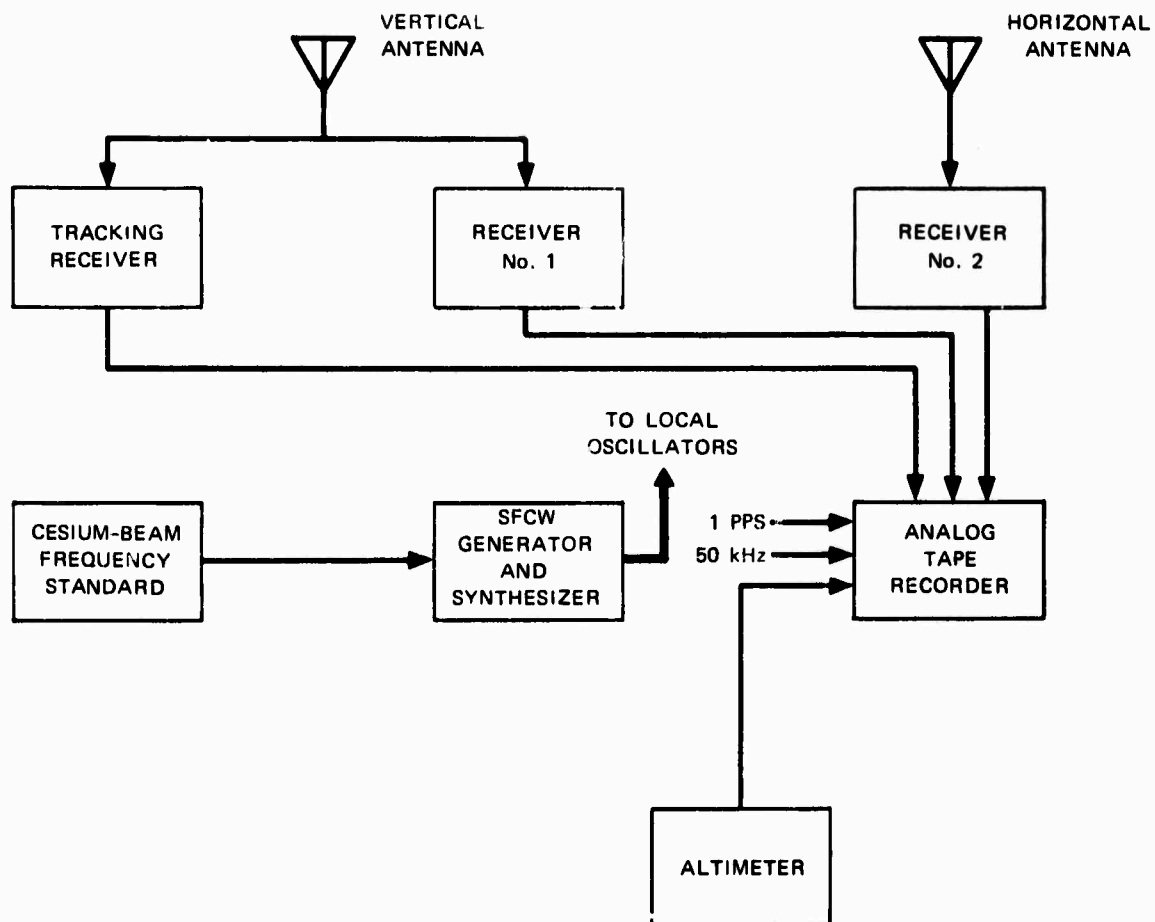would pass over it. Thus this signal could be processed to give the
position of the plane along the flight path, and also could be used as
a real-time precision speed indicator. The Los Banos site is line-of-
sight to the plane if the latter is on the flight path at an altitude
of 6000 ft. The site was furnished with a cesium-beam clock which was
required to guarantee that phase variations in the transmitted signal
would not be responsible for more than 5 m of error in the coordinates
of the plane. A Johnson Viking II transmitter with close to 100 W
output, and an HP frequency synthesizer (5100 A) were used to generate
the CW signal.

The second transmitter was located at a point near the perpendicular
bisector of the flight path. This site was at the FAA VHF radio facility
on Bear Mountain near Copperopolis, Calif. at an altitude of 2893 ft.
The site was selected to be line-of-sight to Los Banos and the entire
flight path, which is a difficult selection owing to the many inacces-
sible areas in the Sierra foothills. The Bear Mountain site also used
a Johnson Viking II transmitter and a Manson Frequency Synthesizer with
an internal crystal standard to transmit a CW signal 3 kHz higher than
the signal from Los Banos. To make the average signal strengths of both
transmissions approximately the same over the flight path, the Bear
Mountain transmitter was operated below 100 W. A 13 ft vertical whip
with two 30 ft radials was used at this location.

The frequency band used (20-26 MHz) is well above the critical
frequency of the ionosphere and therefore vertical ionospheric reflec-
tion is not likely. It is possible for a ground-reflected path between
the ground transmitter and the airborne receiver to interfere with the
desired line-of-sight path. This interference is readily detectable as
amplitude modulation on the received signal. Fortunately, this inter-
ference was not observed during most of the experiment. The lack of
such interference is attributed to the low gain of the Bear Mountain
transmitting antenna at elevation angles close to zero degrees. It is
also possible that the vertically polarized wave and the low ground-
reflection angles make the ground reflected signal small. A more likely

132

problem is that the omnidirectional antenna would propagate a wave backward which could be reflected by the High Sierra. Such a reflection would be aspect-sensitive, and therefore the interference would vary greatly with the plane's position. In fact, amplitude fluctuations were observed on occasion at the north end of the flight path.

The crystal standard at the Bear Mountain site had a stability on the order of one part in 10^8, which is three orders of magnitude less than required. Rather than using another cesium-beam clock, the problem was solved by receiving the Bear Mountain signal at Los Banos. The received signal from Bear Mountain and the locally generated signal were recorded using the same scheme as used in the plane. The analog tape was later processed with the airplane tapes on the Sigma 5 computer; the instability of the Bear Mountain crystal standard is therefore compensated in the digital processing.

The receiver in the aircraft was a Collins 75S-3 with the same modification for external coherent frequency conversion injections as the receivers used for the SFCW data. The 6 kHz pass band made it possible to receive both CW transmissions simultaneously, since they were only separated by 3 kHz. The receiver output consisted of CW tones at 3 and 6 kHz, which were recorded.

The 3 kHz Los Banos tone was also used to measure ground speed in real-time with extremely high precision. The average period of 1000 cycles of the 3 kHz was measured continuously by an HP 5245L frequency counter. The measurement was made with a 1 MHz reference; thus the precision was 1 μsec for the 333 msec interval of the 1000 cycles. A three digit HP 5280A digital-to-analog converter was employed to obtain a meter reading using the three least significant digits. The measured period was inversely proportional to ground speed; but since only small variations in speed occurred, the indicated meter reading was essentially proportional to ground speed (with a change in sign). A full-scale reading was approximately 4 m/sec or 5 per cent of the nominal ground speed. In practice it was found possible to hold the ground speed to about ± 1.5 m/sec.

A sensitive aneroid altimeter made and donated by Rosemont

133

Engineering Company was used which had a full-scale reading of ± 40 m.
The meter had a zero adjustment, so that when a desired altitude was
attained the meter could be used by the pilot to maintain that altitude
(usually at ± 10 m). A dc signal proportional to the meter reading was
recorded for later use in the off-line computer tracking program. The
meter had an error due to hysteresis which was less than 3 m. To
account for variations in the ambient air pressure, temperature-cor-
rected barometric readings were obtained from the Sacramento and
Stockton, weather bureaus. For most flights, this correction was less
than an equivalent of 10 m of altitude and was therefore not used in
the tracking program for these very stable cases. Both ground-speed
and altimeter readings were provided by remote meters in the cockpit.

The CW signals permit the measurement of changes in the distance
to the two CW transmitters at Los Banos and Bear Mountain, respectively.
This information can be accurately translated into the plane's position
coordinates only if the coordinates of the starting point are known
accurately. The latter measurement is made by taking a stereoscopic
pair of aerial photographs of a ground marker using photogrammetry
techniques. A ground marker was accurately positioned at each end of
the flight path by an aerial survey firm. One marker was near the new
Sacramento fair grounds, the other near Manteca (see map, Fig. 15). The
error in the measurement was specified to be less than ± 50 m on the
horizontal, and ± 100 m in altitude. Using one marker as the starting
point, the other marker can be used to test the accuracy of the tracking
data. On four flights the error was between 20 and 60 meters; consider-
ing that the two markers were separated by about 60 km, this result
represents a high degree of accuracy.

E. AIRBORNE ANALOG TAPE RECORDER

An HP 3917B 7-track analog tape recorder was used in the plane.
The half-inch tape ran at 30 in./sec (ips) to reduce inter-channel
timing jitter and to give the necessary band width to record a 50 kHz
reference signal. Extra long reels of tape (4600 ft) were used to make
the data cover as long a time interval as possible. Even so, the 30 min

134

duration of the tape was barely adequate to cover the distance between the two ground markers if a moderate head wind was encountered. The inter-channel timing jitter is specified by the manufacturer to be less than 1.0 μsec which causes a 2 deg phase jitter in a 5 kHz CW signal. While this phase jitter is not negligible, it was judged quite tolerable for the tests being made.

The 50 kHz reference signal derived from the cesium beam standard was used to synchronize the sampling signal during the A/D conversion process In this way tape speed variations were compensated for, and only inter-channel variations were a source of phase errors.

The tape recorder channel assignments and recording method are given in Table 4.

TABLE 4

TAPE RECORDER CHANNELS

Channel #	Method	Signal
1	direct	CW tracking
2	FM	voice (experiment log)
3	direct	1 pps
4	FM	altimeter
5	direct	50 kHz reference
6	direct	horizontal SFCW
7	direct	vertical SFCW

The recorded signals were about 40 dB above internal tape recorder noise, if the input signal level was adjusted properly. Thus noise from the recorder was not significant.

F. HF REPEATERS

Two HF repeaters were used in the experiment. The principal

135

repeater is fixed in Bearden, Arkansas. It consists of two Collins Log-Period Antennas (LPA's) which are horizontally polarized; a 2 MHz bandpass filter; and a Marconi HT00-1000-02 1000 W broad-band amplifier. The receiving antenna is located 1000 m north of the transmitting antenna. The antennas are oriented to point their beam west, and to have a minimum mutual coupling. This repeater introduces about a 5 μsec delay in the signal.

The second repeater was portable, and used a single antenna--a 12 ft whip. The repeater is switched rapidly between transmitting and receiving modes. The signal is amplified, then stored in a delay line for the duration of the receive period. At the end of that period it is transmitted. The keying introduces frequency components not in the received signal; however, for the SFCW signal used in the experiments, these frequencies lie outside the receiver passband. The delay line was 63 μsec, which placed the side bands about 16 kHz away from the repeated signal. The delay difference in the two repeaters is therefore about 58 μsec. A report describing the portable repeater is available.[32]

For best results in the synthetic aperture experiment, both repeaters should have a linear phase-vs-frequency characteristic, and a phase which does not vary with time. Over a 1 MHz band width they satisfy this requirement. Multiple echoes due to impedance mismatch appear to be more than 40 dB down from the main signal. The largest phase change with time was expected to be caused by the 1000 m above-ground cable run, which connects the receiving and transmitting sites of the fixed repeater. Measurements at the site indicate that the fixed repeater is phase stable. The portable repeater is less susceptible to temperature fluctuations and is also phase stable.

The portable repeater was operated at several locations near Bearden.

On various occasions the portable repeater was operated at the receiving site for the fixed repeater; at the Naval Reserve Center in Harrell Field, about 17 km southwest of Bearden; at a cemetery a few miles from Bearden; and in Sheridan, about 40 miles north of Bearden.

136

When the portable repeater was situated at the receiving site of the fixed repeater, both repeaters shared the Collins LPA. The cable to the transmitter site was connected to the switch in the portable repeater so that the fixed repeater and the portable repeater were keyed on and off with a 63 μsec period. Both repeaters received simultaneously. The LPA has considerably more gain than the whip normally used on the portable repeater.

G. CW FORWARD PROPAGATION SUBSYSTEM

The CW forward propagation subsystem used a crystal frequency standard, a 1000 W linear amplifier and a vertical monopole antenna at Bearden, Arkansas. The receiving equipment in the plane was exactly the same as for the backscatter experiment except that the SFCW generators were operated in a mode where they provided a CW signal used for the first frequency conversion external to the receivers. A receiver was provided at Los Banos also which used one of the whips from the 2.5 km phased array there. The output of this receiver was recorded on magnetic tape in exactly the same fashion as the output of the airborne receivers.

H. OPERATIONAL PROBLEMS

1. Communications

It was necessary for the plane, the Bear Mountain site, and the Los Banos site to be connected by some form of communication. Available VHF radio equipment was used between the plane and Bear Mountain site; and a commercial telephone was used between Bear Mountain and Los Banos. The standard VHF transmitter and receiver normally used in the plane had adequate power (10 W) to provide usable communication to Bear Mountain over the entire flight path, but not to Los Banos. The use of Bear Mountain as a message relay point was decided on in order to avoid installing new radio equipment. This was satisfactory for routine messages, but for debugging the experiment it proved to be a handicap.

An intercom in the plane was also provided. The co-pilot and

137

navigator had a direct line as did the three SEL staff members.
Interconnection of the two direct lines could be made manually by the
flight coordinator (one of the SEL staff). The high acoustic noise
level of the plane made both shouting and the intercom only partially
successful. (On several occasions, hand signals were the only recourse.)
Even though special acoustic noise reducing microphones were used, a
much more satisfactory solution could have been found with more time and
money. The intercom communications and a tone marker actuated by the
camera shutter were recorded on the tape recorder.

A major drawback of the VHF communication link was that only
FAA authorized frequencies were used. These frequencies had to be
shared with others which made long conversations difficult. (One day
flocks of Civil Air Patrol planes were searching for a downed plane;
on that day voice transmissions were limited to occasional 15 sec
bursts.)

2.   Local Weather Limitations

Ideal conditions were clear skies, no wind, and plentiful
light. These rarely occur. The most important condition is no clouds
up to 6000 ft, the nominal altitude of the plane. Cloud cover beneath
the plane makes it impossible for the navigator to maintain a straight
course, although he did remarkably well if the ground was only 50 per
cent obscured. If both ground markers were obscured by clouds then
the absolute coordinates of the plane could not be found. This deter-
mination is essential to the accuracy of the CW tracking system.

After sunset the light was not adequate to take the aerial
photos, even if the eye could discern ground features. A moderate
steady head wind made it difficult for the DC-3 to cover the distance
between the two ground markers in 30 minutes, which was the duration
of the extra long reel of tape on the analog recorder. Changing winds
made it very difficult for the pilot to maintain constant speed and
altitude, and a straight course.

138

3. Preferred Ionospheric Conditions

To make an unambiguous backscatter map of the ground, only a single ray path should exist at the operating frequency between the region of the ground to be imaged and the transmitter and receiver. This is usually satisfied by the one-hop lower ray F mode during winter conditions. Unfortunately, summer conditions occurred some of the time during the April 1969 tests. The summertime conditions are characterized by a strong wide band upper ray, and the existence of an "s" turn in the mid-frequency band of the lower F ray. The general experience during that April was that satisfactory conditions prevailed after local noon.

It was desirable that the maximum usable frequency (MUF) not be changing. Not only did this aid in reducing phase distortion for the synthetic aperture but it made it unnecessary to keep changing the operating frequencies of the radio equipment.

4. Airplane Navigation

The co-pilot and navigator work for an air mapping company (Western Aerial Photos) and are experienced in flying prescribed courses. United States Geodedic Survey (USGS) maps (7½ min) showing every farm house, etc., along the course were used. The aerial camera was equipped with a telescope with cross-hairs, which enabled the navigator to make precise corrections to the plane's course (by giving commands such as "two degrees right!" to the co-pilot). The co-pilot is sensitive to wind shifts by noting small bearing changes by sighting on distant landmarks. He makes independent course corrections which improves the short term variations of the flight path. Evaluation of the radio tracking data indicated that the plane was almost always within 500 meters of the straight line course.

The pilot (who came with the plane and made the takeoff, etc.) was responsible for maintaining constant ground speed ($\pm$ 1.5 m/sec) and constant altitude ($\pm$ 10 m). The DC-3 responds slowly, and has a limited dynamic range in the throttle and propellor pitch settings. There is an obvious interaction between speed and altitude which further

139

complicates the problem. Constant speed is very important for both compensated and uncompensated synthetic apertures; therefore these problems cannot be over emphasized. Several flights were required to gain experience and familiarity with each person's task.

5. Personnel Required and Scheduling Problems

The operation of the experiment required 12 people at 5 sites. The Lost Hills transmitting site had a full time operator permanently assigned there. The frequency equipment problems there, however, made it often necessary for people to travel the several hundred miles to the site for repairs. The Bearden repeater also has a permanently assigned operator. The Bear Mountain site is about a four hour trip from Stanford. Two operators were assigned there when flights were scheduled. Two people were required for safety and in order to relay messages more easily from the plane to Los Banos.

An operator and a research assistant were at the Los Banos site. Besides providing the CW tracking signal, this site also received oblique ionograms from Bearden. The research assistant determined the proper operating frequencies, helped debug inoperative equipment by phone, and was in contact with each site.

There were 6 members of the flight crew. A pilot, assigned by the owner of the plane, was responsible for take-off ang landing and, when the plane was on the flight path, for maintaining a constant ground speed as indicated by the meter provided to him. The co-pilot and navigator were a highly trained two man team from Western Aerial Photos, a company which specializes in aerial mapping. They kept the plane on an exceptionally straight course. The three other members of the flight crew were SEL employees. One was an operator, responsible for adjusting the equipment and keeping it working. Another was a "flight coordinator" who organized much of the activity and kept a detailed log of the experiment both on paper and by comments on the voice channel on the tapes. The sixth flight crew member was the author. The author's only defined duty was to maintain communication with the Bear Mountain operators and through them with Los Banos. The

140

author was responsible for the backscatter sounding experiment and for assessing, in flight, the importance of the various parameters and equipment malfunctions. At one point he took over as pilot to determine if it was possible to keep the ground speed of the plane more constant than it had been. (It was.)

The plane was kept at San Jose airport which is about 40 min by car from Stanford and about 40 min by air to the flight path. This distance contributed difficulties in scheduling experiments and moving equipment.

BLANK PAGE

Appendix B

DESCRIPTION OF SIGNAL PROCESSING

A.   ORGANIZATION OF DIGITAL COMPUTER PROGRAMS FOR BACKSCATTER PROCESSING

The signal processing for the synthetic aperture backscatter data is composed of four digital computer programs. The first converts the analog demodulated SFCW backscatter data to sampled digital form. The second program reads the sampled data and does a Fourier transform for each equivalent element (each second of data); the output is another digital tape. The third program combines the elements at each range increment to form array beams, i.e., amplitude vs azimuth; the output is yet another digital tape as well as line printer and plotter displays. The fourth program displays the data. In the descriptions to follow, nominal values of parameters are used. Most of these are established at run time.

The Analog to Digital (A/D) conversion and the final display are done on an XDS Sigma 5 general purpose computer. This machine has a 16,000 word memory, a cycle time of less than a μsec, and is equipped with A/D and D/A converters, multiplexers, a CalComp plotter, one 9 track tape transport, and a 750,000 byte (1 word = 4 eight bit bytes) disk memory system.

The two processing programs (delay processing and beam forming) were written for an IBM 360/67. This computer has a 250,000 word core memory of which 64,000 are available to the user, a rapid access drum, a disc, a CalComp plotter, two 7 track and two 9 track tape transports.

The cost of time on the machine varies, but is approximately $1/minute on the Sigma 5, $7/minute on the 360.

B.   A/D CONVERSION

The demodulated SFCW data is bandpass filtered and sampled at a 5 kHz rate. The sampling signal was derived by dividing a filtered version of the 50 kHz signal on the tape by 10. To avoid aliasing,

143

the full 2 to 8 kHz band width of the data is not used. The band pass filtering of the data eliminated all signals not within 0.5 kHz of a center frequency of 4 kHz. The delays in the SFCW generators were set so the Bearden repeater signal was at 4 kHz. The band pass filter allowed signals within a slant range of ± 75 km to pass. This filtering caused a loss of data which is considered minor and resulted in a five fold saving of the number of samples, and a substantial saving in program size and running time. Even with this saving, the number of samples stored per tape is over 4×10^6 .

Of the 5000 samples taken every second, only 4096 (2^{12}) are stored on the tape. These are stored as one complete record. The discarded samples are taken during the time that the transmitter is off, thus no information loss is incurred. The A/D converter has 14 bits including sign, which represents a dynamic range of over 80 dB.

The 1 pps signal recorded from the cesium beam standard is used to restart the sampling program each second. Sufficient rise time of the 1 pps signal is preserved to insure that the first samples of each record are exactly 50,000 cycles of the 50 kHz reference signal apart. Thus the recording and A/D conversion process preserves coherence.

The output tape is 9 track with between 1024 and 1400 records. Each record has 4096 words written at 800 bytes per inch.

C. DELAY PROCESSING

The demodulated SFCW signal is a representation of the backscatter as amplitude and phase vs frequency. To convert this to amplitude and phase vs delay (range) a Fourier transform is performed. In conventional backscatter using SFCW signals the processing is often done by an analog spectrum analyzer. The available analog spectrum analyzers did not preserve phase information; the phase information is essential to the beam forming operation and therefore a phase preserving digital process was used.

A popular algorithm[31] for performing a fast Fourier Transform (FFT) was used. The version used is based on simplifications in the computation if the number of points to be sampled is a power of 2 (in the

144

present case, 2^{12}). The computation time is $k_1 n\log(n)$ seconds where k_1 is a constant which depends on the machine and the coding, and n is the number of complex points to be transformed. On the 360 the constant k_1 was about 60 μsec. This includes the bookkeeping and data handling in the processing program. Thus the 1024 transforms (one for each second or equivalent element) each with 4096 points would take about 40 minutes of machine time. The conventional transform requires an operating time of $k_2 n^2$ seconds, where k_2 is another constant. Using the conventional algorithm, the processing time would have been 400 times longer, or about one week of computer time (at a cost of $80,000!). Thus the FFT is essential to the digital processing.

The output of the FFT is 4096 complex points. Because the input data is real, only 2048 of these are unique. Of the 2048 unique points only 1024 points are written on a 9 track digital tape. The ± 512 points surrounding the Bearden repeater (at 4 kHz) are saved. (This is 2048 numbers since each point is complex).

The delay processing program is organized so each record is read, the FFT performed and the result then written on another tape. The program has many other features which are included for debugging purposes. Any number of records or samples per record can be processed, the amplitude of some of the FFT's data can be plotted, and the tape writing can be omitted. A simulated data input is also useful for debugging. The length of the program is about 700 cards, half of which are comment cards.

The delay increment between samples is the inverse of the band width of the data transformed. This is $(4096/5000 \times 1.0 \text{ MHz})^{-1}$ or about 1.2 μsec (180 meters of slant range). The delay resolution is determined by the SFCW band width (600 kHz) and the degradation due to side lobe weighting. The resolution (3 dB pulse width) is about 2 μsec.

D. AMPLITUDE, PHASE, AND DELAY COMPENSATION

The signal from the fixed Bearden repeater should be approximately 20 dB above the average level of the backscatter after the delay processing. The amplitude, phase, and delay of the repeater can therefore

145

be accurately measured. The delay vs element number (i.e., position along aperture or time) changes due to several factors. The repeater is not located on a line perpendicular to the flight path. Lines of constant range from the Bearden repeater are curved, while the flight path is essentially straight. In addition there are random deviations of the flight path. Finally, the ionosphere can introduce a delay perturbation. Backscatter returns from an area close to the repeater should have the same delay variations, therefore compensation for the backscatter is achieved by shifting the signals at each element so the repeater has the same delay at each element. The repeater return may be spread over two or three delay samples; the sample with the maximum amplitude defines the delay of the repeater for that element.

The phase of the repeater is also seemingly random due to the same effects, and is about two orders of magnitude more sensitive than delay. The phase is sensitive to path length changes on the order of a fraction of a wave length, about 2 meters, while the delay is sensitive to changes the size of the range increment, about 200 meters. In order for the array to image the repeater, the signal from the repeater must have a phase which depends linearly on the element position where it is measured. The phase compensation therefore is made by adding a phase to every delay increment so the phase of the repeater (which is now at a known delay) is zero. This procedure is done for each element independently. The phase is added by multiplying the complex number at each delay by e^{-jX_i}, where X_i is the phase of the repeater at the ith element.

This compensation includes the effects of the array geometry, flight path variations, and ionospheric variations. The compensation of just the geometrical effects, and the flight path variations is considerably more complicated and is described later.

The amplitude compensation (if used) is achieved by multiplying the complex number at each delay increment by $\dfrac{|A_i|}{|A_i|^2 + 0.01}$, where A_i is the amplitude or the repeater at the ith element and where 0.01 is selected to bound the amplitude correction.

146

E. BEAM FORMING

1. Basic Technique

The region surrounding the reference repeater is imaged by Fourier transforming the amplitude and phase data as a function of element number. This is done for each range increment. The beam forming program reads in one digital tape, does the Fourier transforms, and writes another digital tape of the normalized two dimensional HF ground reflectivity. The data handling problems are described in the next section; the mathematics of the processing for various situations is described here. Compensating for variations in aircraft speed is described after the basic equations are presented. The basic equations will also indicate when the curvature of the wave front is not adequately compensated by the reference. The problem of compensating for geometrical effects and flight path deviations using the airplane tracking data is also discussed. The conventional side lobe reduction technique is also applied here.

The basic geometry of an array receiving a plane wave was shown in Fig. 1. The elements are equally spaced by an amount Δs, and the plane wave is at an angle of θ_o radians relative to the line of the array. Assume the phase at element $i = 0$ is zero radians. The phase at the ith element is

$$\varphi_i = \frac{2\pi \Delta s \cdot \sin \theta_o}{\lambda} \cdot i \tag{47}$$

This phase depends linearly on the element number "i".

Let the received signal be r_{ik}, where "k" is the delay increment. In other words $\tau = k \cdot \Delta\tau$, where τ is delay and $\Delta\tau$ is the delay increment. Assume the look angle θ is small, so $\sin \theta \approx \theta$. Denote the output map as M_{pk}, where p is an integer indicating the angular increment. Therefore

147

$$\theta = p \cdot d\theta \quad , \quad \text{and} \quad \Delta\theta = \lambda/L$$

where L is the array length.

The number of elements in the array is "I" , therefore

$$L = \Delta s \cdot I$$

The response of the array in a direction θ is given by

$$\sum_{i=0}^{I-1} r_{ip} \, e^{-\frac{j\,2\pi\,\Delta s\,\theta_o}{\lambda} \cdot i} \tag{48}$$

or

$$M_{pk} = \sum_{i=0}^{I-1} r_{ik} \, e^{-j\,2\pi\,\frac{pi}{I}} \tag{49}$$

This equation is the discrete Fourier transform.

The range and angle coordinates of the map are approximately longitude and latitude, respectively. This is not exactly true because the angles are not small enough and because of the spherical geometry of the earth. The angular coordinate can also be interpreted as cross-range. The cross-range increment is the angular increment times the range.

2. Defocusing

The above equation images only points which have linear wave

148

fronts, i.e., linear phase vs element number. Ordinarily, for a large array the wave front for a point source would be curved. Let x be the array coordinate, $R(x)$ the range from a point source to the array at position x. Assume the point source, as shown in Fig. 36, is opposite the array midpoint. The phase along the array is

$$\varphi(x) = 2\pi \frac{R(x)}{\lambda} \qquad (50)$$

where

$$R^2(x) = R^2(0) + x^2$$

If $\lambda = 20$ m then $\varphi(x) = $ constant $+ 1/20 \cdot x^2$ radians. For a ± 2 km array the quadratic phase change is 0.2 radians which is negligible, while for a ± 50 km array the quadratic phase change is 125 radians which makes it essentially impossible to form a beam. If known, the quadratic phase term can be compensated for, thereby focusing the array on a certain range. In the synthetic aperture data which uses the Bearden repeater as a reference, the quadratic phase for the Bearden range (2600 km) is compensated for. However, signals from different ranges have different wave front curvatures. It is therefore necessary to determine over what range interval the data will be focused.

Let R_o be the range to Bearden and let $R_o + \Delta R$ be the range to some other source. Let $\varphi(x)$ be the phase difference due to the difference in wave front curvature, then

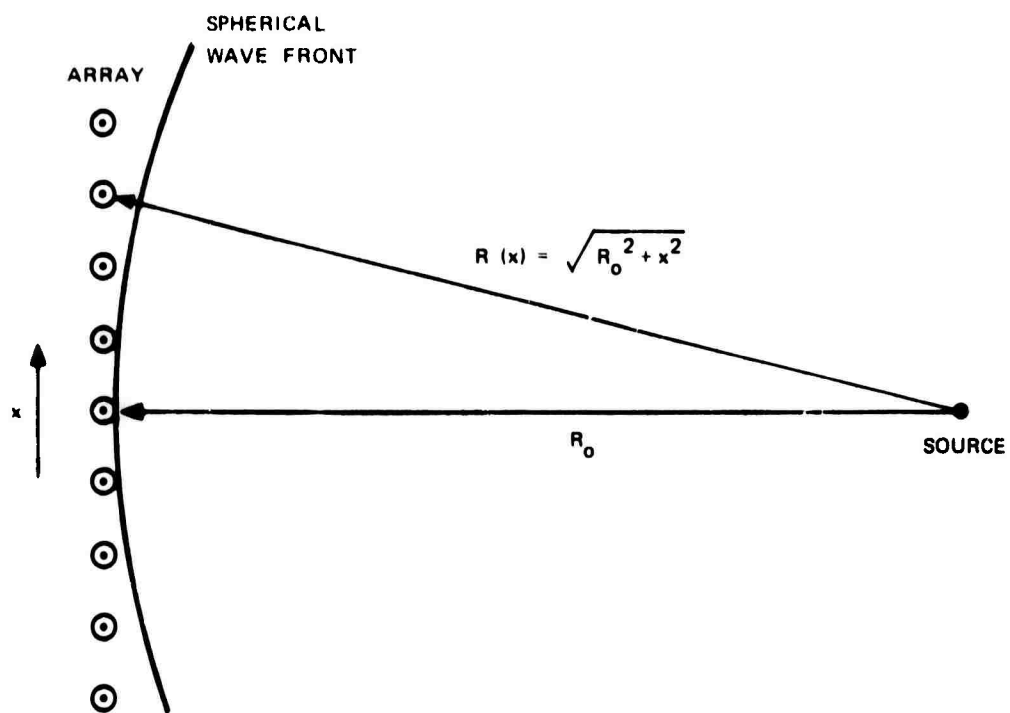$$\varphi(x) = 2\pi \frac{x^2 \, \Delta R}{\lambda \, R_o^2} \qquad (51)$$

149

Figure 36   Geometry for spherical wave-front calculation.

Let the maximum array coordinate be ± 50 km, and λ = 20 m, then the quadratic phase difference $\varphi(x)$ is 0.4 radians, which introduces little distortion. For range intervals larger than 50 km significant phase distortion occurs and defocuses the array. These limitations on the processing must be adhered to or appropriate compensation made. This calculation can be interpreted to indicate that the range resolution obtainable through focusing is about 50 km.

3. Beam Slewing

It is now shown that if the synthetic aperture is to focus on a point which is more than 0.5 deg of azimuth from the repeater, the phase processing of Eq. 49 is not valid. The pulses have such a small width that the delay difference from the end equivalent elements to the point source is greater than the delay resolution. Another point of view is that the proper phase shift to slew the beam depends on λ , but because the signal is wide band the variation of λ makes the required phase change undefined. Delay line steering is used in many arrays to solve this problem.

The difference in delay for a signal from a direction θ from the center to the end element is $x_{max} \cdot \theta$. The pulse width in meters in c/W where c is the speed of light (3×10^{8} m/sec), and W is the system band width (600 kHz). If x_{max} = 50 km then the error is small for small angles θ , namely

$$\theta < \frac{c}{W\,x_{max}} \approx 0.01 \text{ radian} \approx 0.6 \text{ deg}$$

At 20 meter wave length, a ± 50 km array has about a 0.01 deg beam width, thus ± 60 azimuthal increments may be imaged without compensating for the narrow pulse problem.

The delay line steering solution to the problem can only be approximated on the digital computer (without unreasonable difficulty)

151

because the signals can only be shifted in delay by discrete amounts. The required linear delay vs coordinate x can be approximated by delay steps of size 1/W seconds. The phase of the signal can be adjusted by the right amount. The question to be answered is how does the discrete delay approximation degrade the array performance. An amplitude variation is introduced as a result of not shifting the pulse the right amount. The amount of amplitude variation depends on the pulse width and the delay increment. The variation is about 25 per cent. A random 25 per cent amplitude variation can cause a side lobe level on the order of $0.25/\sqrt{I}$, where I is the number of elements. For the 1000 element array the side lobe level introduced is approximately 40 dB down, which is not considered important.

4. Compensation for Changes in Airplane Speed

If the array elements are not equally spaced, the basic array processing equation (Eq. 48) must be rewritten with $\Delta s \cdot i$ replaced by s_i , where s_i is the actual coordinate of the ith element. Thus the processing is no longer exactly a Fourier transform. For small angles θ , the distinction is small, as is now shown.

The difference in phase between that computed using the array element coordinates and that computed assuming equally spaced elements is:

$$\frac{2 \pi \theta}{\lambda} \ (s_i - \Delta s \cdot i) \tag{43}$$

If the rms phase is specified to be less than $\pi/10$, a wave length is $\lambda = 20$ m then the rms deviation of s_i from a straignt line must be constrained to satisfy

$$\theta \cdot rms \ (s_i - \Delta s \cdot i) < 1 \tag{44}$$

152

For example, if the rms deviation is 100 meters, the angle imaged by the array must be less than .01 radians or 0.6 deg.

It is also possible to slew the beam some large amount, say 2 deg, apply a single phase compensation, then only vary the beam ± 0.6 about the offset angle.

5. Compensation for Flight Path Variations

One of the desired tests is to determine the beam width achievable without compensating for ionospheric effects. It is necessary, however, to compensate for geometrical effects and flight path deviations.

Since only arrays less than 12 km long were synthesized the curved wave front significantly affected the phase but not the delay. Flight path deviations from the tracking program are available on punched cards as the slant range to Bearden for each second (array element). The delay compensation for flight path variations is in discrete steps as discussed earlier. The phase compensation depends on the cosine of the array pointing direction. But for angles less than 10 deg the cosine is approximately unity, therefore the compensation is independent of angle and the Fourier transform processing can be used.

F. DATA HANDLING PROCEDURES

The data handling for the delay processing program is straight-forward since only one record is processed at a time. The beam forming program is much more complicated. The input to the beam forming program is a sequence of records, each record representing a synthetic element. The beam forming processing requires data indexed in the opposite manner, that is, the processing requires data for a single range increment but all elements. Tape reading is slow and therefore cannot be repeated 1024 times for each range increment, and the core size is far too small to accommodate the (1024 × 1024 × 2) two million numbers to be processed.

153

To solve the data handling problem a procedure is used to reduce the number of data samples which are required at any given time. The procedure is shown in a flow diagram in Fig. 37. The program starts by reading each equivalent element or record on the digital tape. As each record is read compensation is made by modifying the amplitude and phase of each range increment in the same way.

Sub-arrays are then formed by adding successive equivalent elements at each range increment in groups of four. Thus the number of equivalent elements is reduced from 1024 to 256. Each sub-array has a beam width of about 4 deg thus limiting the azimuths which can be imaged.

In the next step, 384 range samples of the original 1024 range samples are stored on the drum. The 384 range increments represent 12 range blocks of 32 range increments each. The range block is a convenient grouping to facilitate subsequent processing. There are 160,000 samples stored on the drum.

In the next step one range block for all sub-arrays is read from the drum into the core memory. There are now 16,000 samples in core. The beam forming processing is then performed on that one range block.

The drum is used to store the output of the processing which is necessary in order to use the same program to give an immediate display of the map. A display requires the entire output to be normalized to accommodate the limited dynamic range of any practical display (about 20 dB). The beam forming procedure is then re-applied if another range block is to be processed. The end result of the beam forming program is then written on a digital tape for permanent storage.

G. CW FORWARD PROPAGATION PROCESSING

The recorded CW data was sampled at a 50 kHz rate. The sampling signal was derived from the 50 kHz reference signal on the tape. The program used the time of zero crossings of the sine wave at one second intervals to measure the phase of the CW signal. The measured value of the amplitude and phase for each second of data is then stored on digital tape. (The CW data was processed by P. A. Fialer for other purposes. A more complete description of the sampling program may be
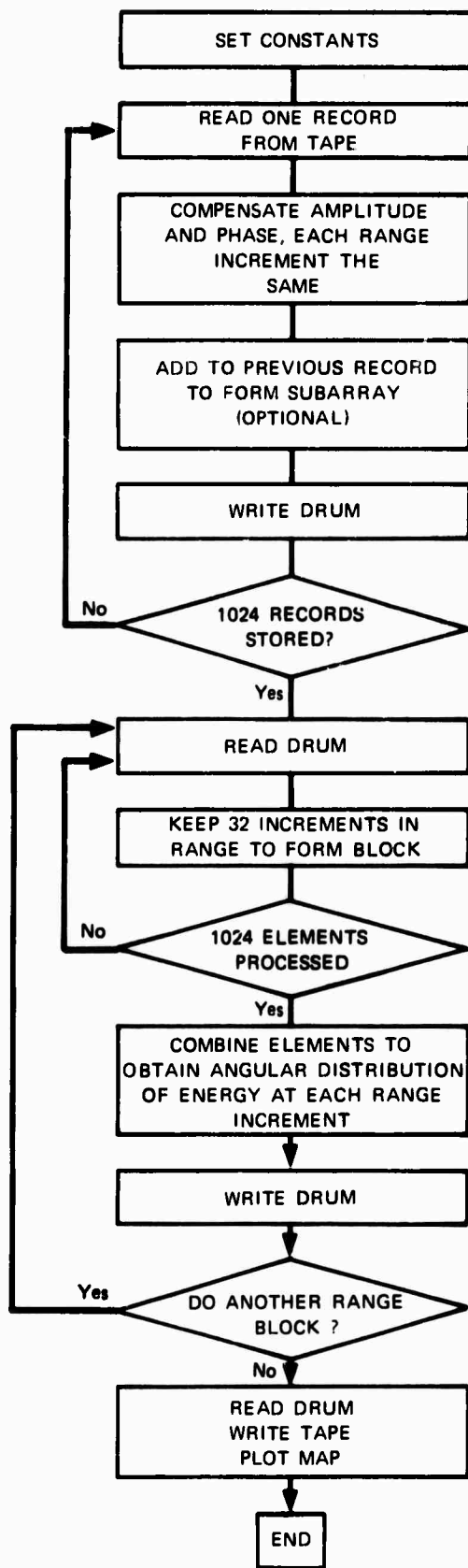
154

Figure 37   Flow chart for beam-
            forming program.

155

found in his dissertation.)

A second program analogous to the beam forming program described for the backscatter processing is then run. This program converts amplitude and phase data (A_i , θ_i) to complex form $(A_i e^{j \theta_i})$ and, after compensating phase for the airplane's position, takes a Fourier transform using 32, 64, 128, or 256 points. The phase compensation, χ_i for the position of the plane is

$$\chi_i = \frac{d_i \, 2\pi}{\lambda}$$

where d_i is the distance between Bearden, Arkansas and the plane at the ith second. The distance to Bearden is based on the airplane tracking data and a nominal reflection height for the ionosphere.

The compensation for aircraft motion includes the effect of a changing range between Bearden and the plane. There should not be therefore any focusing distortion caused by curved wave fronts. The output of the program is a sequence of array patterns (or equivalently-Doppler spectra) drawn by a CalComp plotter.

REFERENCES

1. L. E. Sweeney, Jr., "Spatial Properties of Ionospheric Radio Propagation as Determined with Half-Degree Azimuthal Resolution," Report SEL-70-034 (TR No. 155), Stanford Electronics Laboratories, Stanford, Calif., Jun 1970.

2. W. M. Brown, "An Introduction to Synthetic Aperture Radar," IEEE Spectrum, 52, Sep 1969.

3. Robert O. Harger, Synthetic Aperture Radar Systems: Theory and Design, Academic Press, New York, 1970.

4. E. D. R. Shearman and J. Clarke, "Aperture Synthesis in Ionospheric Radar," Nature, 219, Jul 1968, pp. 143-144.

5. T. M. Georges, "Ionospheric Effects of Atmospheric Waves," IER 57-ITSA 54, Institute for Telecommunication Sciences and Aeronomy, Boulder, Colorado, Oct 1967.

6. K. C. Yeh and G. W. Swenson, Jr., "F-Region Irregularities Studied by Scintillation of Signals from Satellites," Radio Science, 68D, 8, Aug 1964, pp. 881-892.

7. B. H. Briggs, G. J. Phillips and D. H. Shinn, "The Analyses of Observations on Spaced Receivers of the Fading of Radio Signals," Proc. Phys. Soc., B, 63, 1950, p. 106.

8. G. D. Thome, "Incoherent Scatter Observations of Traveling Ionospheric Disturbances," J. Geophys. Res., 69, 19, Oct 1964, pp. 4047-4049.

9. G. D. Thome, "Long-Period Waves Generated in the Polar Ionosphere During the Onset of Magnetic Storms," J. Geophys. Res., 73, 19, Oct 1968, pp. 6319-6336.

10. E. N. Bramley and W. Ross, "Measurements of the Direction of Arrival of Short Radio Waves Reflected at the Ionosphere," Proc. Roy. Soc., A, 207, Jun 1951, p. 251-267.

11. E. N. Bramley, "Direction-Finding Studies of Large-Scale Ionospheric Irregularities," Proc. Roy. Soc., A, 220, Oct 1953, pp. 39-61.

12. P. J. D. Gething, "High-Frequency Direction Finding," Proc. IEE, 113, 1, Jan 1966, pp. 49-61.

REFERENCES (Cont)

13. J. T. Lynch, R. B. Fenwick and O. G. Villard, Jr., "Measurement of Maximum Time-Delay Resolution of Oblique Soundings on East-West and North-South Paths," Report SEL- - (TR No. 146), Stanford Electronics Laboratories, Stanford, Calif., Jun 1968.

14. P. A. Fialer, "Irregularities in the Quiet Ionosphere and Their Effect on Propagation," Report SEL-70-037 (TR No. 156), Stanford Electronics Laboratories, Stanford, Calif., Jul 1970.

15. M. Balser and William B. Smith, "Some Statistical Properties of Pulsed Oblique HF Ionospheric Transmissions," J. Res. NBS, 66D, 6, Nov-Dec 1962, pp. 721-730.

16. R. A. Sheperd and John B. Lomax, "Frequency Spread in Ionospheric Radio Propagation," IEEE Trans. Comm. Tech., COM-15, 2, Apr 1967, pp. 268-275.

17. J. W. Goodman, W. H. Huntley, D. W. Jackson and M. Lehmann, "Wavefront-Reconstruction Imaging Through Random Media," Applied Phys. Lett., 8, 12, Jun 1966, pp. 311-313.

18. R. N. Bracewell, The Fourier Transform and its Applications, McGraw-Hill Book Co., Inc., New York, 1965.

19. Charles E. Cook and Marvin Bernfeld, Radar Signals--An Introduction to Theory and Application, Academic Press, New York, 1967.

20. D. L. Fried, "Optical Resolution Through a Randomly Inhomogeneous Medium for Very Long and Very Short Exposures," JOSA, 56, 10, Oct 1966, pp. 1372-1379.

21. G. R. Heidbreder, "Image Degradation with Random Wavefront Tilt Compensation," IEEE Trans. Antennas and Propagation, AP-15, 1, Jan 1967, pp. 90-98.

22. J. D. Gaskill, "Holographic Imaging Through a Randomly Inhomogeneous Medium," Ph.D. Dissertation, Systems Techniques Laboratory, Stanford University, Stanford, Calif., May 1968.

23. N. Wiener, The Extrapolation, Interpolation and Smoothing of Stationary Time Series, John Wiley and Sons, Inc., New York, 1949.

24. H. L. Van Trees, Detection, Estimation and Modulation Theory, Part 1, John Wiley and Sons, Inc., New York, 1968, pp. 198-202.

REFERENCES (Cont)

25. C. W. Helstom, "Image Restoration by the Method of Least Squares," JOSA, 57, 3, Mar 1967, pp. 297-303.

26. David Slepian, "Linear Least-Squares Filtering of Distorted Images," JOSA, 57, 7, Jul 1967, pp. 918-922.

27. Joseph Horner, "Optical Spatial Filtering with the Least Mean-Square-Error Filter," JOSA, 59, 5, May 1969, pp. 553-558.

28. D. Belknap, R. Haggarty and D. Perry, "Adaptive Signal Processing for Ionospheric Distortion Correction," presented at the Fall URSI meeting, Boston, Mass., 1968.

29. John V. Evans and Tor Hagfors, (Editors), Radar Astronomy, McGraw-Hill Book Co., Inc., New York, 1968.

30. J. D. Gaskill and J. W. Goodman, "Use of Multiple References to Increase the Effective Field of View in Lensless Fourier-Transform Holography," (Ltr.) Proc. IEEE, 57, 5, May 1969, p. 823.

31. R. B. Fenwick and G. H. Barry, "Sweep-Frequency Oblique Ionospheric Soundings at Medium Frequencies," IEEE Trans. Broadcasting, BC-12, 1, Jun 1966, pp. 25-27.

32. A. C. Phillips, "A Single Antenna Repeater for HF Radio Propagation Studies," Report SEL-69-064 (TR No. 154), Stanford Electronics Laboratories, Stanford, Calif. Oct 1969.

33. W. T. Cochran, et. al., "What is the Fast Fourier Transform," IEEE Trans. Audio and Electroacoustics, AU-15, 2, Jun 1967, pp. 45-55.

DOCUMENT CONTROL DATA - R & D		
Security classification of title, body of abstract and indexing annotation must be entered when the overall report is classified)		

1 ORIGINATING ACTIVITY *(Corporate author)*	2a. REPORT SECURITY CLASSIFICATION
Stanford Electronics Laboratories	Unclassified
Stanford University	2b GROUP
Stanford, California 94305	

3 REPORT TITLE

APERTURE SYNTHESIS FOR HF RADIO SIGNALS PROPAGATED VIA THE F LAYER OF THE IONOSPHERE

4 DESCRIPTIVE NOTES *(Type of report and inclusive dates)*

Technical Report No. 161, September 1970

5 AUTHOR(S) *(First name, middle initial, last name)*

J. T. Lynch

6 REPORT DATE	7a. TOTAL NO. OF PAGES	7b. NO OF REFS
September 1970	159	33

8a. CONTRACT OR GRANT NO	9a. ORIGINATOR'S REPORT NUMBER(S)
Nonr-225(64), NR 088-019	SU-SEL-70-066
b. PROJECT NO	TR No. 161
3834	
c. ARPA Order No. 196	9b. OTHER REPORT NO(S) *(Any other numbers that may be assigned this report)*
d	

10 DISTRIBUTION STATEMENT

This document has been approved for public release and sale; its distribution is unlimited.

11 SUPPLEMENTARY NOTES	12. SPONSORING MILITARY ACTIVITY
	Office of Naval Research

13 ABSTRACT

A portable high-frequency (HF) radio aperture up to 70 km in length was synthesized by receiving ionospherically propagated signals in a DC-3 airplane. By thus moving a small antenna rapidly over a long distance, a narrow receiving beam width (high azimuthal resolution) was achieved. It is believed that the synthetic aperture described here is the first in the world developed for HF, although the concept has been used successfully at microwave frequencies.

When HF radio signals are propagated by refraction from the ionosphere, inhomogeneities in the electron density of the medium distort the refracted signals and limit the azimuthal resolution which can be achieved. Using a statistical model of the ionospheric distortion a theoretical analysis was made to predict the performance of the HF synthetic aperture, determine its limitations and compare its performance with that of a ground-based fixed array.

Using continuous wave (CW) signals transmitted from a point 2600 km to the east, it was shown that with compensation for the deviations of the airplane from a straight line course, a 10 km aperture yielded a 1/12 deg beam width (at 23 MHz) for about 20 per cent of the data tested, while a 5 km aperture yielded a 1/6 deg beam for about 50 per cent of the data tested. Based on results obtained by receiving the same signal at a fixed antenna on the ground, it is believed that both spatial and temporal variations of the ionosphere were limiting the achievable beam width. In another method of operation a sequence of swept frequency CW (SFCW) signals was transmitted

14 KEY WORDS	LINK A		LINK B		L	
	ROLE	WT	ROLE	WT	ROLE	

SYNTHETIC APERTURE
HF RADIO PROPAGATION
ANTENNAS
IONOSPHERIC RADIO
SIGNAL PROCESSING

Abstract (Cont)

from California, backscattered from ground areas
2600 km to the east, and received in the airplane,
thus yielding an HF reflectivity image of the area.
An HF repeater was located near the terrain to be
imaged and was used as a reference to compensate for
flight-path deviations and ionospheric distortion.
A second repeater located 1000 m away from the
reference repeater was used to simulate a strong
backscatter return. An HF backscatter map was made
using a 70 km synthetic aperture which had a 500 m
range and a 500 m cross-range (lateral) resolution.
The two repeaters were distinguishable in cross
range. On the basis of the theoretical analysis,
and the characteristics of the two repeaters as
revealed in the backscatter map, it is believed that
objects should be within 3 to 5 km of the reference
repeater in order to be imaged without significant
distortion.

The above results were obtained on a midlatitude
east-west path which is known to have favorable
characteristics. The data were taken during a
period of low magnetic activity and in general the
ionosphere was undisturbed.

It is concluded that aperture-synthesis
techniques at HF are particularly attractive for
apertures of between 1 and 10 km in length. For the
shorter apertures, 1 to 3 km, it should be possible
to obtain full benefit of the aperture by using a
medium-sized airplane and simple processing techniques
which would not compensate for course deviations of
the plane from a straight line. Longer apertures,
6 to 10 km, could be used effectively at least part
of the time, if compensation for course variations
could be provided.